INFORMATION TO USERS

This manuscript has been reproduced from the microfilm master. UMI films the text directly from the original or copy submitted. Thus, some thesis and dissertation copies are in typewriter face, while others may be from any type of computer printer.

The quality of this reproduction is dependent upon the quality of the copy submitted. Broken or indistinct print, colored or poor quality illustrations and photographs, print bleedthrough, substandard margins, and improper alignment can adversely affect reproduction.

In the unlikely event that the author did not send UMI a complete manuscript and there are missing pages, these will be noted. Also, if unauthorized copyright material had to be removed, a note will indicate the deletion.

Oversize materials (e.g., maps, drawings, charts) are reproduced by sectioning the original, beginning at the upper left-hand corner and continuing from left to right in equal sections with small overlaps. Each original is also photographed in one exposure and is included in reduced form at the back of the book.

Photographs included in the original manuscript have been reproduced xerographically in this copy. Higher quality 6" x 9" black and white photographic prints are available for any photographs or illustrations appearing in this copy for an additional charge. Contact UMI directly to order.

UMI

A Bell & Howell Information Company
300 North Zeeb Road, Ann Arbor MI 48106-1346 USA
313/761-4700 800/521-0600

THE EFFECTS OF PASSIVE JOINT MOVEMENT ON HUMAN ANKLE STRETCH REFLEX DYNAMICS

Luckshman Parameswaran

Department of Mechanical Engineering

McGill University

Montréal, Québec, Canada

August 1996

A Thesis submitted to the

Faculty of Graduate Studies and Research

in partial fulfillment of the requirements for the degree of

Master of Engineering

Abstract

The role of the monosynaptic stretch reflex in the realm of human motor activity has been controversial for many years. A non-linear parallel-cascade system identification technique was recently developed to non-invasively elucidate the ankle reflex dynamics. Identification of these dynamics requires the application of stochastic signals to the ankle joint. The stretch reflex is known to be highly modulated and attenuated during on-going cyclical movements and passively applied perturbations. The aim of this study was to investigate these effects.

The stretch reflex gain was found to decrease progressively as the average velocity of the applied movement increased. The velocity-mediated effects were a function of the amplitude distribution characteristics, rather than the spectral properties, of the applied motion. The experiments confirmed that although the stretch reflex response is large enough to be important its effects will depend on the functional context.

Résumé

Le rôle du réflexe myotatique dans le contrôle du systéme neuromusculaire chez l'humain est depuis des années un sujet controversé. Un technique non-linéaire d' identification de systèmes a été développé récemment pour élucider la dynamique du réflexe à la cheville. L'identification de cette dynamique requiert l'application de signaux stochastiques à la cheville. On sait que le réflexe myotatique varie et est largement atténué pendant les mouvements cycliques et les perturbations appliquéees passivement. L'objectif de cette thèse était d'étudier ce phénomène.

Nous avons découvert que le gain du réflexe myotatique diminue progressivement lorsque la vitesse moyenne des perturbations augmente. De plus, nous avons trouvé que les charactéristiques du réflexe dûs à la vitesse de perturbation dépendent de la distribution de l'amplitude du mouvement appliqué et non des propriétés spectrales. Les experiences ont confirmé que le refléxe myotatique est suffisamment grand pour être important, mais que ses effets dépendent du contexte fonctionnel.

Acknowledgments

I am greatly indebted to my supervisor Rob Kearney for his probing questions and insightful comments. My research experience was enriched by his flexibility in letting me explore and his ability to make me focus.

I have experienced many fruitful consultations and discussions with the denizens of the Department of Biomedical Engineering. In particular, Andrzej Kozakiewicz, Mireille Lortie, Mehdi Mirbagheri, Helen Qiao, Michael Steszyn, Ross Wagner and David Westwick must all be mentioned. I would also like to thank Jacqueline Chen, Bert Haverkamp, Rachel Holmes, Hanif Ladak, Thomas Ranger and Tom Kennedy for being willing participants in my endless experiments.

My deepest appreciation goes to Frank Chan, Jan Duha, Andrea Green, Sunil Kukreja, Barb Naber, Natasha Ramachandran and Tanisha Ramachandran for their invaluable friendship. I would especially like to acknowledge Stacy Shoemaker for her unfailing support, endless encouragement and companionship.

I am extremely grateful to my parents for their unfaltering love and guidance, and for the sacrifices they have made.

This work was supported by grants from the Medical Research Council and from the Natural Sciences and Engineering Research Council.

Contents

List of Figures

List of Tables

The human body is the only known machine that can run for more than a century with proper care and at worst, several years with poor care. It needs no maintenance other than fuel and rarely requires replacement parts. It is watertight, airtight, and can run well in both hot and cold environments after adjusting itself accordingly. It can repair itself and can withstand both internal and external assaults...The human body is the only machine that becomes more esthetically pleasing and efficient when it is worked harder. Should a defect in its workings occur, it has the remarkable ability to bypass that defect and compensate for it using any of its other resources. Most importantly, although external programming and instruction enhance the body, it is able to run and exist without being told how [87].

Chapter 1

Introduction

There is grandeur in this view of life, with its several powers, having been originally breathed by the Creator...from so simple a beginning endless forms most beautiful and most wonderful have been, and are being evolved.

- Charles Darwin [27].

Joint Dynamics

The human body is supported by a collection of rigid skeletal elements connected by joints and articulated by muscle. The maintenance of posture and the execution of motion is effected by the active involvement of the *neuromuscular system* integrating sensory receptors and physiological actuators that communicate with each other via ingenuously connected nerve fibres.

How does the neuromuscular system control posture and movement?

In an attempt to answer this complex question, neuromuscular function has been described using the mechanical properties of joints. In engineering terms, the study of dynamics deals with the mechanical relation between the forces acting on a body and its resulting movement. *Joint dynamics* thus refer to the relation between the angular position of a joint and the torques acting about it. They determine the perturbing forces during postural control and the forces needed to perform voluntary movement: in other words, they describe the interaction between the neuromuscular system and

the external environment.

Understanding the nature and functional importance of the innate mechanisms contributing to joint dynamics will yield important benefits. Neuromuscular diseases can be objectively assessed using quantitative diagnostic tools. Orthosis design, prosthetic control, and functional electrical stimulation (FES) all require a knowledge of joint dynamics. Human operator performance must be understood in order to construct man-machine interfaces, such as tele-robotic actuators.

System identification techniques have been used to investigate and construct mathematical models of biomedical systems. Since they allow the deduction of system behaviour from easily measured inputs and outputs, these techniques afford a non-invasive means of determining neuromuscular dynamics in the intact functional human (as opposed to the anaesthetised animal or the dead human).

Stretch Reflex

The *stretch reflex* is the term given to a seemingly simple phenomenon : when a muscle is stretched via an external perturbation, it will contract and produce force. The evocation of the stretch reflex in the quadriceps muscle group is popularly referred to as the knee jerk; tapping the patellar tendon elongates the quadriceps and the resulting reflex contraction causes the lower limb to swing upwards.

The stretch reflex is thought to be instrumental in the control of movement and the maintenance of posture. It is known to be context-sensitive and phase-dependent within that context. Although the neurophysiological mechanisms underlying stretch reflexes have been studied extensively, their functional importance in the neuromuscular system remains a matter of controversy. Researchers in the Neuromuscular Control Lab at McGill's Department of Biomedical Engineering have successfully measured the *reflex contribution to ankle joint dynamics* using a non-linear parallel-cascade technique.

Some interesting results were noted during the investigation of stretch reflex dynamics at the human ankle. The system identification scheme was more effective using a pseudo-random binary perturbation signal in place of the traditional filtered

Gaussian white noise input. The nature of the signal determined the efficacy of the identification scheme. In addition, the reflex activity evoked by pulse displacements decreased in the presence of an externally imposed passive motion.

Performing experiments on the ankle joint simplifies the logistics of investigating joint dynamics. Due to its distal location, it can be studied without interference from other limb segments. The results are crucial for locomotion and posture studies as the foot interfaces the musculoskeletal system with the ground. Furthermore, the dynamics may be representative of other joints operating under similar conditions.

Thesis Outline

The objective of this research was to determine the effect of an ongoing imposed passive movement on stretch reflex dynamics. An attempt was made to discover which properties of the imposed movement were responsible for the decrease in reflex activity. This work is a continuation of the efforts to understand the functional activity of the stretch reflex.

In order to fully understand the rationale behind the project, it is necessary to place it within the proper context. *Chapter 2* describes the structure of the ankle joint, the mechanics of muscle fibre and the physiology of the peripheral neuromuscular system. The concepts involved in ankle joint dynamics are described along with the system identification techniques used to describe them. A brief review of previous studies of stretch reflex function concludes the chapter.

The parallel-cascade identification technique and the experimental apparatus used to study reflex dynamics are presented in *Chapter 3*. The experimental protocol is described in detail with emphasis placed on the input perturbation signals used to investigate the effect of different movement parameters on stretch reflexes.

The experiments were conducted in two stages. The first looked at the effect of motion on the dynamic model developed using the system identification methods. The second concentrated on the attenuation of the ankle reflex response evoked by a brief stretch of the calf muscles. These results are revealed in *Chapter 4*; their significance is expounded in *Chapter 5*.

Chapter 2

Background

This chapter commences with the basic anatomy of the ankle joint followed by a brief description of muscle mechanics. The physiology of the stretch reflex is reviewed within the context of the peripheral neuromuscular control system. The second half of the chapter introduces the concept of joint dynamics and the system identification techniques used to measure them. The resulting quantitative descriptions of the neuromuscular system are summarized. The chapter concludes with a review of the studies that have attempted to characterize the stretch reflex.

2.1 Ankle Joint

The ankle, a versatile joint adapted for both stability and flexibility, contains the extremities of the tibia, fibula and talus as illustrated in Fig. 2.1.

The ankle is capable of rotating about 2 axes. The *talocrural joint* (henceforth referred to as the *ankle joint*) forms the proximal connection between the talus and the leg and is responsible for motion in the sagittal plane. (The sagittal plane slices the body into left and right halves). Supination and pronation of the foot occurs about the *talcocaneal* (or *subtalar*) joint which forms the distal connection between the talus and the leg. Both joints have single axes of rotation [50]. Although the ankle and subtalar joints constitute an integrated mechanism, the dominant motion of the ankle is restricted to the sagittal plane; the following research work is restricted

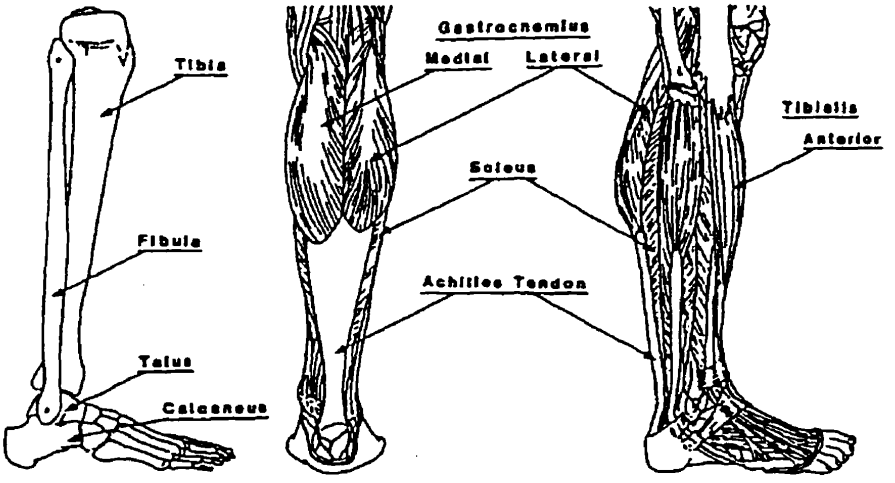

Figure 2.1: Skeletal structure and musculature at the ankle joint(from Yunan[102])

to the ankle joint in order to simplify the experimental and analytical procedures.

Axis of Rotation

The position of the ankle joint can be estimated as a line passing beneath the ankle malleoli, 82^o from the sagittal plane and $20^o - 30^o$ from the frontal plane [93]. (The frontal plane separates the body into front and back halves). The experimental determination of the axis[1] and the uncertainties associated with the procedure[2] for locating it are described later.

Notation and Terminology

As shown in Fig. 2.2, *dorsiflexion* is the rotation of the foot towards the rest of the body. Lab convention assigns a positive sign to a dorsiflexing position or torque change. *Plantarflexion* refers to the downward movement of the foot.

The *range of motion (ROM)* quantifies the angle of rotation between the points of maximum plantarflexion and maximum dorsiflexion. Total ankle ROM was measured to be 0.99 ± 0.12 rad (mean ± 1 s.d.) in a study of six healthy subjects by Weiss et al [97] and approximately 1.75 rad by Sinkjaer et al [86].

[1]Section 3.3.3 on page 51
[2]Section 5.7.2 on page 93

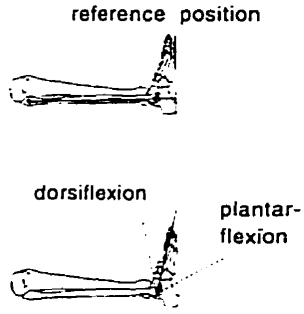

Figure 2.2: Ankle notation (adapted from Weiss[95])

The *neutral position* (NP) is the ankle angle associated with no net passive joint torque. The *reference position* is located where the plantar surface of the foot is perpendicular to a line joining the head of the fibula and the medial malleolus. Rotating the ankle from the reference position increases the passive joint torque to about 4 Nm in plantarflexion (-0.8 rad) and 9 Nm in dorsiflexion (0.15 rad) [97].

Musculature

The dorsiflexing muscles are comprised of the *tibialis anterior*, *extensor hallucis longus*, *peroneus tertius* and *extensor digitorum longus* muscles. They are all innervated by branches of the deep peroneal nerve. Due to its superficial location, the *tibialis anterior* (TA) was chosen to represent the global action of the dorsiflexor group of muscles.

The *soleus* muscle and the lateral and medial heads of the *gastrocnemius* muscle, collectively known as the *triceps surae* (TS) muscle group, constitute the major plantarflexors. The TA and TS muscle group are illustrated in Fig. 2.1.

2.2 Muscle Mechanics

The ankle joint articulates and exerts force on the external environment through the mechanical action of the muscle fibres attached to the rigid skeletal structure. Muscles in the human body can be differentiated into cardiac, skeletal and smooth categories on the basis of structure, contractile properties and control mechanisms.

Unlike cardiac and smooth muscle, skeletal muscle is under voluntary control and is responsible for movement and posture. Figure 2.3 shows how skeletal muscle attaches to the bone via tendons at each end.

The mechanical properties of the muscle are a function of both the **contractile mechanics** and the **activation dynamics.**

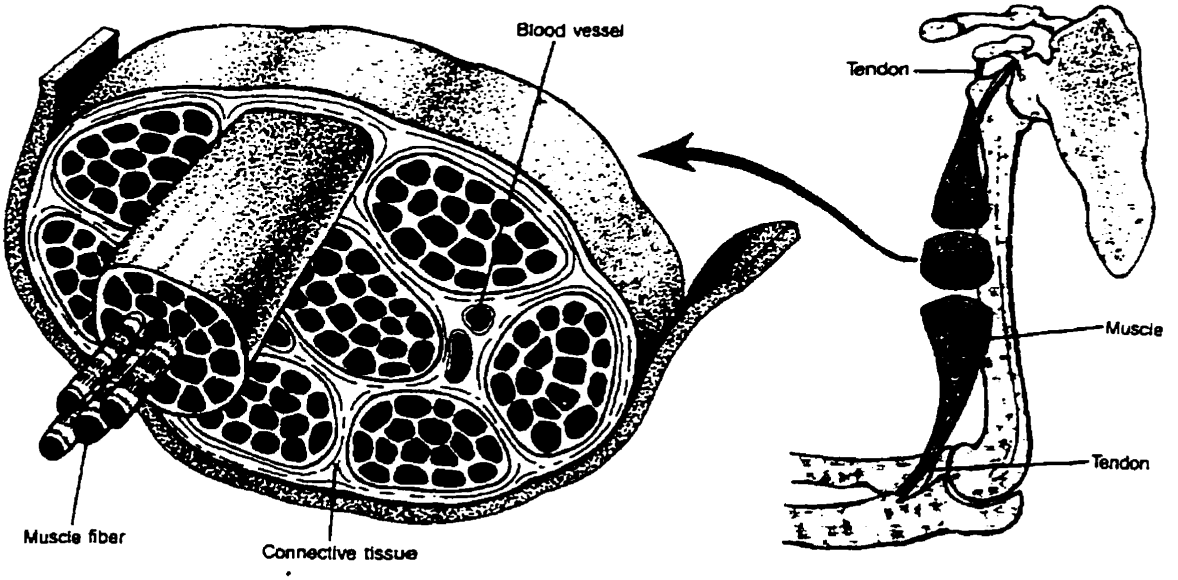

Figure 2.3: Muscle attachment in the upper limb (from Vander[94])

2.2.1 Anatomy

As shown in Fig. 2.4, whole *skeletal muscles* consist of bundles of *muscle fibres* bound by connective tissue. The connective tissue from the ends of each fibre join together to form the tendon which attaches muscle to bone. Muscle fibres, which range in diameter from 10 μm to 100 μm, are comprised of bundles of *myofibrils*. A myofibril is 1 – 2 μm in diameter and extends the length of the muscle fibre (and whole muscle). Myofibrils are parallel and partially overlapping collections of thick and thin *myofilaments*. *Thick* filaments, constructed from myosin protein, have diameters between 12 and 18 nm. Actin, troponin and tropomyosin are the protein subcomponents of *thin* filaments, which have diameters ranging from 5 to 8 nm.Myofibrils are striated: they have alternating dark and light bands as a result of their repeating structure. The

repeating unit of this periodic structure is called a *sarcomere* and is between 1.5 and 3.6 μm in length.

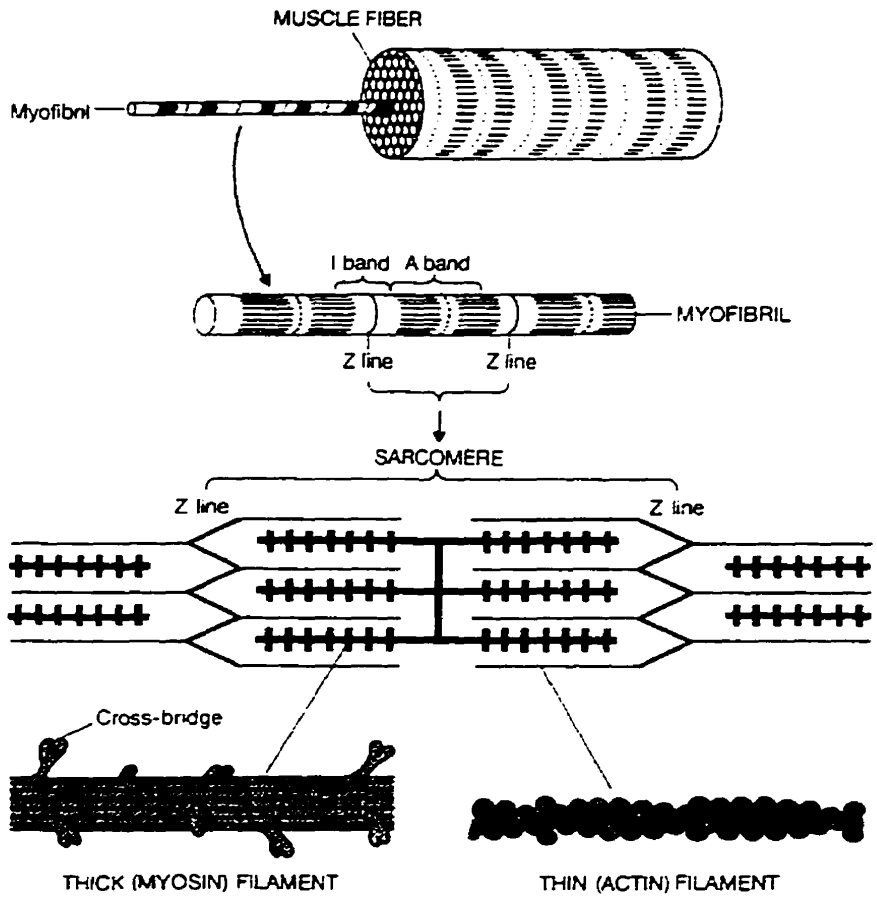

Figure 2.4: Muscle structure (from Vander[94])

2.2.2 Physiology

According to the *sliding filament theory* proposed by Huxley in 1957, thick and thin filaments slide relative to each other. Sarcomere length varies with the degree of overlap. Large heads of myosin, known as crossbridges, lie in proximity to the actin filaments in the region of overlap. The crossbridges are thought to attach onto the thin filaments and exert force by rotating through an angle of 45 degrees. As illustrated in Fig. 2.5, the crossbridges cycle through a process of attachment, rotation, detachment and reattachment. The collective effort of a huge number of crossbridges

result in the substantial force and shortening action observed in contracting muscle. Although muscle length does not change during isometric (constant length) operating conditions. force is still generated during crossbridge cycling.

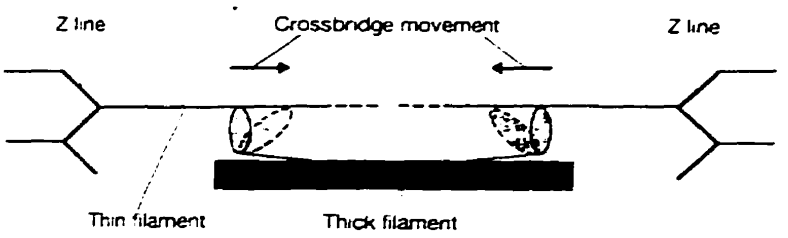

Figure 2.5: Crossbridge cycling (from Vander[94])

2.2.3 Contractile Mechanics

The forces generated by changes in muscle length are described by the contractile mechanics which have been studied in isolated muscle preparations.

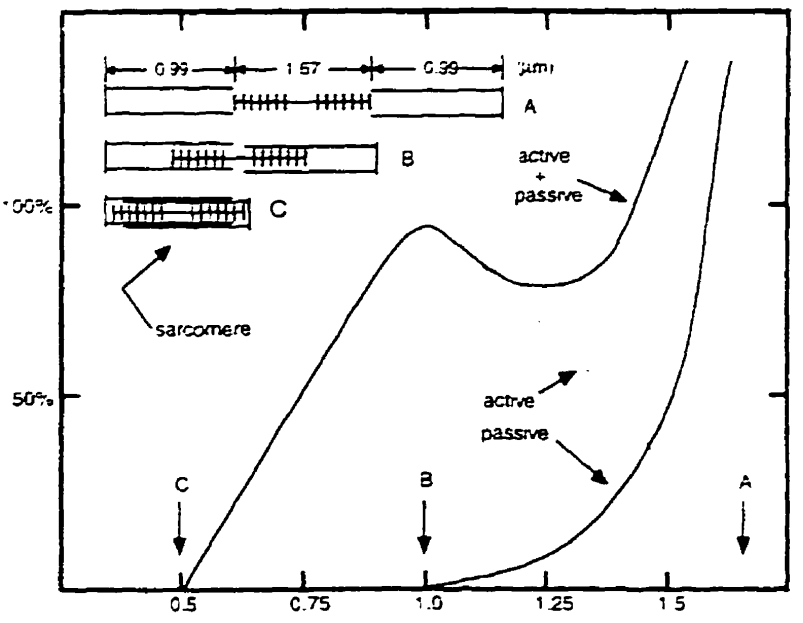

Figure 2.6: Tension as a function of length in isolated muscle (adapted from Trainor[92])

Figure 2.6 demonstrates the the non-linear passive and active length tension properties. Length is normalized with respect to the resting length. The tension corresponding to the resting length is fixed at 100%. Stretching or shortening the muscle

beyond certain limits restrict the number of possible crossbridge attachment points and consequently diminish force generation potential. It should be noted that the curve is a static interpolated relation.

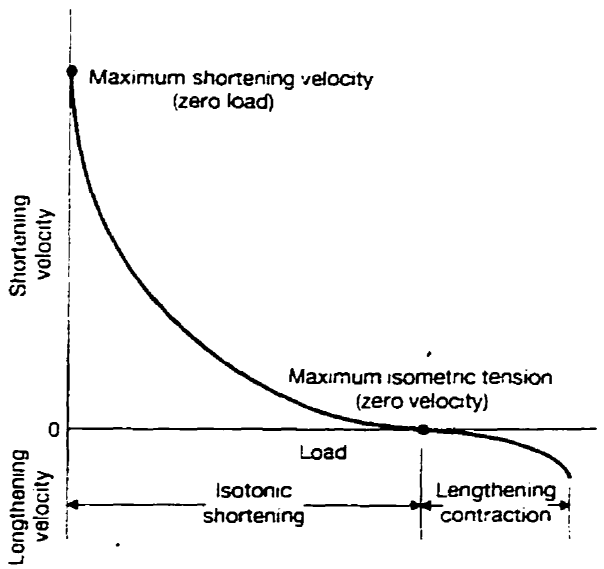

Figure 2.7: Relation between muscle tension and velocity (from Vander[94])

Shortening velocity is a non-linear function of load: as illustrated in Fig. 2.7, an actively shortening muscle produces less force than one that contracts isometrically.

Contractile muscle force thus depends on limb position as well as the rate and direction of change in limb position.

2.2.4 Activation Dynamics

Activation dynamics describe how electrical signals from the neuromuscular system relate to the force generated by the muscle. Muscle fibres are innervated near their centre by fibres arising from a single alpha (α) motorneuron originating in the anterior horn of spinal grey matter.

Neural Activation

Under steady state conditions, a potential difference of -70 mV exists across the muscle fibre and nerve membranes. Electrical or chemical stimulation, resulting in an above-

threshold membrane depolarization, causes the membrane's permeability to sodium (Na^+) ions to rapidly increase. The influx of Na^+ ions elicits a transient change in membrane potential (to +40 mV). This localized depolarization, known as an *action potential* induces local current flows in adjacent sections of the membrane and results in the generation of new action potentials. Areas that have just undergone an action potential enter a refractory state and are temporarily unable to sustain a new action potential. Action potentials consequently *propagate* along neurons at speeds ranging between 30 m/s and 120 m/s. The *frequency modulation* of action potentials is the primary means of information transmission in the neuromuscular system.

The waves of depolarization release a neurotransmitter known as acetylcholine (Ach) at synapses, which are the junctions between two neurons or between neurons and muscle fibres. The neurotransmitter causes the depolarization of adjoining nerve and muscle fibre membranes. The binding of Ach to receptors on the muscle membrane elicits waves of action potentials, propagating at 4 – 5 m/s in opposite directions, along the muscle membrane. The depolarizing wave travels along the transverse tubules to the fibre's interior and releases calcium (Ca^{++}) ions from the lateral sacs of the sarcoplasmic reticulum. The Ca^{++} ions enable the coupling of actin and myosin proteins and the consequent generation of muscle force. [72, 94]

Motor Units

The smallest functional unit of the neuromuscular system is the *motor unit.* As illustrated in Fig. 2.8, the motor unit is a group of muscle fibres, innervated by the same nerve fibre, and thus activated in near synchrony. A single muscle can contain many motor units varying in both size (2 fibres in laryngeal muscle; 2000 in the gastrocnemius medial head [8]) and speed of contraction.

Each action potential will elicit a twitch contraction within the motor unit. The twitch is a smooth increase and decrease of muscle force that last significantly longer than an action potential (see Fig. 2.9).

Each motor unit contains fibres with similar properties. Small motor units have low diameter neurons with slow conduction velocities and highly vascularized non-

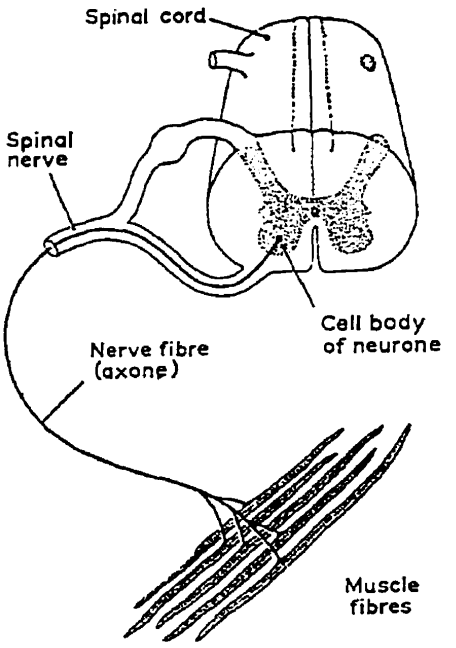

Figure 2.8: Motor unit (from Basmajian[8])

fatiguing muscle fibres capable of generating slow twitches of long duration at low force levels. Conversely, large motor units have rapidly conducting axons, produce large fast contractions and fatigue easily.

The neuromuscular system uses the dual mechanisms of **rate coding** and **recruitment** to control the force output of whole muscle. *Rate coding* refers to the adjustment of the motoneuron firing rate. If a second action potential arrives before the effects of the first action potential have expired, the resultant twitches sum to produce a larger tension. As the action potential frequency increases, a smooth sustained tension known as tetanus is eventually reached. Figure 2.10 illustrates this mechanism. Tetanus force is 2 – 4 times greater than the maximal twitch tension.

The *recruitment* of motor units is determined by the size principle. At low contraction levels, small fatigue-resistant motor units are activated first. As the force requirement increases, recruitment proceeds from the small low-force units to the large quickly-fatiguing motor units.

The relative importance of either control mechanism depends on the level of contraction and the type of muscle [56]. Muscle force is modulated primarily by firing

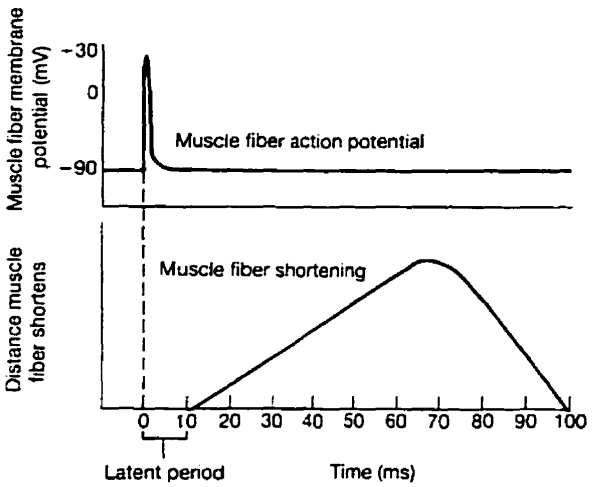

Figure 2.9: Action potential and the resulting muscle twitch (from Vander[94])

rate in small muscles and by recruitment in large muscles. There is also evidence to show that in certain muscles, recruitment is the primary mechanism at low contraction levels, while rate coding assumes importance as muscle forces increase to 70% of their maximum. [8]

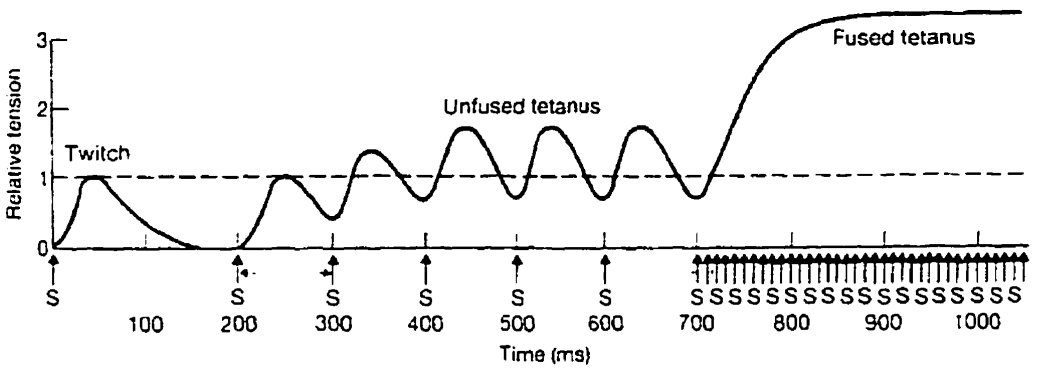

Figure 2.10: Effect of AP frequency on muscle force (from Vander[94])

EMG

Motor unit action potentials (MUAP) are manifested as changes in voltage in the skin above the muscle. The voltage change, known as an *electromyogram (EMG)*, can be detected using a surface electrode. The surface EMG represents the spatial and temporal summation of electrical activity, in a large number of motor units, filtered by the intervening skin and muscle fibre [8]. Although the EMG detected

by a surface electrode is an indirect measure of neural input to the muscle, it is convenient, non-invasive and corresponds to a substantial portion of the activated muscle.

Recorded EMG's are in the microvolt range. Since the background noise has comparable power, the EMG signal is recorded using a *bipolar electrode* configuration and *amplified differentially.* Signals picked up simultaneously are assumed to be background noise and are rejected. The common-mode signal (noise) can be reduced by using a third reference electrode that acts as a virtual ground [82].

The surface electrodes are placed in pairs parallel to the fibre direction. This configuration allows the recording of the overall activity of the muscle and minimizes the sensitivity to changes in distance between the electrode and muscle fibre.

Raw differentially measured EMG resembles zero-mean amplitude-modulated random noise. Information about muscle activation can be obtained from the signal's envelope and is thus expressed using root mean square (or standard deviation) values. EMG detection circuits usually combine full-wave rectification with low-pass filtering. The mean rectified EMG is proportional to the r.m.s. value of raw EMG provided that the EMG has a Gaussian distribution [56].

2.3 Peripheral Neuromuscular Control

The human body uses central and peripheral mechanisms to control movement and posture. Central mechanisms, involving the portion of the nervous system above the spinal cord, are responsible for command and trajectory generation, movement coordination and muscle selection. Commands originating in central mechanisms are translated into appropriate muscle forces and joint movements by peripheral mechanisms such as the previously described muscle mechanics and motoneuron activity. *Segmental reflexes* are another important peripheral mechanism [55].

Reflexes are involuntary, unpremeditated, unlearned responses to a stimulus. They are an invaluable part of the body's homeostatic mechanisms; they are compensating regulatory responses that maintain the stable conditions of the body's internal

environment [94].

The anatomy and function of a segmental reflex is embodied in its reflex arc. This consists of a sensory receptor, afferent and efferent pathways, an integrating centre and an effector. Data from these receptors are fedback through sensory neurons (afferent pathway) to the spinal cord (intergrating centre). The response, transmitted via the motoneurons (efferent pathway), is effected by the muscle fibres. Muscles are thus activated by voluntary and reflex inputs.

2.3.1 Peripheral Sensory Receptors

The two most important receptors in the peripheral nervous system are the Golgi tendon organs and the muscle spindles. They sense the body's position in space by transducing position and force information. Although the stretch receptors have cortical projections, they do not produce conscious perception of limb position kinesthesia). The relative significance of proprioceptive feedback is exemplified by the fact that the nerve fibres associated with proprioceptors outnumber the α-motorneurons. [72]

Golgi Tendon Organs

Golgi tendon organs are found in the tendon close to their junction with muscle fibres (see Fig. 2.11). These receptors are 0.8mm long and 0.5mm in diameter. They transduce muscle force by detecting tendon stretch. Since they are attached only to a few muscle fibres, they are not very sensitive to passive forces or external perturbations (which are distributed between all the muscle fibres), but are instead extremely sensitive to active muscle forces [72].

Muscle Spindles

As illustrated in Fig. 2.11, muscle spindles are fusiform capsules, 2 – 3 mm in length and 0.15 mm in diameter, embedded within the muscle. They are attached at both ends to the muscle, lie parallel to the extrafusal muscle fibres, and consequently

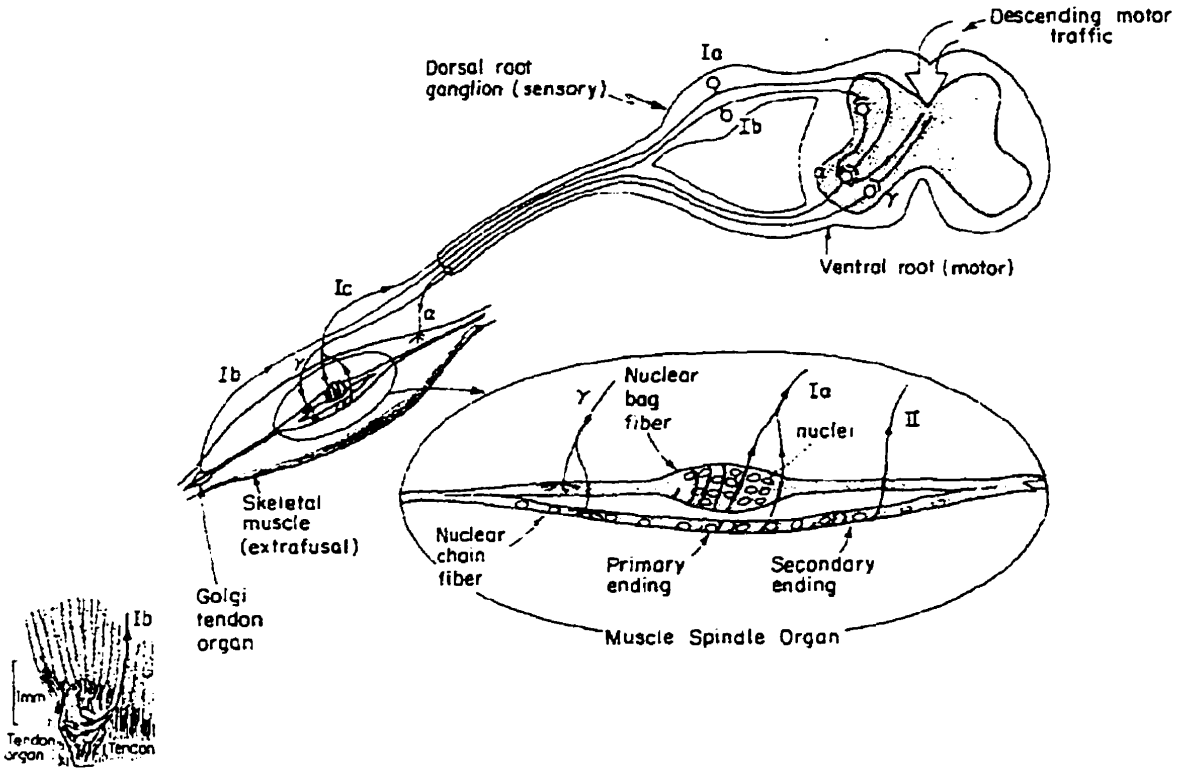

Figure 2.11: Spindle anatomy (from McMahon[74])

experience the same length change. Spindles transduce muscle length and velocity. The density of spindles in muscle ranges from 120 spindles/gram in the small finely-controlled muscles of the hand to 5 spindles/gram in the large gastrocnemius muscle [74].

The *intrafusal fibres*, which lie within the spindle, can be differentiated into nuclear bag and nuclear chain fibres. Bag fibres have closely packed nuclei at their centre and are longer and larger than the chain fibres. The latter have a single row of nuclei and their ends are attached to the bag fibres. 2 chain and 3 - 5 bag fibres are present within each spindle.

Two types of *afferent* fibres carry information from the spindles to the spinal cord. The **primary sensory fibres (Group Ia)** are large (12–20 μm in diameter) and myelinated, with unmyelinated endings coiled about the central non-contractile portions of the intrafusal fibres. **Secondary (Group II) afferents** are small (4–12 μm and terminate on chain fibres in flower-spray endings. Group Ia fibres transmit nerve

impulses at speeds ranging from 70–120 m/s. while Group II fibres have conduction velocities in the 20–70 m/s range. [72]

The afferent endings are mechanoreceptors that modify discharge rate in the afferent fibres in response to elongation. The latter is brought about by a muscle stretch or by contraction of the intrafusal fibre's contractile ends. [8]

Spindles receive *efferent* innervation through two distinct groups of **fusimotor** (γ) motoneurons which synapse onto the contractile ends of the intrafusal fibres. **Static** γ activation increases the firing rates of both primary and secondary endings when the muscle length remains constant. **Dynamic** γ activity increases the response in the primary endings during a ramp stretch of the muscle: it has no effect on the secondary endings or on the static response of the primary endings [72]. γ fibres conduct impulses at speeds of 10–50 m/s.

The primary endings are sensitive to both the static component (instantaneous muscle length) and the dynamic component (instantaneous muscle velocity) of an applied stimulus [72]. The primary endings are more sensitive to longitudinal vibration than the secondary endings. Secondary endings are not very sensitive to dynamic stimuli in the presence or absence of fusimotor activity. [15. 16. 17]

Using sinusoidal inputs. the primary afferent response to velocity inputs has ben characterised as a high-pass filter with a corner frequency of 1.5 Hz. The primary afferents are more sensitive to smaller displacements than to large amplitude stretches. The primary endings have a smaller linear range and are more sensitive to stretching than shortening. They also exhibit sensitivity to acceleration. [14. 72]

2.3.2 Peripheral Reflexes

The Tendon Jerk was first described in 1875. During the last century. researchers have proved that it is a monosynaptic reflex action originating in the primary spindle afferents. Also known as the *stretch (or myotatic) reflex*. the Group Ia - mediated response refers to the phasic contraction resulting from a brief stretch of a muscle. The stretch is detected by the muscle spindles: theGroup Ia discharge excites the α motorneurons. The reflex pathway is illustrated in Fig. 2.12. Each Ia fibre synapses

with up to 90 % of the homonymous motorneuron (MN) pool and varying portions of the synergistic MN pool. (Soleus MN's receive substantial heteronymous excitation from Ia afferents in the lateral gastrocnemius).

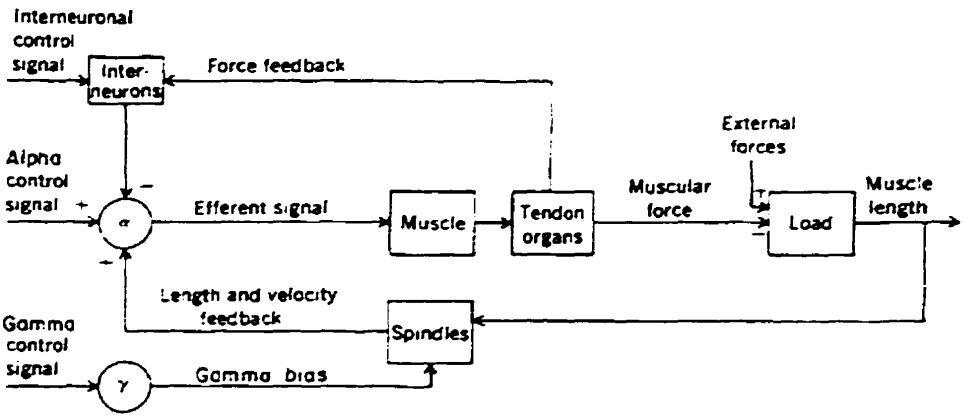

Figure 2.12: The effects of peripheral reflex mechanisms (from Brooks[14])

Several polysynaptic reflex arcs originate in the spindles and tendon organs. Although they may be functionally important, they are difficult to study.

Ia afferents are also responsible for reciprocal inhibition: a stretch in the extensor muscle inhibits flexor activation. The reflex is mediated via a disynaptic pathway [8]. Longer latency stretch reflexes such as the Functional Stretch Reflex involve trans-cortical pathways. (See section 2.6.2) for more details).

Ib afferents from the Golgi Tendon organs excite interneurons that inhibit synergist α motoneurons and facilitate antagonist α motoneurons.

Secondary afferents have fewer monosynaptic connections. The Group II neurons make excitatory polysynaptic connections with flexor α - motoneurons and possibly inhibitory polysynaptic connections with extensor α - motoneurons [8]. It is difficult to elucidate the function of group II fibres since they also originate in joint receptors and Pacinian corpuscles. Group II afferents from the latter two receptors together with group III fibres (collectively called the Flexor Reflex Afferents) mediate the crossed-extensor and ipsilateral flexion reflex responses to noxious stimuli [84].

Control Scheme

Muscles are activated by voluntary and reflex inputs. In the soma of α - motoneurons. the collective influences of the central command (size principle & recruitment). excitatory inputs from the spindle afferents. inhibitory inputs from the Golgi tendon organs and the influences from complex polysynaptic pathways are integrated. If the summation of signals is greater than the motoneuron threshold. the muscle fibres in that motor unit will contract.

During a voluntary muscle contraction. the α and γ neurons are activated simultaneously. As a consequence of α–γ coactivation. the spindle length follows muscle length and keeps the spindle sensitivity at a high level.

An axon terminal that is presynaptic to the target neuron and is postsynaptic to another pathway is termed an axo-axonic synapse. If the synapse is activated at the same time that an AP arrives at the nerve terminal. the consequent reduction in quantal content of neurotransmitter is called *presynaptic inhibition.* The decrease in synaptic potency is thought to be due to depolarization of the inhibited terminal. One nerve ending can consequently regulate the actions of another. [72. 94]

Post-synaptic inhibition. as the name implies. involves the termination of neuron pathways onto the post-synaptic portion of α motorneurons. The axons of motorneurons. while still in the grey matter of the spinal cord. give off branches called *recurrent collaterals* that synapse onto *Renshaw cells* which synapse onto the parent motoneuron and provide inhibitory inputs [74]. Figure 2.13 illustrates the action of the Renshaw cells.

Renshaw inhibition. a form of post-synaptic inhibition. can also be exerted on homonymous and synergist α motorneurons. inhibitory interneurons and on γ motorneurons [14]. Supraspinal convergence on the Renshaw cells allows recurrent inhibition to serve as a variable gain regulator at the motorneuronal level [44].

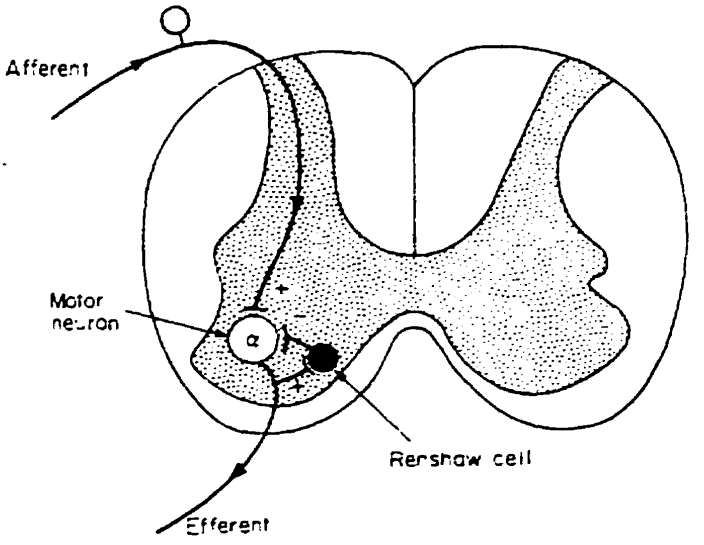

Figure 2.13: Renshaw cell (from McMahon[74])

Descending Control

Originally considered to be fixed and automatic, the stretch reflex is now known to be subject to descending control from the higher centres of the nervous system [14, 84]. Examples of reflex modulation by higher motor centres can be found in daily situations: a hot but valuable object will be placed rapidly rather than dropped.

Muscle movement is controlled by the sensorimotor cortex, a term used to refer to several regions in the cerebral cortex of the brain. Multineuronal and corticospinal pathways connect the brain and the peripheral neuromuscular apparatus.[94]. A number of centres have descending projections onto the α - motoneurons in the spinal cord. It has been postulated that they control voluntary actions and that they may alter sensitivity to reflex signals. Monosynaptic connections have been found from the brainstem to the γ motorneurons. Stimulation of many areas of the reticular formation in cats have been shown to activate γ motoneurons. This may be evidence for the supra-spinal determination of spindle sensitivity. In addition, central control has been found to modulate the effects of tendon organs via interneurons. As mentioned above, Renshaw cells are also under strong descending control from the motor cortex [44]

2.4 Ankle Joint Dynamics

In order to fully comprehend their intricacies, body movement and the maintenance of posture may be viewed in more macroscopic terms. The concept of joint dynamics defines the interactions between a joint, its associated limbs and the environment. Joint dynamics quantify the relation between the angular position of the ankle and the torques developed about it. Figure 2.15 illustrates the complexity of this relation.

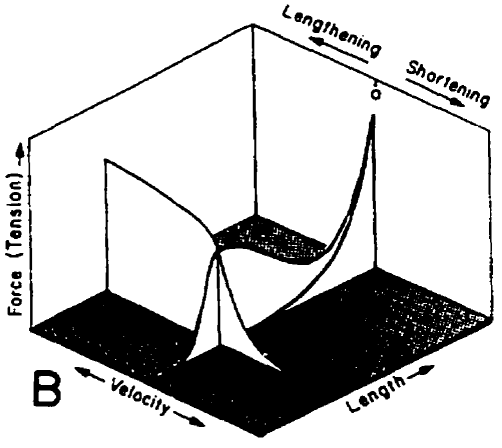

Figure 2.14: Force as a function of length and velocity (from Brooks[14])

As described before, *muscle mechanics* are influenced by crossbridge overlap and the crossbridge cycling dynamics. Under physiological conditions, muscle length and activation level will change at the same time. *Interactions* will consequently occur, since the muscle forces are influenced by joint position and velocity and controlled by rate coding and recruitment. The interaction is shown in Fig. 2.14. *Reflex dynamics* describe the muscular activities originating in the muscle proprioceptors. The basic anatomy and physiology behind these mechanisms were described in previous sections.

The *articular mechanics* involve the viscoelastic properties of joint surfaces, ligaments, and other connective tissue. Although these dynamics may be small in comparison to other contributions in the middle of an ankle's ROM, they become important near the limits [98].

The limb is considered to be a rigid body rotating about a single fixed axis; the *limb dynamics* can thus modelled as a pure inertia. In practice, joint surfaces slide

relative to each other and the centre of rotation varies with joint position.

The relation between joint position and muscle length *kinematics* is hard to determine. Muscle length is governed by the origin and insertion points and the articulation geometry. Muscle and tendon are connected in series; the length changes between the origin and the insertion are consequently the result of a cascade of muscle and tendon properties. The properties of tendon have to be accounted for.

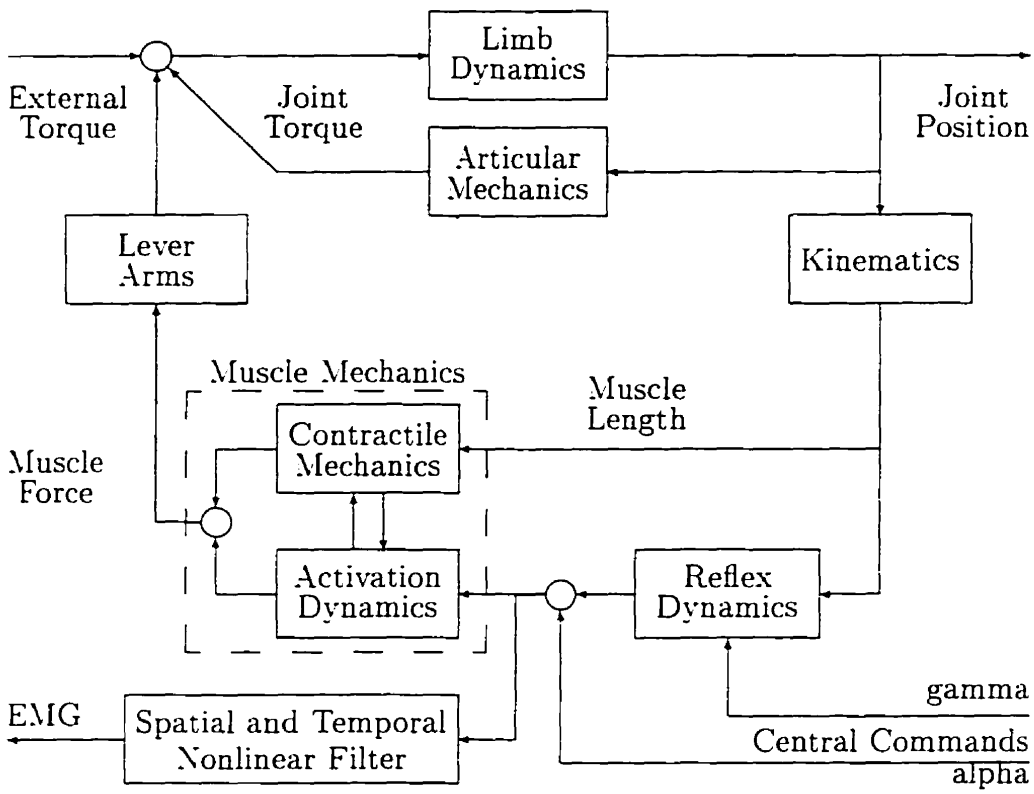

Figure 2.15: Joint dynamics (from Westwick[100])

The *external torques* caused by interactions with the environment may be unpredictable. The *relation between muscle force and torque* is determined by the lines of actions and the lever arms. However, predictions from biomechanical models are impossible to verify without using invasive procedures.

Joints are controlled by two sets of muscle generating force in opposite directions. In addition, sensory receptors make reflex connections with homonymous motoneurons as well as synergist and antagonist motoneurons. A simple symmetric structure

cannot always be assumed; assymmetry has been shown between the functions, morphologies, contractile properties and reflex behaviours of the TA muscle and the TS muscle group [59, 60, 90, 98].

The figure does omit gain modulation, via interneurons, in the α-motor command signal, as well as numerous non-spindle receptors.

2.5 System identification – ankle joint dynamics

The characteristics of the various independent subsystems and the interactions between them are difficult to determine due to experimental and ethical limitations. Position and torque are the only important signals that can be readily observed and manipulated. The EMG is an additional, indirect measure of the neural input to the muscle.

System identification deals with the problem of determining quantitative models of system behaviour through the analysis of the relationship between its inputs and outputs. It is a non-invasive means of studying the functional human being. Although no *direct* functional or structural information is provided about the system, a "black box" model can serve as a reference against which other morphological models can be validated [100].

2.5.1 Systems Approach

To gain knowledge of a system is to formulate a mathematical description of it. One needs to identify an analytical model that is detailed, quantitative and capable of predicting system behaviour under general conditions.

As is the case in human joint dynamics, the system is not well understood and too complex to model from a priori knowledge. Consequently, it is necessary to develop empirical non-parametric models from the input-output experiments. A non-parametric model does not make any assumptions about the system structure.

Joint dynamics system identification has been performed by perturbing the joint with a stochastic signal. A model identified using a sufficiently rich stochastic in-

put is theoretically capable of predicting the response to any arbitrary input signal. The model's efficacy was obtained by comparing its predictions with experimentally observed data.

Based on the sensitivity to measurement noise in the inputs and outputs, the optimal experimental technique has been to drive the system with a desired wide-band position input and record the resulting torque response [62]. The ankle joint was driven by a position controlled actuator stiff enough to remove the feedback path between the stretch reflex and joint position. Another assumption used to simplify the identification procedure is that there is a minimal interaction between the activation and passive dynamics [81].

A model explains reality only when all the assumptions of the methodology are satisfied. One must know how deviations from the assumption will affect the model's inferences [75]. It has been assumed that the process of identifying the model, by stochastically perturbing the system, does not alter the system itself. However, as developed in later sections, the use of stochastic perturbation may alter the system.

2.5.2 IRF Estimation

A linear system can be specified by a parametric or non-parametric linear filter. An *impulse response function* (IRF) is a non-parametric vector representation of a system in the time domain.

$$Y(t) = \int_{-t_{max}}^{t_{max}} h(\tau).X(t-\tau)d\tau \tag{2.1}$$

The IRF, $h(\tau)$, is best understood within the context of an input-output equation (see Eqn. 2.1); convolving the input, X, with the IRF yields the output, Y. Unlike causal physical systems, biological systems can exhibit anticipatory or predictive behaviour and are consequently represented by a 2-sided IRF. The latter is determined using the input auto-correlation function and the 2-sided cross-correlation function, as shown in [49]. The algorithm accounts for the spectral characteristics of the input. The estimated IRF minimizes the sum of squared differences between the actual and

predicted outputs. The simple form of an IRF does not imply simple responses.

Actuator and Fixation Dynamics

In order to perturb the ankle joint, the foot must be attached to the perturbing actuator. The ideal fixation should have an infinite stiffness and zero inertia while providing a secure attachment between the actuator and the limb. In reality, the effect of the fixation device on the observed dynamics must be considered in addition to the dynamics from the finite stiffness and the non-zero inertia of the actuator and fixation device.

2.5.3 Quasi-Linear Techniques

System identification has been used extensively to describe the joint dynamics in the neck, elbow[31], wrist, ankle[62] and knee[91]. Linear dynamic models describe the joint dynamics well, provided that operating conditions remain relatively constant. Research conducted in our lab has focused on identifying the dynamic stiffness of the ankle.

Ankle stiffness, defined as the *dynamic* relation between ankle position and torque, was found to be well described by a simple second-order quasi-linear model having inertial (I), viscous (B) and elastic (K) parameters [62] :

$$TQ(t) = I(\lambda)\frac{d^2\theta(t)}{dt^2} + B(\lambda)\frac{d\theta(t)}{dt} + K(\lambda)\theta(t) \tag{2.2}$$

where TQ and θ are the torque about and the angular position of the ankle joint respectively, t is the time, and λ defines the operating point.

The equation can be expressed in the Laplace domain as a *stiffness* transfer function :

$$\frac{TQ(s)}{\theta(s)} = Is^2 + Bs + K \tag{2.3}$$

The transfer function is a frequency-domain representation of the system dynamics. If X and Y (in Eqn. 2.1) were replaced by θ and TQ, the transfer function shown

in Eqn. 2.3 is merely the Fourier Transform of the IRF, $h(\tau)$.

Another formulation commonly used to discuss second-order linear dynamics is shown below. The ratio of angular position to torque is known as *compliance*; it is the inverse of the stiffness transfer function :

$$\frac{\theta(s)}{TQ(s)} = \frac{G\omega_n^2}{s^2 + 2\zeta\omega_n s + \omega_n^2} \tag{2.4}$$

where G, ω_n and ζ are the static gain, natural frequency and damping parameter respectively. G specifies the magnitude of the response, ω_n determines the length of the response and ζ expresses the nature of the system oscillation.

Changes in the operating conditions were shown to affect the mechanical characteristics of the ankle joint. The **joint position** and **muscle activation level** were found to have particularly strong effects. Passive ankle joint dynamics are constant over the middle of the ROM but the elastic parameter increases sharply at the limits of the ROM. Active contraction causes a linear increase in K if mean position is held constant. The two effects appear to be independent. Incremental effects of active contraction show little dependence on mean joint position. [46, 96, 97, 98]

The increase in the elastic parameter was accompanied by an increase in the viscous parameter. This translates into an increase in the natural frequency and low frequency gain of the stiffness dynamics. However, the damping parameter remained constant. The invariance of ζ indicates that the shape of the transient response (IRF) remains constant, while the amplitude and time scale of that response change with the level of muscle contraction and the angular position of the joint.

Increasing the **displacement amplitude** of the input perturbation (desired position signal) caused a decrease in the elastic and viscous parameters. Stiffness was found to decrease rapidly as amplitudes increased from 0 to 0.05 rad. The rate of decrease declined at higher amplitudes[58].

Quasi-linear models have also been used to describe the relation between EMG and ankle torque defined as the ankle muscle activation dynamics. The relation was well-described by a second-order low-pass transfer function, whose parameters depended

on the contraction characteristics and muscle length [37].

The efficacy of the identification procedure was measured by computing the percentage of the output variance that was accounted for by the model (%VAF) :

$$\%\text{VAF} = 100 \times \left(1 - \frac{V_{obs} - V_{pre}}{V_{obs}}\right) \tag{2.5}$$

where V_{obs} is the variance of the observed output and V_{pre} is the variance of the predicted output.

The models described above generally accounted for 80 - 90 % of the output variance. The %VAF was not affected by changes in the operating conditions.

The squared coherence between the measured and observed outputs was used to describe the *frequency range* where the model components accurately described the model output [62]. The coherence squared function between an input, x, and an output, y, is defined as :

$$\gamma_{xy}^2 = \frac{|S_{xy}|^2}{S_{xx}S_{yy}} \tag{2.6}$$

where S_{xx} and S_{yy} are the input and output power spectra and S_{xy} is the input-output cross spectrum.

An ensemble of linear models obtained for different sets of operating conditions can thus be used to define a quasi-linear model of joint dynamics.

2.5.4 Time-Varying Identification

Joint dynamics can change considerably in a short period of time; the changes occur on a time-scale comparable to the system's dynamic response. In order to characterize ankle joint mechanics during non-stationary time-varying conditions, a non-parametric ensemble-based method was developed by MacNeil et al [70]. The technique uses singular value decomposition to obtain the least-squares estimate of the time-varying IRF from an ensemble of statistically independent input-output realizations having the same time-varying behaviour.

Ankle stiffness dynamics were investigated during a rapid voluntary isometric

contraction [70]. There was a decrease in low-frequency (0.6 Hz) stiffness during the transient increase in joint torque. During the contraction, the dynamics could not be adequately described by a linear second-order model. Similar findings were reported when time-varying studies were used to examine an electrically-evoked twitch contraction of the TS muscle group [92]. The ankle stiffness dynamics had to be described by higher-order models during the twitch.

2.5.5 Non-Linear Identification

Although ankle dynamics can be summarized using sets of quasi-linear models, one must realize that the overall joint dynamics are *non-linear* and may involve multiple inputs. Traditionally, Wiener or Volterra functional expansions were used to describe non-linear dynamics. The structure of certain systems could be obtained from the analysis of the first and second order kernels. However, these techniques are generally unusable because of problems with the input. Westwick provides an excellent description of current (and previous) techniques in non-linear single- and multiple-input system identification [100].

Empirical nonlinear models have also been developed to explain stretch reflex dynamics. The evolution of these models, in the context of other attempts to characterise reflex dynamics, is discussed in the following section.

2.6 Stretch Reflex Dynamics

Overall dynamic joint stiffness is determined by contributions from passive, intrinsic and reflex mechanisms. Elucidating and understanding the reflex portion would not only contribute to the development of a better dynamic model but would also aid in explaining the functional role of the stretch reflex.

Passive stiffness is related to the properties of the joint articulation, connective tissue and limb inertia. The intrinsic properties arise from the contractile apparatus (non-passive portion) of the muscle. The reflex contribution is due to the muscular activity that originates in the muscle spindles.

The stretch reflex has been studied in a wide variety of muscles. Traditionally, the reflex has been quantified by measuring changes in EMG or torque resulting from externally applied position or torque inputs or by using the electrically stimulated H-reflex, an indirect analogue of the stretch reflex. The following section summarises the various reflex identification attempts: it concludes with a review of what is known about the stretch reflex at the human ankle.

2.6.1 H-reflex

The Hoffmann-reflex is a brief muscular contraction elicited by the electrical stimulation of afferent nerves from the muscle. It is a monosynaptic reflex which, from the point of stimulation on, uses the same pathways as the tendon jerk. The H-reflex is used as a convenient, albeit unphysiological, means of studying stretch reflex function. However, it is impossible to draw conclusions from H-reflex studies alone since the reflex ignores spindle activity [19].

2.6.2 Transient Stimuli

Transient stimuli such as ramps and pulses (used to approximate ideal steps and impulses) have been used extensively to study reflex mechanisms. They correspond to disturbances encountered in functional situations and provide direct insight into system behaviour without requiring the assumption of linearity [62].

EMG studies

Researchers have extensively studied the stretch reflex by stretching a muscle and measuring the changes in EMG. The muscles under study have been stretched in a variety of ways. In the case of the TS muscle, this has been achieved by direct stretching of the calcaneous tendon (in mesencephalic cats)[3], tapping the Achilles tendon[1], and by rapidly displacing the foot.

The application of a ramp change to the ankle position [6, 10, 57] generated a synchronous burst of EMG in the stretched muscle after a short latency. The EMG

response, dubbed the *monosynaptic stretch reflex* (MSR), was found to be strongly dependent on the velocity of the stretch, suggesting the importance of the primary spindle afferents.

Gottlieb and Agarwal (1979) used torque perturbations and found that reflex EMG in soleus and gastrocnemius were well correlated with joint velocity [39]. The gain, defined as the relation between the reflex EMG and velocity, was linearly proportional to the level of tonic voluntary activation.

Other studies have revealed the presence of a long-latency reflex named the *functional stretch reflex* (FSR). The FSR, whose presence can be explained using segmental mechanisms alone [54], is a preprogrammed *voluntary response* triggered by kinesthetic stimuli [10, 24]. Requesting the subject *not* to resist the applied stretch eliminates the evocation of the FSR [57].

Torque Studies

The EMG is an indirect measure of the mechanical consequences of the stretch reflex. It is difficult to relate EMG changes to muscle force due to the nonlinear activation dynamics and their complex interaction with contractile mechanics. Hoffer and Andreassen observed differences between the reflex EMG response and the resulting torque [42]. Researchers have consequently attempted to measure the reflex torques directly, after applying ramp stretches. However, one must separate the reflex torque responses from those originating in the intrinsic mechanisms.

One method, performed on animals, involved the surgical removal of the afferent signals from the muscle spindles. The stretch reflex in the neck muscles of monkeys were studied after the section of cervical dorsal roots [11]. Nichols and Houk similarly transected dorsal roots to study the response to ramp displacements in decerebrate cats [79]. Hoffer and Andreassen removed reflex effects by inducing deep anaesthesia (using halothane gas) in pre-mamillary cats [42]. Differences in the muscle response with and without afferent feedback were attributed to reflex function.

The deafferentation has also been performed indirectly in humans: electrical stimulation was used by Sinkjaer et al to suppress stretch reflex and voluntary activity

[85, 86]. In certain subjects, the stimulation tended to be painful, elicited muscle spasms and caused problems with co-contraction. Carter and colleagues used a similar technique to investigate the response to ramp displacement stretches of the first dorsal interosseus muscle [23]. The protocol required instructing subjects to "relax" - a procedure that is not always tenable[3]. Allum et al (1984) employed ischaemia and tendon vibration to temporarily reduce reflex activity [5].

Less obtrusive procedures have exploited the nerve conduction delay inherent in all reflex pathways to separate reflex and intrinsic responses. A series of seminal experiments by Kearney and Stein [90] used rapid, small-amplitude pulse displacements to briefly stretch the TS muscle group. The brief duration of the perturbation ensured that the intrinsic response ended before the reflex response commenced. The reflex contribution was seen to be highly nonlinear and dependent on the duration, direction and amplitude of the pulse displacement in addition to the angular position of the ankle and the level of muscular contraction.

Inadequacies of transient stimuli

All of the above studies have looked at the reflex responses to a particular perturbation. These responses cannot be generalized to predict the effect of other inputs: they present a measure of the system's output and provide indirect information about the underlying reflex mechanisms. Transient stimuli do not explore the full range of frequencies encountered during functional situations[4]. The transient response depends upon the stimulus displacement trajectory and is affected by the actuator's dynamics.

Static vs. Dynamic Reflex Stiffness

Transient stimuli provide a static measure of the reflex stiffness. Although they provide some pertinent information, static measures do not fully characterise the dynamics of a system.

[3] especially in spinal cord injury, cerebral palsy or stroke victims

[4] perturbations resulting from a heel strike during normal gait have a bandwidth up to 75Hz [7]

Sinusoidal stimuli

Joyce and colleagues (1974) investigated reflex dynamics at the elbow using sinusoidal perturbations [52]. They relied on the reflex conduction delay to separate the reflex and intrinsic contributions; components of the mechanical response whose phase varied with frequency were regarded as being reflex in origin. A similar approach was used to investigate reflex mechanics at the human jaw[26], thumb[18], and ankle[36].

The downfalls of sinusoidal perturbation include the presence of voluntary responses to predictable stimuli and the evocation of non-linearities due to phase locking [62]. In addition, they are inadequate for exploring nonlinear relations when stimuli having more complex frequency structures are used [81].

2.6.3 System Identification

Studying reflex stiffness using a black-box systems approach, as mentioned in section 2.5.1, generates a more complete explanation of the reflex mechanisms. The approach enables the noninvasive study of functional human subjects. Perturbing the system with a wide-band stochastic input allows the study of the system dynamics over a large frequency range in a relatively short period of time. The use of a stochastic input also allows for the easy removal of the effects of the input waveform and the actuator dynamics [62]. In addition, stochastic perturbations eliminate voluntary mechanisms such as the FSR [59].

Quasi-stationary techniques

Stochastic torque inputs were used by Dufresne et al(1979) to study the relation between motor activity and angular position at the human forearm. A linear combination of position, velocity and acceleration terms with different delays modelled the rectified EMG [32]. The data suggested that the short-latency reflex response was primarily velocity-sensitive. Bennet et al (1992) used pseudo-random torque disturbances to study the mechanical properties of elbow joints [9].

Attempts to identify the ankle reflex dynamics at specific operating points, have

been made using non-linear non-parametric techniques. The dynamic relation between ankle velocity and TS EMG was identified by perturbing the ankle with a stochastic position displacement, while the subject maintained a steady TS contraction. The best VAF estimates (approximately 70% with 25 averaged trials) were obtained when a directionally-dependent velocity-sensitive non-linearity (half-wave rectifier) was added in series prior to the linear IRF in the dynamic model. The IRF was dominated with a large peak at 40ms; this was interpreted as velocity feedback via a pathway with a 40ms delay. Increasing the tonic activity (as measured by EMG) increased the reflex gain (as observed in the IRF amplitude). In addition, the IRF amplitude decreased when the peak–to–peak amplitude of the stochastic input was increased[59]. Dorsiflexion increases TS stretch reflex magnitude, but has no effect on the IRF shape or the reflex latency. Plantarflexion has no effect on the TS reflex magnitude. [99]

A similar study for the TA stretch reflex yielded an IRF with two excitatory peaks at delays of 40ms and 70ms. The effects of modulating the peak-to-peak amplitude of the input position signal and the level of muscular contraction were similar to those for the TS muscle group. The 2 peaks were attributed to two velocity feedback pathways, the action of secondary spindle afferents or the mediation of the primary spindle afferents by long-latency pathways. The presence of a directionally-dependent non-linearity did not improve VAF estimates. [60]

The systematic development of a non-linear model of TS stretch reflex dynamics using Wiener kernel analysis suggested a cascade structure with a Hammerstein configuration [61]. A static non-linearity in series with linear dynamics and a pure delay provided an adequate estimate of the TS stretch reflex dynamics during stationary conditions. Using a higher-order polynomial in the place of the half-wave rectifier did not increase the model VAF.

Time-varying conditions

Ensemble-based time-varying techniques, mentioned in section 2.5.4, were used to study the stretch reflex dynamics during a rapid voluntary isometric contraction[69]

and during a rapid imposed stretch[68] of the TS muscle group. The dynamic relation between half-wave rectified ankle velocity and TS EMG was used to measure the reflex dynamics. Although the reflex dynamics remained constant during the *voluntary contraction*, the reflex gain covaried with the average EMG.

During and for a brief time after the *imposed stretch*, the reflex magnitude decreased substantially. However, the decrease in the EMG was moderate, suggesting that peripheral mechanisms had an increased importance after an externally applied stretch.

Parallel-cascade techniques

Parallel-cascade techniques were developed to completely characterise ankle stiffness.

Perreault developed a parallel-cascade structure that combined the elements of the Hammerstein cascade with the delay inherent in the reflex pathway [83]. The structure consisted of a pre-reflex linear pathway, a pre-reflex non-linear pathway to account for large amplitude non-linearities and a reflex pathway. The pre-reflex components were assumed to decay quicker than the reflex latency. The reflex dynamics were estimated in two stages. The linear estimated between half-wave rectified ankle velocity and reflex EMG were used to identify the reflex latency. The EMG–torque dynamics were estimated after subtracting the torque, due to the short-latency passive mechanisms, from the total ankle torque.

Reflexes were found to be of great importance in the 3–15Hz frequency range. The non-linear parallel-cascade technique used in this thesis, and presented in section 3.1, incorporates many of the features of the Perreault model. The uniqueness of the Perreault model lies in its ability to identify both the reflex and intrinsic contributions to ankle joint stiffness under dynamic conditions using the powerful techniques of system identification.

2.6.4 Effect of Vibration

High-frequency (50–150Hz) vibration of the tendon and muscle belly results in a slowly developing muscle contraction known as the *Tonic Vibration reflex* (TVR). The reflex probably involves monosynaptic and polysynaptic pathways and requires descending facilitation. A similar, though smaller, contraction can be evoked by vibrating cutaneous receptors. The TVR cannot be recorded in the lower limbs of paraplegics. It is also possible to voluntarily prevent the reflex contraction. [41, 72, 84].

When the joint is held isometrically, vibration results in illusions of movement [2, 72].

Often termed the vibration paradox, high-frequency vibration is also known to inhibit the stretch reflex. Vibration of the Achilles tendon decreases the magnitude of the Triceps Surae reflex EMG response to a ramp displacement of the ankle [2, 10]. The degree of inhibition of the TS myotatic reflex was shown to be directly proportional to the vibration frequency [2]. Another study discovered that the Soleus H-reflex inhibition was directly proportional to the vibration amplitude and inversely proportional to the vibration frequency [28].

The inhibition of reflexes originating in proprioceptive volleys is generally attributed to pre-synaptic effects.

2.6.5 Reflex Modulation with Behaviour and Movement

The magnitude of the stretch reflex has been shown to change during a number of behavioural tasks; the modulation seems to depend upon the task performed and the instructions given[5]. Doemges and Rack (1992) demonstrated that the long-latency reflex EMG responses at the first dorsal interosseus muscle[29] and in the wrist[30] were different if the subject was asked to maintain a constant position instead of a constant force.

In decerebrate cats undergoing locomotion induced by stimulation of the mesen-

[5]see references in [69]

cephalic motor region, the stretch reflex was found to be deeply modulated during the step cycle [3]. Similar variations were seen in high decerebrate cats suspended above a treadmill [89].

The monosynaptic component of the spinal reflex, often considered to be a fixed and stereotyped action, can be modulated greatly during voluntary activity in humans. Gottlieb and Agarwal (1973,1980) found that the H-reflex was greatly inhibited during voluntary muscle stretch and facilitated during muscle shortening [38] and inferred that descending control modulated the reflex response to a sudden torque during a phasic contraction at the ankle [40].

Experimenters have examined the reflex response during more complex coordinated movements. The magnitude of spindle - mediated responses are modulated considerably during different phases of locomotion. This modulation is thought to be due to changes in gamma drive and changes in the state of interneurons regulating spinal reflex arcs originating in the peripheral receptors.

For a given starting muscle length, and perturbation magnitude, different stretch responses can be evoked in the TS in different postural conditions (reviewed in [88]). The adaptive non-sterotyped changes are tailored towards maintaining a stable posture.

Capaday and Stein (1986) observed that H-reflex magnitude was heavily modulated during the walking cycle, in a manner related to the soleus EMG. The H-reflex was strongest during the stance phase (where they would assist posture maintenance) and weakest during the swing phase (where they would interfere with ankle flexion)[20]. Yang et al also noted that H-reflexes were more pronounced later in the stance phase, when the body needs to be propelled up and forward[101].

For a given stimulus strength and EMG level, the reflex response was much larger while standing than during walking. When the experiments were extended to running trials, a similar modulation of reflex magnitude was observed; the relation between reflex and EMG level was different for the different task of walking, running and standing. The H-reflex gain was lowest during running and highest during walking. [88]

Similar results were obtained by Brooke et al in their investigation of the soleus H-reflex through the course of a stationary pedalling cycle [12]. Reflex magnitudes were largest during the power-producing phase and near zero near the recovery phase. For the duration of cycling, H-reflexes, were attenuated during movement (as compared with sitting). McIlroy and colleagues extended the findings; they discovered that increasing the speed of passive rotation proportionately decreased the reflex gain [73]. Taken a step further, experiments by Collins et al demonstrated that passive rotation inhibited H-reflexes in the contralateral leg in proportion to the rotation velocity [25].

Stein and Kearney (1995) reported that an on-going passively applied stochastic perturbation decreased the reflex torque and EMG response to a brief displacement pulse in the TS [90]. The reflex attenuation was noted to increase with both the peak-to-peak amplitude and bandwidth of the stochastic perturbation.

2.6.6 Functional Role

Polysynaptic reflex pathways seem to be under adaptive control; inputs to interneurons can be changed to adapt the system structure to the task in question. On the other hand, elucidating the role of the *monosynaptic* stretch reflex has remained elusive in spite of the intrinsic simplicity of the reflex arc.

A number of theories have been proposed to explain stretch reflex function [55]. Stretch reflexes were originally seen as a means of controlling muscle length (Merton). α–γ coactivation seems to suggest the servo-assistance model which proposes that spindle response to the error between the intended movement and the actual movement (Matthews and Stein).

Nichols and Houk noted that during a muscle stretch, the reflex response was large and the mechanical (intrinsic) response was small; the opposite behavour was observed with muscle release [79]. Houk consequently eschewed the servo-regulation models for one that incorporated feedback from the Golgi tendon organs and stabilized muscle stiffness [43]. Allum et al concurred, stating that, the stretch reflex modifies joint stiffness by regulating muscular contraction in response to changes in position

or force[6]. Hoffer and Andreassen found that static stiffness was well regulated for forces over 25 % of the maximum in premammillary cats [42].

Note that these experiments all use a static (and therefore incomplete) measure of muscle stiffness. The static stiffness is defined as the force change for a given position change. Optimally, static stiffness describes the effect of position changes but does not account for velocity and acceleration. (Recall that reflex EMG responses are generally velocity-sensitive).

Although Carter and colleagues noted that the stretch reflex compensates for the inherently non-linear intrinsic properties of muscle; they observed that the total stiffness was not regulated to a constant value independent of the initial torque level [23]. Akazawa et al observed that stiffness covaried with stretch reflex magnitude, with maximum levels experienced during the stance phase, and suggested that the reflex assisted in load compensation [3]. A number of other studies have yielded results that conflict with the stiffness regulation hypothesis [26, 29, 30].

None of the theories can consistently stand up to experimental testing [89]. The apparent modulation with ongoing movement confounds the issue.

Nevertheless, the importance of the MSR cannot be overlooked. They can produce a significant amount of force acting to resist muscle stretch and can make a large contribution to the overall joint stiffness. A recent study by Yang et al (1991) estimated that 30 - 60 % of the EMG generated in the soleus during the normal walking cycle arises reflexively [101].

2.6.7 Reflex Behaviour - Triceps Surae

Although the functional role remains a mystery, the large number of studies performed have generated an immense body of information on the stretch reflex. The following summarises a few pertinent details about reflex behaviour in the gastrocnemius and soleus muscles at the human ankle joint.

The stretch reflex is much larger in the TS than in the TA. The TS stretch reflex occurs at a latency of about 40–45ms after the beginning of the stretch. [90]. Linear dynamics can be identified between half-wave positively-rectified velocity and TS

EMG. Remember that a positive direction is assigned to plantarflexing motion. Thus positive velocities refer to movements that stretch the TS [61].

Reflex EMG and torque evoked by a brief displacement *increase* with the displacement velocity [10, 39, 59, 90]. Dorsiflexing the ankle, or pre-stretching the TS muscle group *increases* the reflex magnitude [90][99]. Increasing the level of voluntary muscular activation *increases* the reflex EMG and torque response to a brief pulse stretch magnitude [90]. A similar effect was noted for the reflex-activation dynamics (relation between ankle velocity and reflex EMG) [59, 69, 76]. Using the parallel-cascade model, reflex-stiffness dynamics (relation between ankle velocity and reflex torque) were observed to *decrease* in magnitude with an increase in the voluntary contraction [76], suggesting that reflex mechanisms are more significant at low contraction levels.

Active and passive movements strongly modulate the magnitude but not the dynamics of the stretch reflex [68, 69]. Increasing the peak–to–peak amplitude of the applied stochastic input *decreases* the magnitude of the IRF describing the reflex dynamics [59]. A passively superimposed perturbation appears to *decrease* the reflex magnitude [90]. The magnitude of stretch reflex dynamics decreased for a brief period (100ms) after a passively imposed stretch [68]. Similar behaviour was noted with H-reflex studies [10]. The response to a brief pulse increased as the pulse duration increased indicating that a previously applied plantarflexing motion can affect the reflex response to a dorsiflexing stretch [90].

2.7 Rationale

Additional work is needed to fully characterise the stretch reflex and understand its role in posture and movement. Although numerous studies have investigated the stretch reflex under static conditions, they present an incomplete measure of the reflex action. Stochastic system identification techniques appear to be promising in their ability to elucidate the dynamic reflex contribution to the overall mechanical characteristics of the joint.

It has been demonstrated that stretch reflexes and the analogous H-reflexes are

modified during cyclical movements, after externally applied stretches and during stochastic perturbations. The inputs used in system identification may alter the reflexes that they are attempting to measure.

This project investigates the effect of externally applied passive movements on the stretch reflex in the Triceps Surae muscle group. The study looks at the variation in the reflex dynamics identified using the parallel-cascade model (described in section 3.1) and in the reflex response to a brief pulse. An attempt is made to discover which of the kinematic parameters of the externally applied perturbation are responsible for the modification of the stretch reflex.

Chapter 3

Methods

The stretch reflex behaviour of the ankle joint was investigated by rapidly and precisely moving the left feet of healthy human subjects with the aid of a servo-controlled rotary actuator. The angular position of the ankle, considered to be the input to the system, was manipulated using various stochastic and deterministic perturbations. The resulting torque and EMG responses, in conjunction with the input position record, were used to extract information about the system. The experiments were performed in 2 stages: the effect of passive movement on reflex dynamics were investigated first. The second part studied the attenuation of reflex responses, to a transient stimuli, using stochastic perturbations with different amplitude and frequency characteristics.

This chapter begins with a description of the non-linear system identification techniques used to distinguish between reflex and passive components of ankle joint dynamics. The experimental apparatus and techniques are subsequently detailed. Special emphasis is given to the "boot" used to fix the ankle to the actuator and to the different stochastic perturbations used to elucidate the kinematic parameters responsible for stretch reflex attenuation.

3.1 Parallel Cascade Model

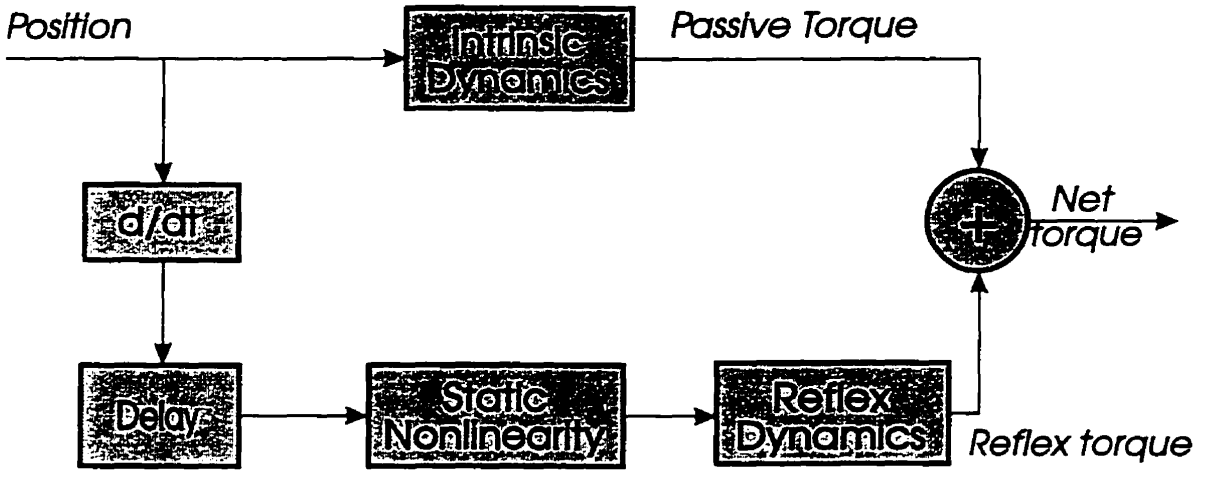

Figure 3.1: Parallel cascade

The *parallel cascade* model, shown in Figure 3.1 is the latest in a series of attempts[1] to determine the reflex dynamics using system identification techniques. The model, which has been outlined elsewhere[66], is based on a parallel-cascade model used by Perreault et al[83].

The model consisted of a linear pathway describing the position-dependent *intrinsic dynamics*, and a non-linear pathway describing the velocity-dependent *reflex dynamics*. This allowed for the differentiation of intrinsic and reflex mechanisms while identifying the overall joint dynamics between angular position and torque.

Overall ankle torque was expressed as the sum of the *voluntary torque* and the *net torque*, TQ_N. The voluntary torque, due to the constant tonic contraction exerted by the subject, was numerically removed during the IRF estimation procedure. TQ_N had two components : intrinsic torque, TQ_I, and reflex torque, TQ_R.

$$TQ_N = TQ_I + TQ_R \tag{3.1}$$

A Hammerstein identification procedure [61] was used to estimate the reflex activation dynamics between ankle position and reflex EMG. These were modelled as

[1] section 2.6 on page 28

a differentiator in series with a delay, a static nonlinear element, $n_{RS}(.)$ and a dynamic linear element, h_{RS}. The resulting IRF gives a measure of the reflex pathway's conduction delay.

The intrinsic dynamics were estimated using an IRF, $\hat{h_{IS}}$, relating the position to the torque. The length of the IRF was fixed to be smaller than the reflex conduction delay. Since the torques due to reflex dynamics were prevented from influencing the intrinsic dynamics, the two mechanisms can be effectively separated. An estimate of the intrinsic torque, $\hat{TQ_I}$, was obtained by convolving the input position, P, with $\hat{h_{IS}}$.

$$\hat{TQ_I} = \hat{h_{IS}} \circledast P \tag{3.2}$$

The intrinsic residual torque, TQ_{IR}, was computed as shown in Eqn. 3.3.

$$TQ_{IR} = TQ_N - \hat{TQ_I} \tag{3.3}$$

Estimates of $\hat{n_{RS}}(.)$ and $\hat{h_{RS}}$ were identified using a Hammerstein procedure with ankle velocity (obtained by numerically differentiating P) and intrinsic residual torque, TQ_{IR}, as the input and output respectively. The identified Hammerstein model was subsequently used to estimate the reflex torque, $\hat{TQ_R}$. From previous results[61], the static nonlinearity has been shown to resemble a half-wave rectifier with a gain near 0 for negative (plantarflexing) velocities and a gain close to 1 for positive (dorsiflexing) velocities.

The percentage of variance in the net torque accounted for by the model ($\%VAF_N$) was calculated using Eqn. 3.4.

$$\%VAF_N = 100 * \left(1 - \frac{\sum_1^l (TQ_N - \hat{TQ_I} - \hat{TQ_R})^2}{\sum_1^l (TQ_N)^2}\right) \tag{3.4}$$

where, l is the length of the data record.

$$TQ_{RR} = TQ_N - \hat{TQ_I} \tag{3.5}$$

The reflex residual torque, TQ_{RR}, calculated as shown in Eqn. 3.5, were used as

the output in re-estimating $\hat{h_{IS}}$. The whole estimation procedure was repeated until, successive iterations did not improve the $\%VAF_N$.

3.2 Apparatus

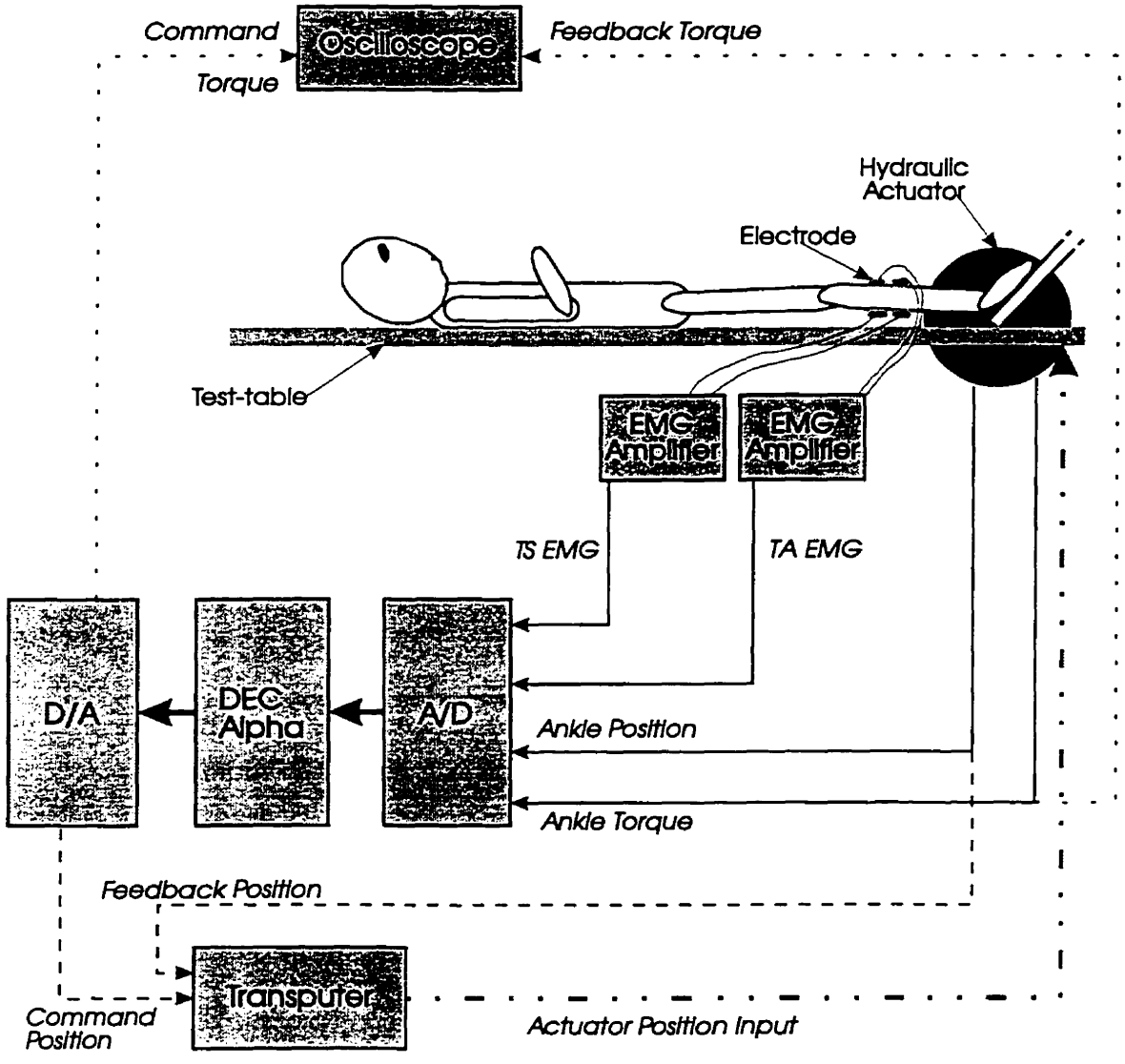

Figure 3.2: Experimental setup

Fig. 3.2 illustrates the experimental apparatus used to perturb the ankle joint. The subject lay supine on a test-table[63], with their left foot attached to the ankle actuator by means of a fibre-glass boot. A wide strap and sandbags were used to secure the the left leg to the table. The following section details the layout of the ankle actuator

and the ankle fixation device (boot) in addition to the techniques and equipment used to transduce and acquire experimental signals. The computer hardware and software modules used to control the experimental process is subsequently outlined.

3.2.1 Ankle Actuator

The ankle actuator used to impart the perturbations was a rotary hydraulic motor[2] controlled by a two-stage servo-valve[3]. The actuator was operated under proportional control using angular position as the feedback signal[4]. The servo-controlled electro-hydraulic system had a frequency response that was flat to 50 Hz and was capable of applying power up to 100 Hz for system identification purposes [102].

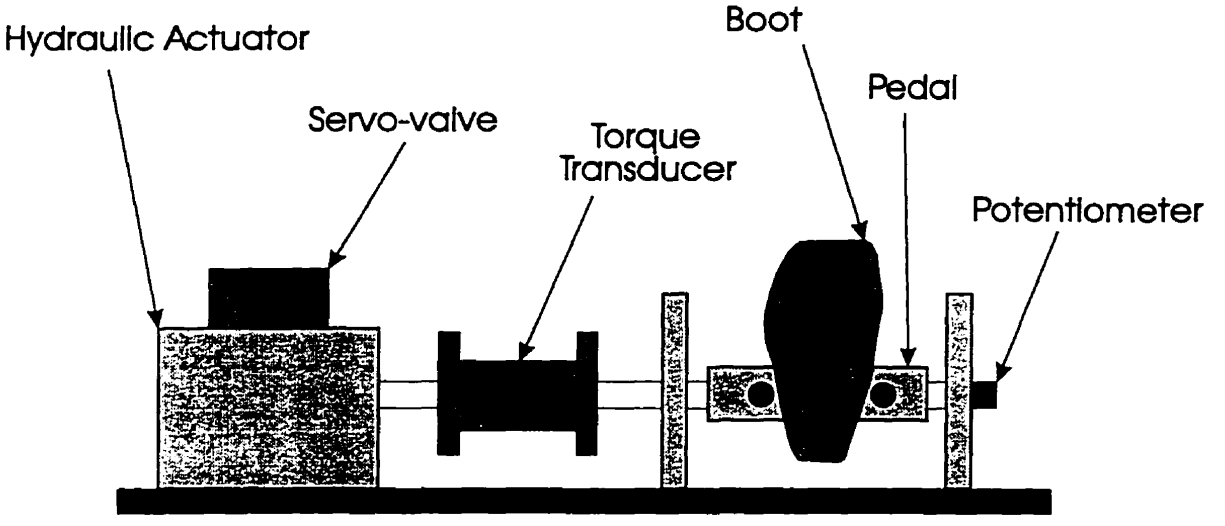

Figure 3.3: Ankle actuator

As shown in Figure 3.3, the actuator shaft is directly coupled to a pedal assembly, thus minimizing backlash. A custom-built boot made of a fibreglass body epoxied to steel posts served as the fixation between the pedal assembly and the subject's left foot. The boot constrained the ankle to a fixed plane of rotation and thus simplified the experimental procedure. The axis of rotation of the ankle was aligned with that of the actuator during the boot construction process. The history, design, material

[2]Rotac 26R-2-1V, Ex-Cell-O Corp., Berne, IN
[3]Moog 73-233, Moog Inc., East Aurora, NY
[4]described in section 3.2.3 on page 48

content and construction procedure of the fixation boot are detailed in section 3.3.

The actuator was operated at pressures up to 3000 psi and was thus capable of rapidly applying massive torques (up to 380 Nm) [102]. In order to protect the ankle joint from potential injury, four independent safety mechanisms were present. The control system, described below, limited displacements and velocities to predetermined values. Two aluminum bolts, fixed to the pedal support at locations corresponding to the extremes of the subject ankle's ROM, served as mechanical stops. An adjustable hydraulic cam removed power by cutting off flow to the actuator before the ROM limits were reached. The hydraulic stops set the boundaries for normal actuator function. The subject could halt actuator operation with a panic button placed in their hand.

3.2.2 Signal Transduction

Angular Position

The input stimulus was transformed by the band-limiting nature of the actuator. An independent measure of the ankle angular position was transduced by a precision plastic film rotary potentiometer[5] located on the axis of the ankle actuator. The potentiometer had a maximum non-linearity of ± 0.2%. Position signals were amplified by a potentiometer module[6]. The ankle velocity was obtained by numerically differentiating the position record.

Joint Torque

Ankle torque was measured by a torque transducer[7] mounted on the shaft between the actuator and the pedal assembly. The transducer had a stiffness of 10^5 Nm/rad and a maximum nonlinearity of ± 0.2%. The torque signals were conditioned by a bridge amplifier module.

[5]Beckman 6273-R5K, Beckman Industrial, Fullerton CA

[6]Detailed information on the custom-built electronics modules can be accessed on-line at http://www.biomed.mcgill.ca/REKLAB/ELECTRONICS/outline_electronics.html.

[7]Lebow 2110-5K, Eaton Corp., Troy NY

EMG

Electromyograms (EMG's), representing the neural activity in the ankle plantarflexors and dorsiflexors, were obtained using disposable, self-adhesive Ag/AgCl surface electrodes[8]. Pairs of electrodes were placed, parallel to the muscle fibre direction, over the lateral head of the gastrocnemius (GS), and over the belly of the tibialis anterior (TA) muscle (about one-third the distance between the kneecap and the lateral malleolus). The ground electrode was attached over the patella. The skin underneath the electrodes was prepared by shaving and vigorous rubbing with ethanol. The leads to the electrodes were taped[9] to the skin to reduce movement artefacts.

The noise removal performance of an amplifier, evaluated as the ability to remove the common signal, is quantified by the common mode rejection ratio. Unfavourable electrode impedance characteristics translate into the recorded voltage being a nonlinear function of the voltage magnitude. In addition, impedance mismatches between the electrodes lowers the effective CMMR of the differential amplifier.

These problems can be minimized by decreasing electrode impedances through adequate pre-experiment skin preparations. The skin underneath the electrodes should be shaved and rubbed vigorously with ethanol. The impedance effects can be further lowered by using differential amplifiers with high input impedances [56, 82].

The EMG's were amplified using custom-built three-stage preamplifiers. The preamplifiers consisted of an AD 625 instrumentation amplifier[10], a passive single-pole RC high-pass filter with a 1 Hz cutoff, and an AD 210 isolation amplifier. The amplifier has an upper cutoff of 15 kHz, and a CMMR greater than 110 dB between 1–250 Hz above which it rolled off at 20 dB/decade. The high-pass filter removes low-frequency artifacts due to electrode polarization, and cable and electrode motion. The overall gain could be switched between 1,000 VV^{-1} and 10,000 VV^{-1}. The RMS output noise was 3.2 mV.

The preamplified EMG signals were then high-pass filtered by a fourth-order But-

[8]Electrotrace ET301, Jason, Huntington Beach CA
[9]3M Micropore Tape, 3M Canada Inc., London, ON
[10]Analog Devices, Norwood, MA

teworth filter[11] with a cutoff frequency of 5Hz. To differentiate between agonist and antagonist muscle groups, the TA signal was positively full-wave rectified while the GS signal was negatively full-wave rectified.

Data Acquisition

The conditioned and amplified EMG, torque and position signals were anti-alias filtered at 200 Hz and sampled at 1000 Hz using an 8-channel, 16-bit analog-to-digital converter[12]. The data was stored on the DEC AXP machines.

3.2.3 Experimental Control

The experimental and analytical procedures were implemented using proprietary MATLAB[13] modules. The procedures were executed on a DEC AXP workstation [14] using the OSF/1 operating system. The desired position of the ankle actuator was generated digitally and output using a 16-bit, 4-channel digital-to-analog converter[15]. The position command was then low-pass filtered at 200 Hz with an 8-pole linear-phase constant-delay filter[16]. The workstation communicated with the external devices via a GPIB[17] interface.

The proportional control law was implemented using a two-processor transputer system configured for servo-hydraulic systems. The transputer was mounted on a Transtech TMB-16 motherboard with a 16-bit PC interface hosted within a 486 PC. The transputer has a 12-bit, 100 kSamp/sec A/D converter with 16 differential inputs and a 12-bit D/A converter with 8 single-ended outputs capable of 50 kHz maximum output rates. The transputer was connected to the DEC AXP workstation using Ethernet.[33]

The transputer used two position inputs and one servo gain input from the DEC

[11] Frequency Devices 711H4B-5Hz
[12] IOtech ADC 488/8S
[13] The MathWorks Inc., Natick, MA
[14] Digital Equipment Corporation, Maynard, MA
[15] IOTech 488HR/4, IOtech Inc., Cleveland, OH
[16] Frequency Devices 9064, Frequency Devices, Haverhill, MA
[17] NI 488, National Instruments, Austin, TX

AXP, and a feedback position input from the potentiometer attached to ankle actuator (refer to Fig. 3.2). The output was converted into a current signal and sent to the servo-valve.

In order for the trials to be executed at constant voluntary contraction levels, subjects were trained to match a command (or target) torque signal with their ankle torque. The passive torque was sampled and removed from the transduced torque signal. The subject's voluntary torque level was then low-pass filtered at 5 Hz with an 8-pole Bessel filter (Frequency Devices 902 LPF). The two torque signals were displayed on an oscilloscope (BK Precision, Model 2120) placed above the subject's head.

The servo gain and command torque signals were generated digitally by the DEC AXP workstations and output via a 12-bit digital-to-analog converter (IOtech DAC488/4).

More information can be obtained online[18].

3.3 Boot Construction

The "boot" was used to attach the foot to the hydraulic actuator. The following section outlines the functional requirements, previous design iterations and provided details on the newly developed fixation device.

3.3.1 Design Requirements

The ankle "boot" has to transmit the stochastic perturbations from the actuator to the foot without interfering with joint function. Consequently, it must conform closely to the foot contours and be rigid and durable without being uncomfortable. These requirements rule out the excessive use of padding. Furthermore, the "boot" must be light; minimizing fixation inertia increases the range of the stimulus amplitude and frequency applied by the actuator, and improves the measurement resolution

[18] http://ralph.biomed.mcgill.ca/REKLAB/SERVO_CONTROL/outline_control.html

of ankle torque [77]. In addition, the construction procedure should be relatively straightforward and rapid, and the materials should be inexpensive and non-toxic.

3.3.2 Construction History

Traditional fixation devices that use straps, clamps, slings and cuffs result in local ischemia, pain and skin injury due to localized concentrations of force. Furthermore, the elasticity inherent in compliant straps introduces spurious dynamics. These methods were judged to be unacceptable [77, 95]. Our lab has favoured the construction of cast-like "boots". The fixation devices have undergone several iterations in a continuous effort to fully satisy the design criteria.

Kearney used sheets of thermoplastic splinting material, reinforced in high-stress areas, closed by straps and bonded to a plastic plate mated with the hydraulic pedal [53]. Adequate fixation was ascertained by measuring heel contact using electrodes on the heel and the cast. A pain free range of 0.5 rad was obtained. Weiss et al used casts made of expanded polyurethane foam [95]. Although comfortable and rigid, the construction process was tedious: a plaster negative and a dental stone positive casting were required before the final polyurethane boot could be fashioned. 85 % of the total ROM (approximately 0.85 rad) was preserved when the ankle was in the cast.

Morier et al [77] introduced the use of fibre-glass casting bandage taking advantage of its high strength-to-weight ratio, moisture permeability and low density. The cast was attached to the actuator pedal using steel-filled epoxy and aluminium sleeves. The "boot" has been previously detailed [77]. The casting procedure could be completed in approximately 90 minutes.

The Morier "boot" had an opening on the dorsal surface; the subject inserted the foot by inverting the subtalar joint and dorsiflexing the metatarsophalangeal joints. The ingress and egress procedures tended to require effort and time. Despite the low fixation forces, the Velcro strap fastened around the instep could become painful in long experiments.

An intermediate improvement was to partially slit open the back of the boot

(between the heel and the Achilles tendon), insert thermoplastic splinting material formed around the heel, and tighten the two halves using hose clamp. Although fixation was improved, tightening the hose clamp induced pain in the medial and lateral malleoli. Ingress and egress was marginally improved.

3.3.3 Improved Design

The current version, jointly developed by Andrzej Kozakiewicz[19] and the author retains advantages inherent in the casting materials and wrapping process originated by Morier et al [77]. The procedure and materials are documented on the WWW[20].

The new "boot" dispenses with the heel slit and hose clamp. Instead, a significantly larger opening is made on the dorsal surface. The removed cast material is refitted to the boot with molded thermoplastic splinting material as the lining. The removable dorsal surface is secured using a wide Velcro strap.

The large dorsal opening enables easy ingress and egress for the foot: the subject can thus take frequent breaks during experiments reducing discomfort and fatigue. The retaining force provided by the velcro strap is spread out over the entire removable dorsal surface and thus ceases to be a problem. The thermoplastic lining compensates for irregular cast shrinkage; the entire assembly, akin to a ski boot, consequently provides remarkable fixation.

Axis of Rotation

The "boot" constrains the foot to rotation about the talocrural (ankle) joint. The axis of rotation is currently determined using anthropometric data obtained from a study of 46 cadaver legs [51].

Anatomical landmarks are used as reference points in ankle axis location, as shown in Fig. C.1 and Fig. C.2 on pages 117 and 118, the axis passes through a point 11mm anterior to and 12 mm distal from the most lateral point of the lateral (fibular)

[19] Neuromuscular Control Lab, Dept. of Biomedical Engineering, McGill University
[20] http://www.biomed.mcgill.ca/REKLAB/HYDRAULICS/Ankle_Act/boot/outline_boot.html

malleolus. On the other side of the foot. the axis is located 1mm posterior to and and 16mm distal from the most medial point of the medial (tibial) malleolus.

A "boot" possessing a properly aligned axis allowed for the rotation of the foot without inducing translational forces in the supine subject.

3.4 Experimental Paradigm

3.4.1 Protocol

The experiments were performed on healthy subjects (aged 20–31) in sessions lasting between 2 and 3 hours. All subjects (8 male and 4 female) gave informed consent. Certain volunteers were used in repeat experiments. The subjects were trained to maintain a tonic contraction of the triceps soleus (TS) muscle group by aligning a low-pass filtered torque signal with a target signal. They were also instructed not to react to the input perturbations.

3.4.2 MVC

The maximum voluntary contraction (MVC) was recorded prior to the experimental trials. with the ankle at an initial reference position[21]. The subjects were asked to execute a maximal contraction in response to a step change in a tracking stimulus displayed on the overhead oscilloscope. A 3 second dorsiflexing contraction was followed by a 3 second plantarflexing contraction after a 1 second break.

Fig. 3.4 illustrates the joint torque and Triceps Surae EMG signals recorded from a MVC trial. Note that signals corresponding to plantarflexion were assigned negative polarity. The difference between the maximum plantarflexing torque and the pre-MVC torque (recorded during the first second) was designated as the MVC torque. A similar calculation was used to determine MVC EMG for plantarflexion.

[21] Section 2.1 on Page 4

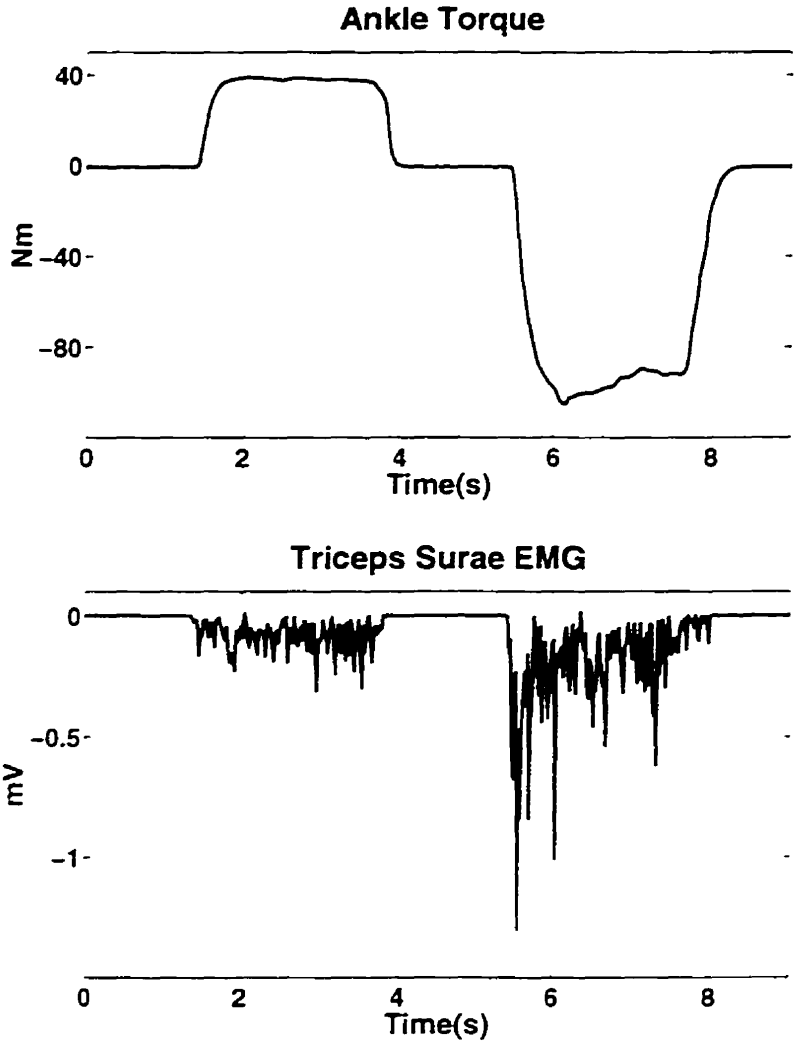

Figure 3.4: MVC trial. Subject - FC

3.4.3 Identification of Reflex Dynamics

The stretch reflex dynamics were identified by applying a PRBS position perturbation to the ankle and recording the torque and EMG responses. The stochastic perturbations are described in detail in section 3.5. In general, perturbations with amplitudes ranging from 0.02 - 0.03 rad and switching intervals of 100 - 200 ms were used. The non-linear parallel-cascade identification scheme described above was used to differentiate between reflex and intrinsic dynamics.

In order to understand the observed effects of movement on the identified reflex dynamics, a different protocol was employed. The effects could have been ascribed

to either reflex attenuation by the imposed movement or spectral problems with the system identification procedure. Based on the hypothesis that the input perturbations (passive applied movements) were decreasing the reflex gain, transient stimuli were used to evoke the reflex. Stochastic perturbations superimposed onto the reflex-evoking pulses enabled us to elucidate the effects of movement on reflexes.

3.4.4 Reflex Evocation

A TS stretch reflex was evoked by briefly stretching the plantarflexors with a pulse input as described in [90]. This is a more physiological means of evoking a stretch reflex than the electrical stimulation used to incite an H-reflex.

The short duration of the position pulse allowed for the separation of the reflex and intrinsic effects of perturbing the ankle. Since the ankle was returned to its starting position within 40 ms, the generated reflex could be easily distinguished since it has a latency greater than 40 ms. A trial would typically consist of 5 – 10 pulses separated by 1 – 3 second intervals.

The evoked reflex is influenced by the mean ankle position, the pulse height (which corresponds to the stretch magnitude) and the subject's voluntary contraction [90]. The optimal operating point was located by adjusting the afore-mentioned factors until a large and consistent reflex was obtained. The optimal ankle position was obtained by dorsiflexing the ankle (and thus prestretching the muscle) by about 0.1 rad from the initial reference position[22]. This pre-stretches the TS muscle group. Pulses ranging from 0.2 – 0.4 rad gave the best results. Voluntary contractions of the GS muscle ranging from 5 – 10 % of MVC (5 – 10 Nm) were generally used.

3.4.5 Reflex Attenuation

Passively moving the ankle while the stretch reflex was being evoked allows for the determination of the effects of passive movement on stretch reflex gain. Various stochastic perturbations characterised by different amplitude spectra and frequency

[22] section 2.1 on page 4

distributions were superimposed onto a series of position pulses, as shown in Figure 3.5.

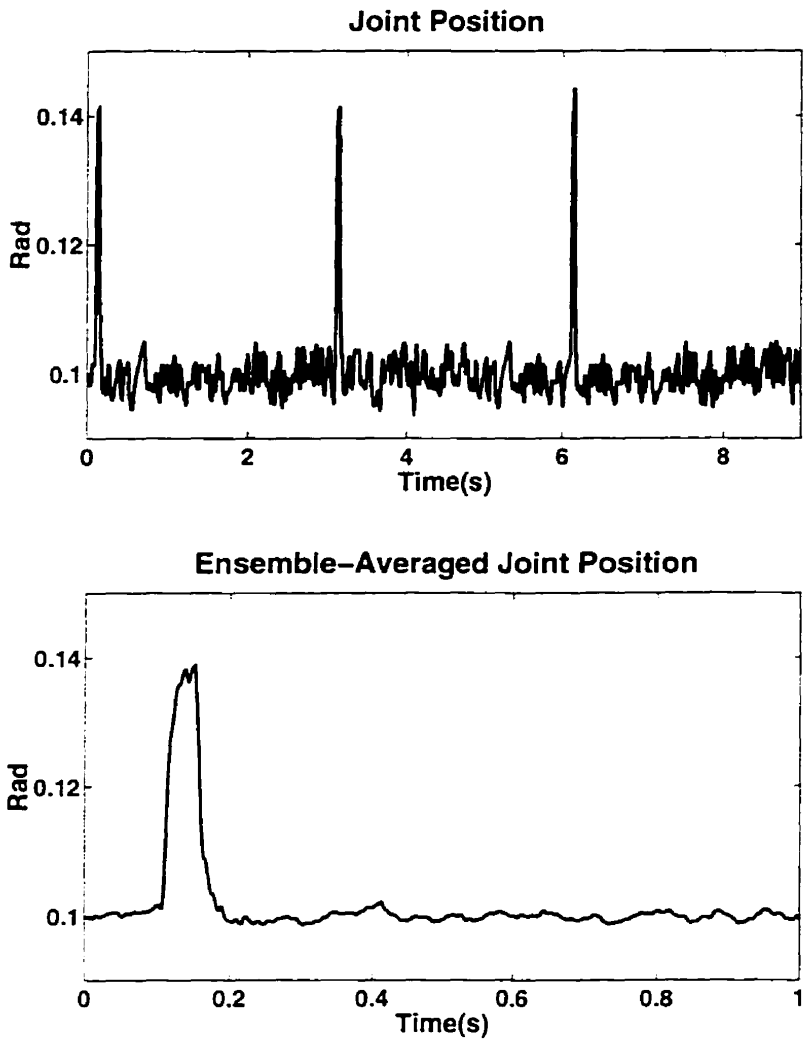

Figure 3.5: Pulse trial with superimposed FGWN perturbation. Subject – DW

The experiments were designed to avoid the deleterious effects of muscle fatigue. The "attenuation" trials were randomized so that fatigue, if present, would contribute to the variability in the data rather than systematic modifications. Control trials composed of series of pulses were used frequently to monitor the magnitude of the reflex response. Section 5.7.1 provides a detailed discussion of the various sources of fatigue and the steps taken to prevent its occurrence.

3.4.6 Actuator–Cast Dynamics Correction

The sampled torque contains contributions from the actuator and boot. In order to identify these dynamics, a post-experiment calibration was used to determine the impulse response function (IRF) between the applied position and the actuator-cast torque. Each experimental position record was then convolved with the IRF to predict the actuator-cast torque contribution, which was then subtracted from the recorded torque signal. A PRBS signal with an amplitude of 0.25 rad and a switching time of 20 ms was used as the input perturbation.

3.5 Stochastic Input Perturbations

System identification studies have traditionally been performed using *filtered Gaussian white noise* (FGWN) signals [71]. Stochastic inputs contain power over a wide range of frequencies and thus ensure that experiments characterizing system dynamics have short durations. Our lab has tended towards the use of both FGWN signals and *pseudo-random binary sequences* (PRBS) [62]. Pseudo-random inputs are relatively easier to generate, and are repeatable yet unpredictable. A joint perturbed by this sequence is moved rapidly between two positions at random intervals determined by the *switching interval*, defined as the average time spent by the signal at one of the two possible levels. (See Fig. 3.7).

The PRBS signals previously used in our lab had switching intervals on the order of a millisecond. When these signals are filtered by actuator limitations, they resembled FGWN signals - they were characterised by a Gaussian amplitude distribution as opposed to a binary one. Recent efforts using PRBS inputs with longer switching intervals (20–200ms) yielded excellent results with the parallel-cascade reflex identification scheme [64, 65]. In order to differentiate between the two sequences, the low switching interval input was dubbed as a FGWN signal (see Fig. 3.6), while the high switching interval input was called a PRBS signal (see Fig. 3.7).

In order to study the effects of different forms of passive movement on stretch reflex dynamics, both FGWN (Gaussian) and PRBS (binary sequence) inputs were

used in this study. In addition, two other inputs, referred to as the *pseudo-random quaternary sequence* (PRQS) and the *pseudo-random triangular sequence* (PRTS), were employed.

Stochastic signals are often specified using the first order probability density function and the first order auto-correlation function. These properties represent independent and useful yet partial statistics of a signal [47]. The Fourier Transform of the auto-correlation function is called the power spectra [71] and describes the amount of power contained by the signal over a range of frequencies. The following figures display the signals in the position and velocity domains along with their power spectra and amplitude distributions.

3.5.1 Gaussian (FGWN) Input

Fig. 3.6 illustrates a FGWN signal with a peak-to-peak amplitude of 0.037 rad filtered at 50 Hz. The input is characterised by a Gaussian amplitude distribution in both the position and velocity domains.

3.5.2 Binary Sequence (PRBS) Input

Fig. 3.7 shows a binary sequence (PRBS) with a peak-to-peak amplitude of 0.027rad and a switching interval of 50ms. Binary sequence (PRBS) signals have a binary position distribution and a trimodal velocity distribution. For similar peak-to-peak amplitudes, the PRBS signal has a lower average (root mean square) velocity and a higher peak velocity than the FGWN signals. Another difference of interest is the concentration of power at low frequencies in the velocity power spectrum.

As explained in Chapter 4, experiments superimposing FGWN and PRBS signals onto reflex-evoking pulse displacements yielded different results. Using multiple linear regression techniques (described in Appendix B), the kinematic parameters of the signal that appear to contribute to reflex attenuation seemed to be the average velocity, the peak velocity and the zero-crossing rate. The zero-crossing (ZC) rate refers to the number of times a zero-mean signal crosses the horizontal in one second and

is used as a signal-independent measure of the frequency spectra. Using specifically designed experiments, it was determined that the frequency spectra was not explicitly important in reflex attenuation (refer to Section 4.5.1).

The downfall of using the PRBS input was the fact that the peak velocity and the average velocity covaried; both measures were dependent on the peak-to-peak amplitude. In order to investigate the effects of peak velocity and other amplitude distribution effects on reflex attenuation, a new set of signals were generated. Both inputs had different position amplitude distributions, and allowed for the independent manipulation of the peak and average velocities.

3.5.3 Quaternary Sequence (PRQS) Input

The PRQS input has a quaternary position amplitude distribution; an ankle joint perturbed by the PRQS input moved rapidly between four position levels at random intervals. Fig. 3.8 displays a quaternary sequence input with a peak-to-peak amplitude of 0.019rad and a switching interval of 100ms. The peak velocity is determined by the peak-to-peak amplitude of the signal. The average velocity is controlled by the time spent at each of the 4 possible positions in addition to the peak-to-peak amplitude. For a given peak velocity, the PRQS input had a lower average velocity than the PRBS input.

It is relatively simple to alter the amplitude structure to have more than four position levels; note that an increase in the number of position levels will make the PRQS similar to the traditional FGWN input.

3.5.4 Triangular Sequence (PRTS) Input

Fig. 3.9 illustrates a PRTS input with a peak-to-peak amplitude of 0.015rad and a switching interval of 125ms. Triangular sequences move the joint between two position levels at variable velocities. The sequence was designed to move the joint at random intervals with either the fastest speed possible (as in the PRBS input) or a speed that could be altered by changing the "slope" variable.

A glance at Fig. 3.9 reveals that in the velocity domain, the signal has large spikes corresponding to the fastest possible switches (and consequently the peak velocity) and smaller spikes corresponding to the variable speed switches. The amplitude of the variable speed switches is controlled by the slope variable, while the amplitude of the large spikes is determined by the peak-to-peak amplitude. The average velocity is thus a function of the *ratio* of high-velocity switches and the variable-velocity switches, the magnitude ("slope") of the variable-velocity switches, and the magnitude of the high-velocity switches.

The independent manipulation of average and peak velocities is constrained by the fact that peak-to-peak amplitude affects both of the velocity measures; there is a degree of covariation.

Fig. 3.10 compares the velocity probability distribution functions for the PRBS, PRQS and PRTS signals shown in Figures 3.7, 3.8 and 3.9. The vertical axes are truncated from 1 to 0.05 to reveal the side lobes of the PDF. The dominant peak at zero velocity, in the previous figures, drowns out the details in the side lobes.

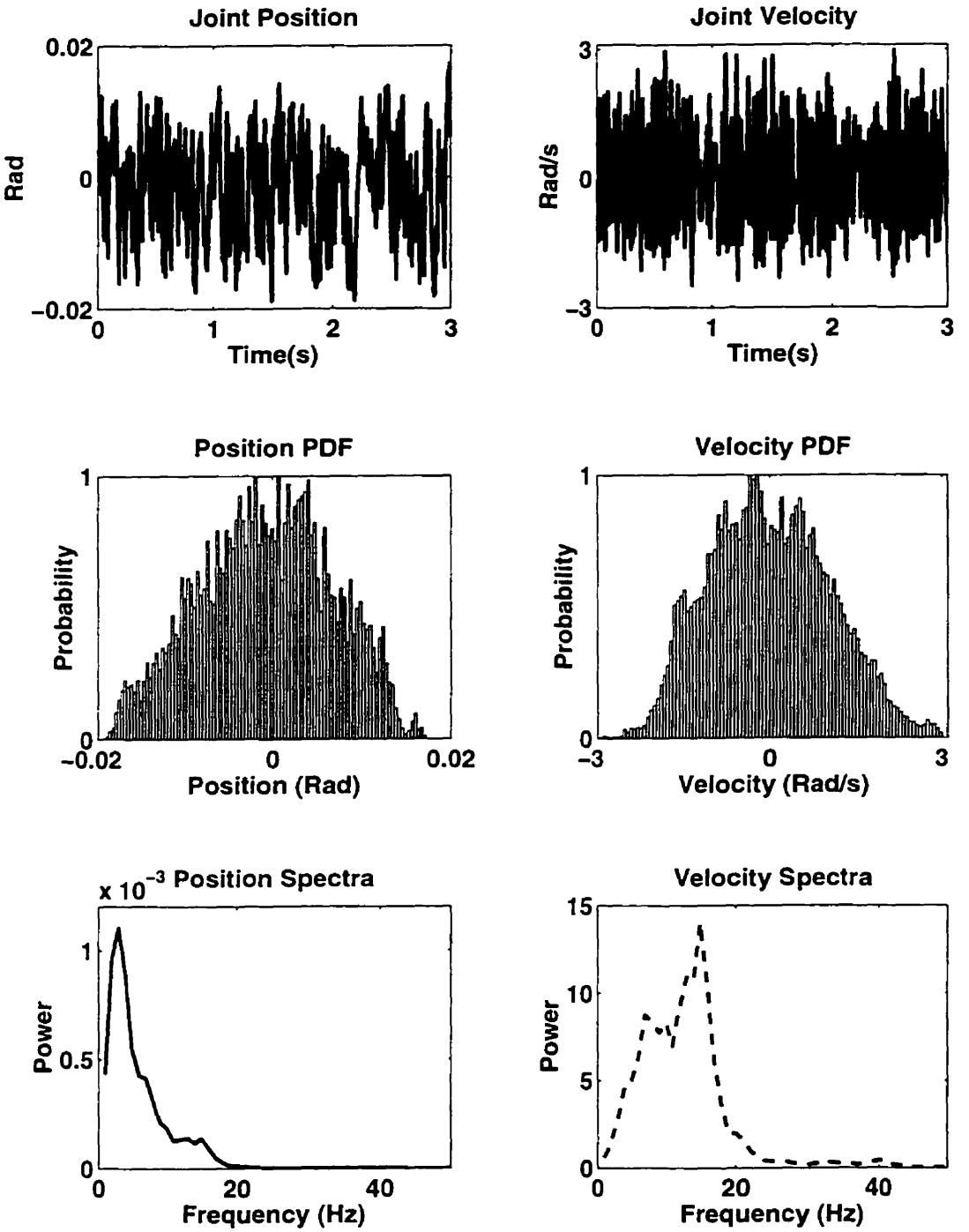

Figure 3.6: Filtered Gaussian White Noise (FGWN) input with a peak-to-peak amplitude of 0.037 rad and filtered at 50 Hz

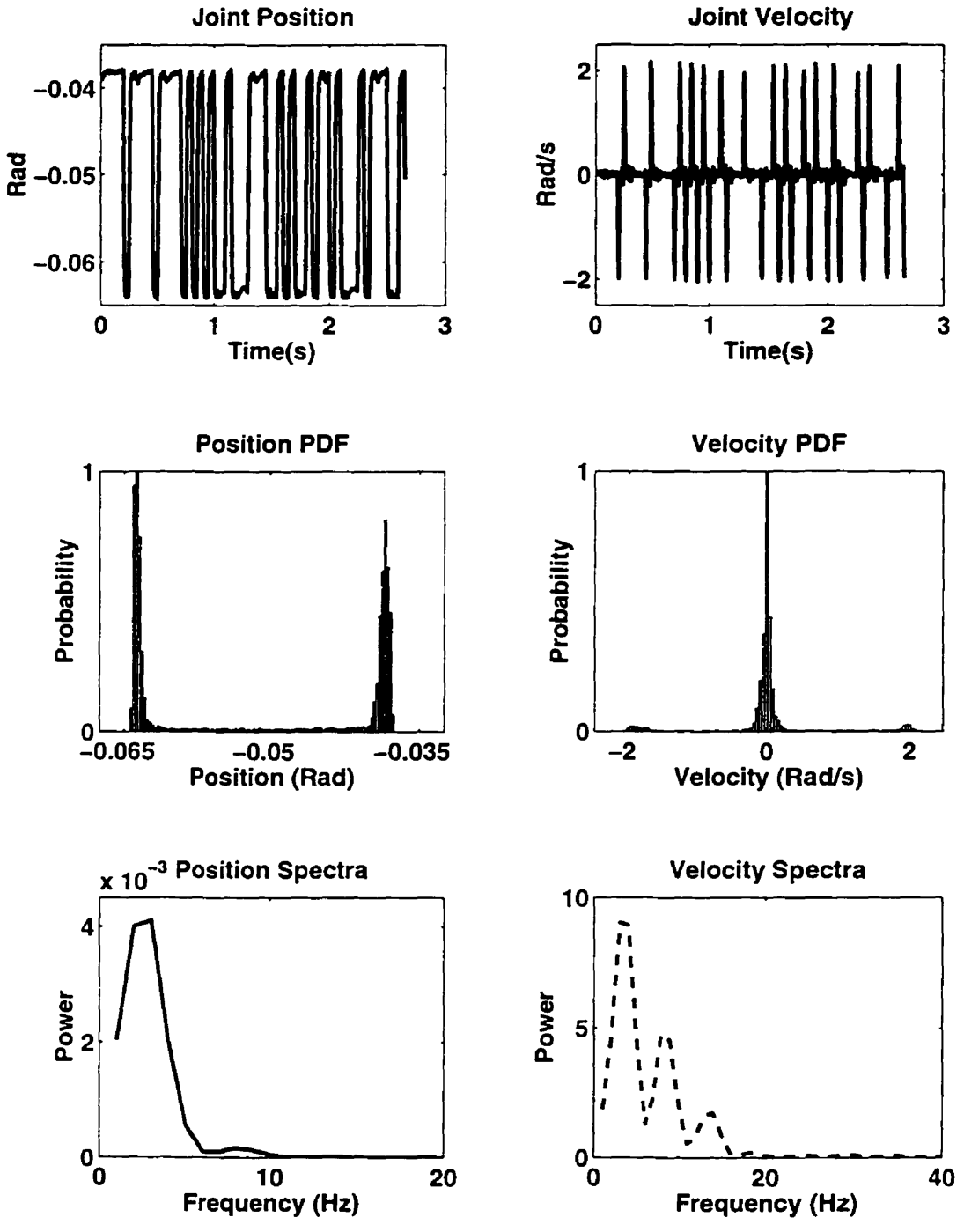

Figure 3.7: Pseudo-random binary sequence (PRBS) input with a peak-to-peak amplitude of 0.027 rad and a switching interval of 50ms

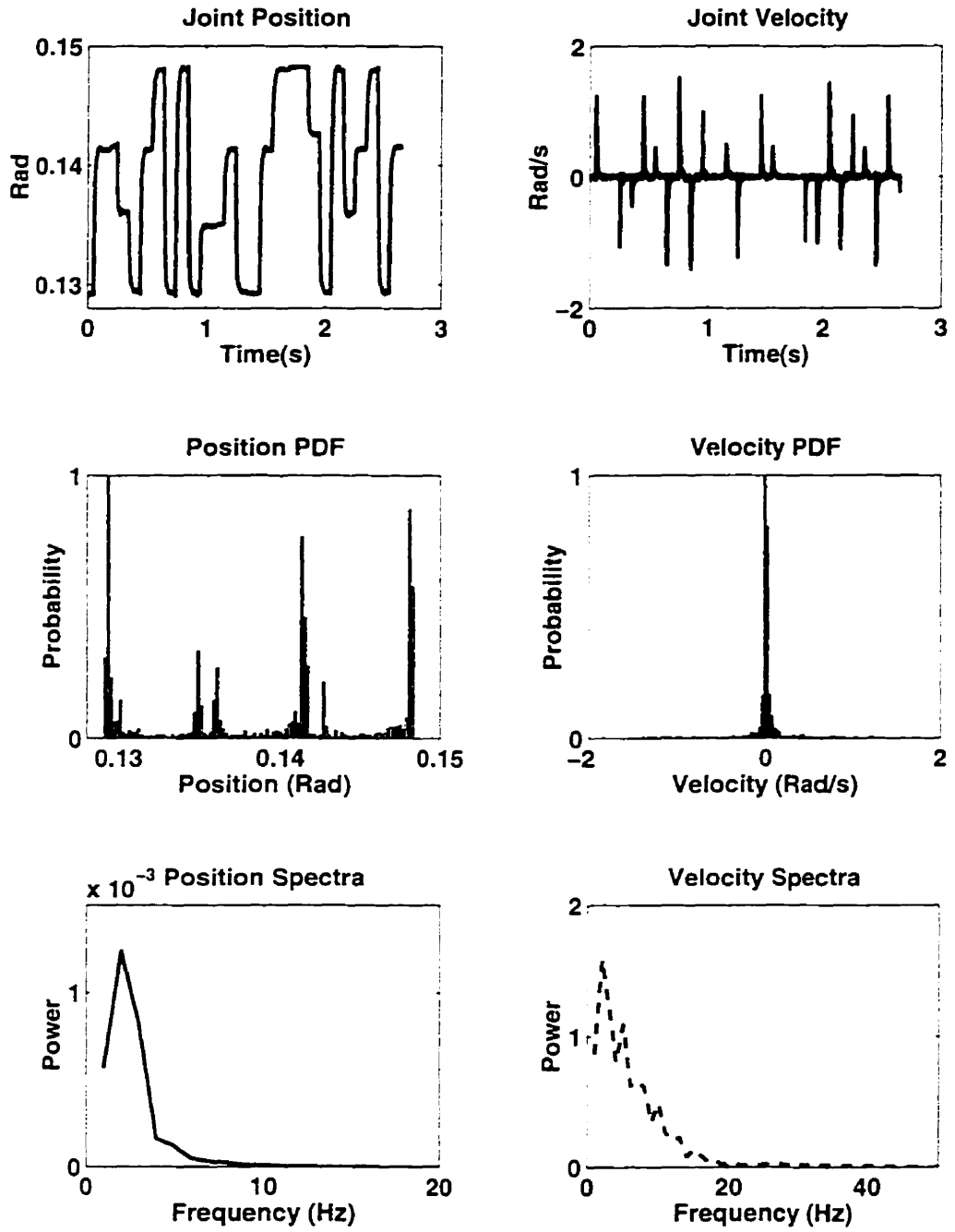

Figure 3.8: Pseudo-random quaternary sequence (PRQS) input with a peak-to-peak amplitude of 0.019 rad and a switching interval of 10ms

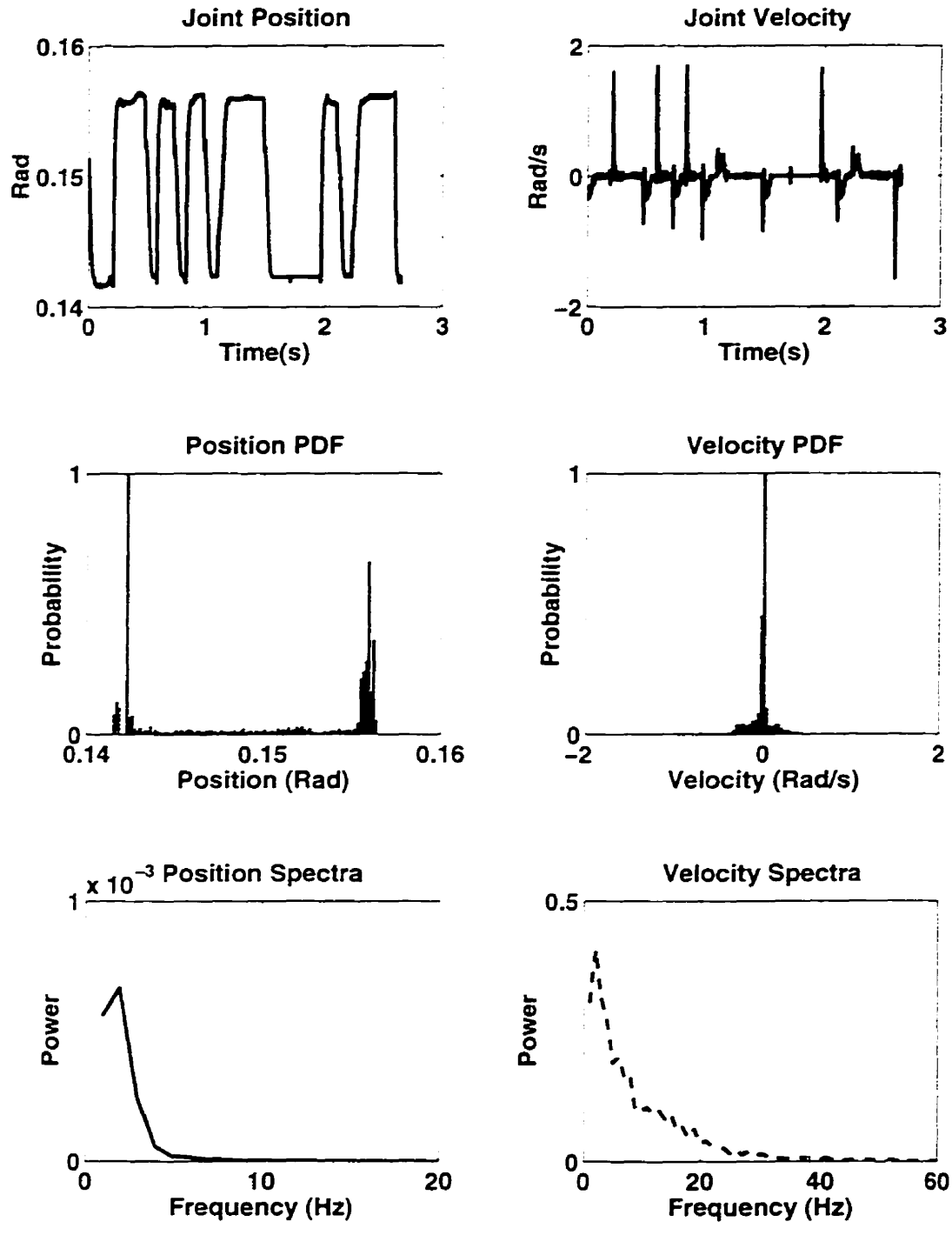

Figure 3.9: Pseudo-random triangular sequence (PRTS) input with a peak-to-peak amplitude of 0.015 rad and a switching interval of 125ms

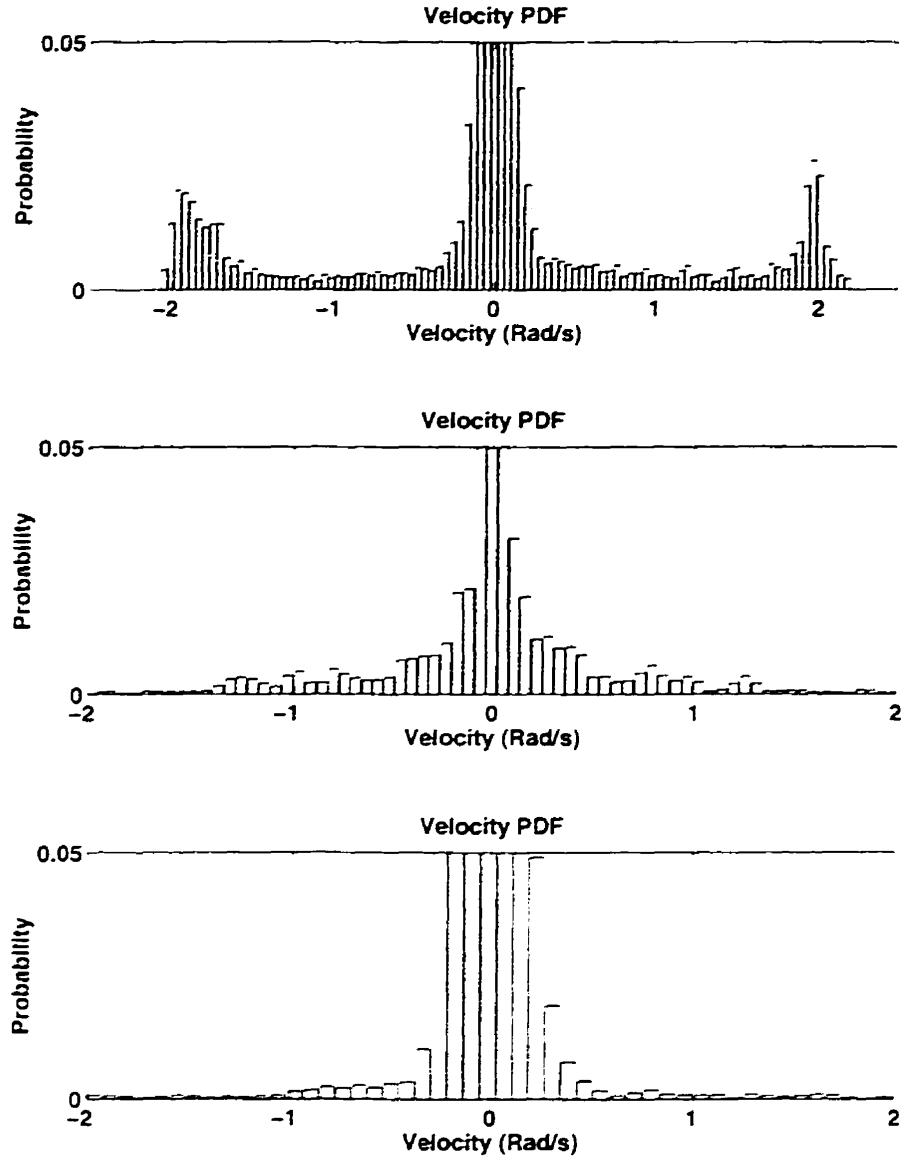

Figure 3.10: A comparison of the velocity PDF's from PRBS (top), PRQS (middle) and PRTS (bottom) signals. These PDF's are plotted with magnified vertical scales to allow a qualitative comparison of the distribution properties at non-zero velocities.

Chapter 4

Results

The chapter commences with a discussion of the stretch reflex evoked by a displacement pulse. In order to give the reader an idea about the strength of the reflex response, a comparison is made between the stretch reflex torques and EMG's with the torques and EMG's generated during a maximum voluntary contraction(MVC). Reflex dynamics estimated using the afore-mentioned parallel-cascade technique are then displayed. The effect of perturbation velocity on the identified dynamics is also shown. We return to pulse displacement experiments to explicitly investigate the effect of random perturbations on the evocation of ankle stretch reflexes. In particular, the effects of changing the amplitude distribution and spectral characteristics of the imposed movement are demonstrated.

4.1 Stretch Reflex Evocation

The reflex response, evoked by briefly stretching the TS muscle group as described in Chapter 3 is illustrated in Figure 4.1. The torque response to the dorsiflexing pulse displacement can be separated into an immediate (< 45ms) transient intrinsic component and a delayed twitch-like reflex component. The dorsiflexing pulse displacement shown as a positive deflection results in a "negative" reflex contraction resisting the original deflection.

This non-invasive technique of separating intrinsic and reflex responses was pre-

viously demonstrated by Stein and Kearney [90]. The start of the plantarflexing (negative) reflex contraction is marked by a large TS EMG pulse. (Neural activity in the TS EMG is associated with plantarflexing torques, and is thus rectified in the negative direction according to our lab's convention).

The reflex response appears to be the Ia-mediated monosynaptic stretch reflex (MSR). Note the absence of a long-latency reflex response. This was due to our experiment protocol which specified that subjects were *not* to resist the applied perturbation.

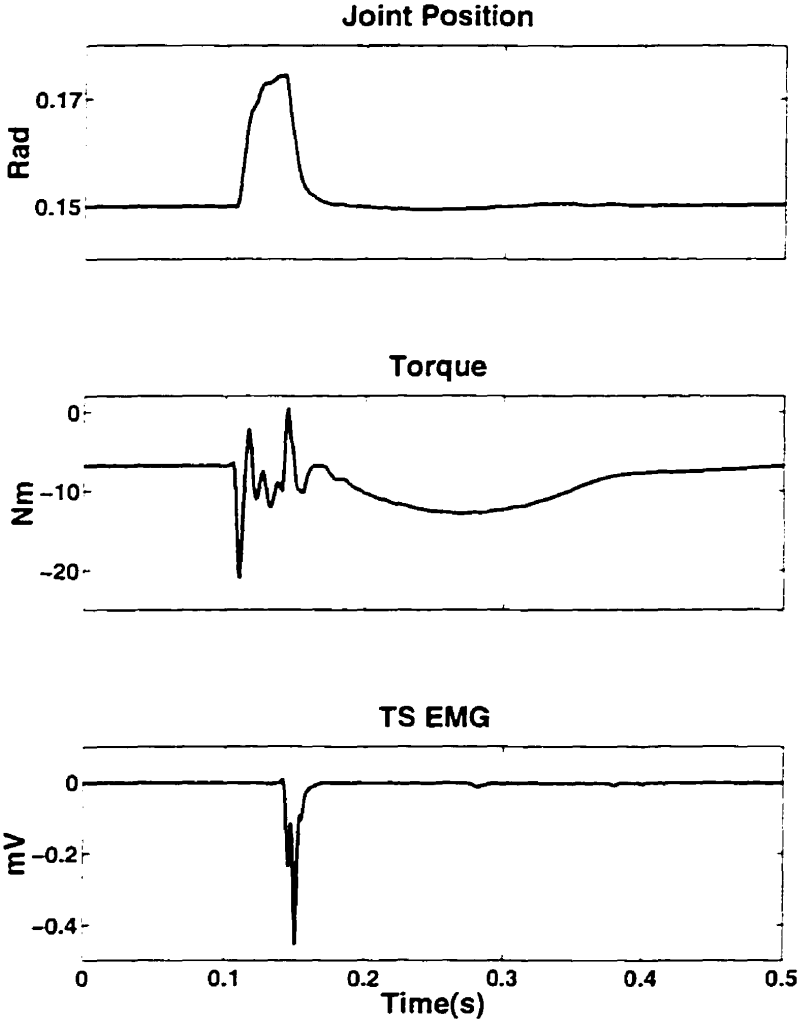

Figure 4.1: Ensemble-averaged joint position, torque and Triceps Surae EMG record during and after a dorsiflexing pulse. Subject - RH

The magnitude of the reflex torque response was measured as the difference be-

tween the mean torque level before the pulse displacement and the maximum torque level reached during the reflex component of the torque record. The procedure was repeated for the EMG response.

A comparison of sample reflex EMG and torque responses with those obtained during a MVC trial would be informative. Tables 4.1 and 4.2 display corresponding values for the MVC and stretch reflex in 12 subjects. The MVC recordings were made at the initial reference position (0 rad). The reflex responses were obtained at various joint angles ranging from 0 rad to -0.15 rad($-8.6°$). Note that the TS reflex response was heightened as the ankle was progressively dorsiflexed. The range of values obtained for the MVC's [67, 90, 98] and reflexes [90] was similar to those reported previously.

Ankle Plantarflexor Responses		
Subject	**MVC**	
	Torque (Nm)	**EMG (mV)**
AK	80.4	0.331
BH	89.6	0.277
BN	46.2	0.158
DW	61.9	0.391
FC	109	1.29
HL	58.1	0.150
HQ	37.0	0.146
JC	81.4	0.855
MS	48.9	0.35
RH	81.7	1.40
TK	73.6	0.560
TR	52.5	0.586

Table 4.1: Triceps Surae MVC torques and EMG's. The MVC's were recorded with the ankle in the initial reference position.

Let us examine subject BN : at a voluntary activation level of 6.3 Nm (14% of

MVC) in the Triceps Surae, a stretch of 0.031 rad (1.8°) elicits a reflex contraction of 13.5 Nm (29% of MVC). (In comparison, the ankle's ROM has been reported to be over 1 rad). Similar behaviour was observed in all the subjects; very small stretches ($1.5° - 3°$) of the ankle plantarflexors could elicit large reflex torques (4–29% of MVC) at physiologically significant operating points.

Stretch Reflex Responses in the Ankle Plantarflexors					
Subject	Operating Conditions		Stretch Reflex		
	Voluntary Activation (Nm)	Pulse Amplitude (rad)	Torque (Nm)	EMG (mV)	% of MVC Torque
AK	-0.4	0.049	4.86	0.695	6.0
BH	-7.0	0.034	7.91	0.538	8.8
BN	-6.3	0.031	13.5	1.015	29
DW	-9.3	0.039	5.99	0.206	9.7
FC	-0.4	0.029	4.75	0.507	4.4
HL	-5.6	0.036	9.99	0.538	17
HQ	-6.8	0.027	7.73	0.468	21
JC	-16.0	0.031	3.30	0.587	4.1
MS	-14.0	0.032	12.4	0.726	25
RH	-6.1	0.030	5.94	0.412	7.3
TK	-10.0	0.029	4.98	0.270	6.8
TR	-8.9	0.049	5.64	0.528	11

Table 4.2: Triceps Surae stretch reflex torques and EMG's. The responses were obtained at various positions – 0 rad to -0.1 rad ($-6°$). The last column expresses the reflex torque as a percentage of the MVC torque.

4.2 Reflex Dynamics

Relative contributions of the reflex and intrinsic mechanisms were estimated using stochastic system identification techniques. Ankle position was randomly altered and

the resulting joint torque and EMG signals recorded. Ankle angular velocity was obtained by numerically differentiating the position signal.

Fig. 4.2 illustrates typical signals from an experimental trial involving the PRBS input. The transduced torque signal can be differentiated into symmetrical components that match the position input and transient twitch-like components aligned with TS EMG spikes. These results are an extension of those reported in Fig. 4.1. The two components can be attributed to intrinsic and reflex mechanisms respectively.

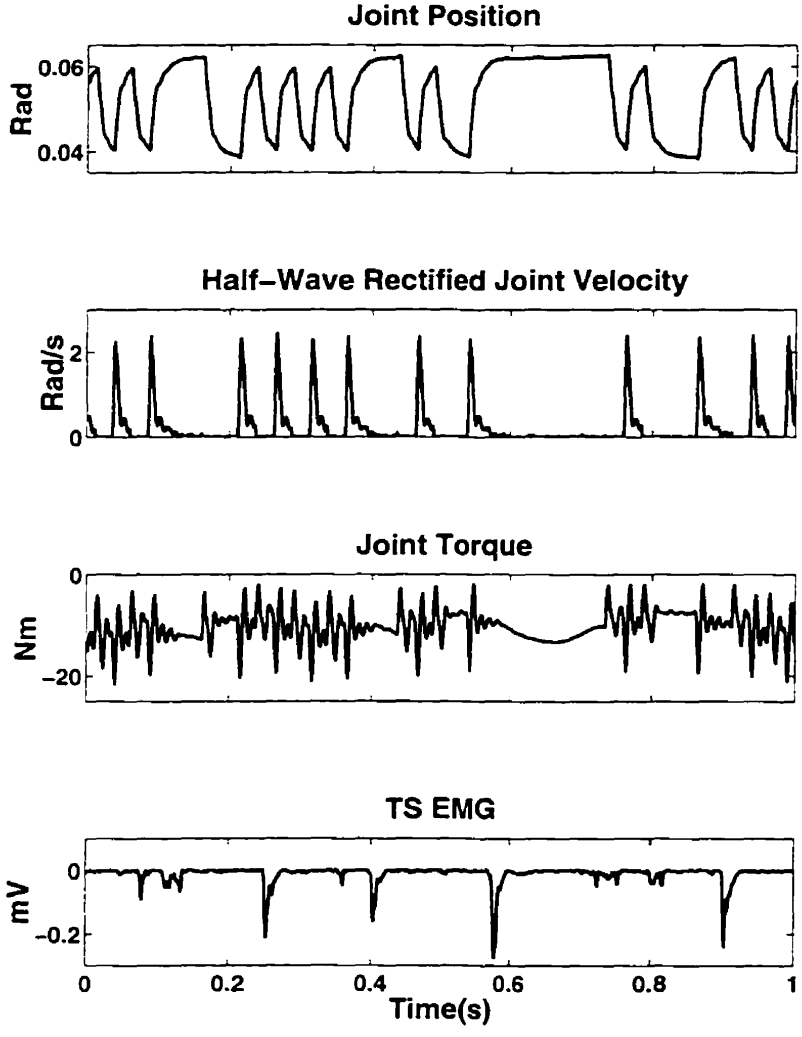

Figure 4.2: Experimentally acquired position, half-wave rectified velocity, torque and TS EMG signals. Subject - TR

The nonlinear parallel cascade technique described in Fig. 3.1 enabled the determination of impulse response functions (IRF's) describing the joint dynamics. Figure 4.3

illustrates the intrinsic stiffness IRF, the reflex stiffness IRF and the reflex activation IRF.

The *intrinsic stiffness* IRF quantifies the dynamic relation between the angular position and the joint torque. The intrinsic dynamics are similar to the previously determined [62] overall joint stiffness IRF's : they describe a second-order system with high-pass dynamics.

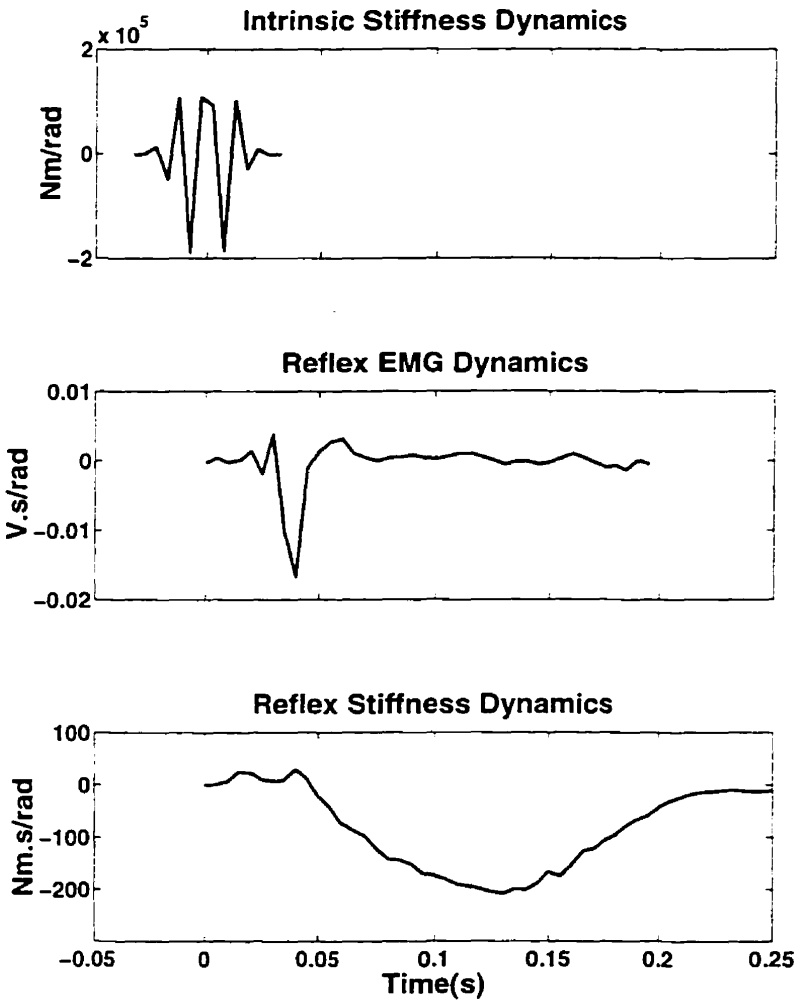

Figure 4.3: Impulse response functions calculated for the intrinsic stiffness dynamics, the reflex EMG dynamics and the reflex stiffness dynamics. Subject - TR

The *reflex stiffness* dynamics identifies the relation between half-wave rectified joint velocity and the "residual" torque. The reflex stiffness IRF consists of a 40ms delay followed by low-pass dynamics. The shape of the IRF (the response to an impulse) is very similar to the reflex evoked by the brief displacement pulse shown in

Fig. 4.1.

The *reflex activation* dynamics, identified between half-wave rectified joint velocity and the TS EMG, represents the neural activity originating in the muscle spindles. Note the large spike that occurs 40ms after the muscle stretch and corresponds to the beginning of the reflex response.

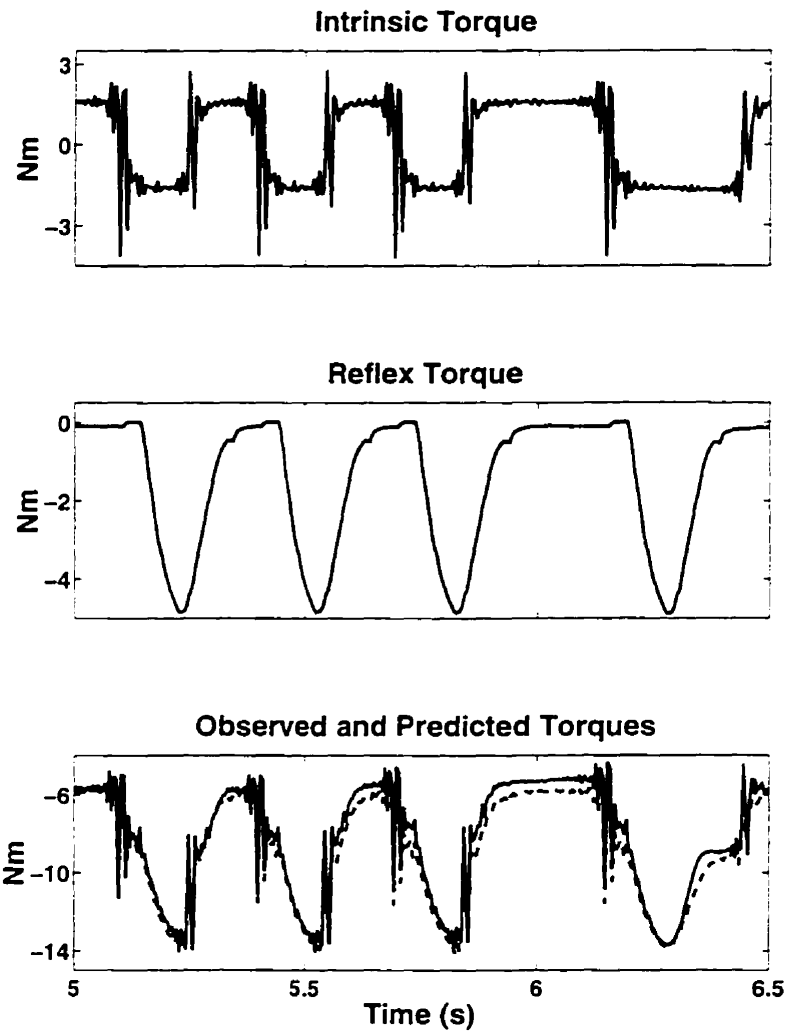

Figure 4.4: Intrinsic and reflex torques predicted by the parallel-cascade model. The last plot compares the *total* predicted (dashed line) and observed (solid line) torques. Note that the subject was exerting a voluntary contraction of -8 Nm. Subject - TR

For the trial presented in Fig. 4.3, the intrinsic mechanisms accounted for approximately 62 % of the overall measured torque variance. The reflex mechanisms accounted for over 90% of the residual torque variance and about 32 % of the overall torque variance. The overall parallel-cascade model accounted for more than 94 % of

the total torque response to the applied position perturbation.

The relative contributions of the two mechanisms can be inferred by examining the predicted intrinsic and reflex torques. As shown in Fig 4.4, the predicted torque signals differ in structure and frequency content but are similar in magnitude. For the trial shown, the reflex mechanisms generated torques as large as those that originated in the intrinsic mechanisms. The predictive ability of the model is also demonstrated in Fig. 4.4: summing the intrinsic, reflex and voluntary torque exerted by the subject yields an excellent estimate of the recorded joint torque.

Figure 4.5 shows the coherence between the predicted intrinsic torque and the measured torque, and the coherence between the predicted *total* torque and the measured torque. The intrinsic torque coherence varied with frequency. Taking the reflex pathway into account increases the measure of total coherence in the 4–9 Hz frequency range. Reflexes thus seem to be significant within this narrow frequency range. The high overall coherence is consistent with the high % VAF obtained for the model.

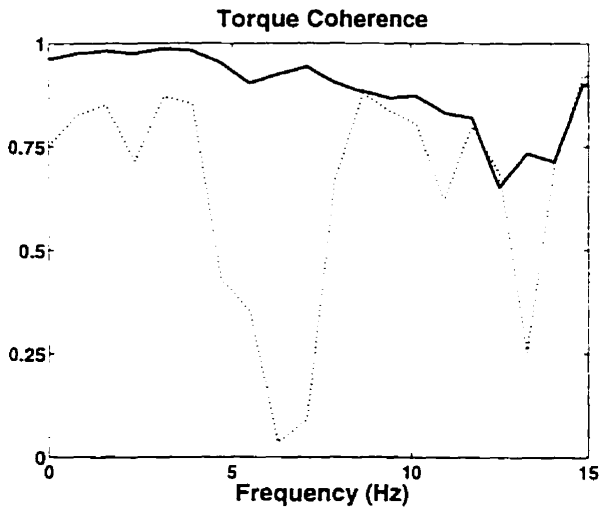

Figure 4.5: Coherence between the actual torque and the estimated *intrinsic* torque (dotted line) and between the actual torque and the estimated *total* torque . Subject - TR

Figures 4.2, 4.3, 4.4 and 4.5 were all obtained from the same experimental trial for the sake of continuity. Similar results were obtained for the all subjects.

The prediction efficacy of the parallel-cascade model seemed to depend on the type of signal used to perturb the ankle joint. The best results were obtained when

a binary sequence (PRBS) input was used [64][65].

4.3 Modulation of Reflex Dynamics with Perturbation Velocity

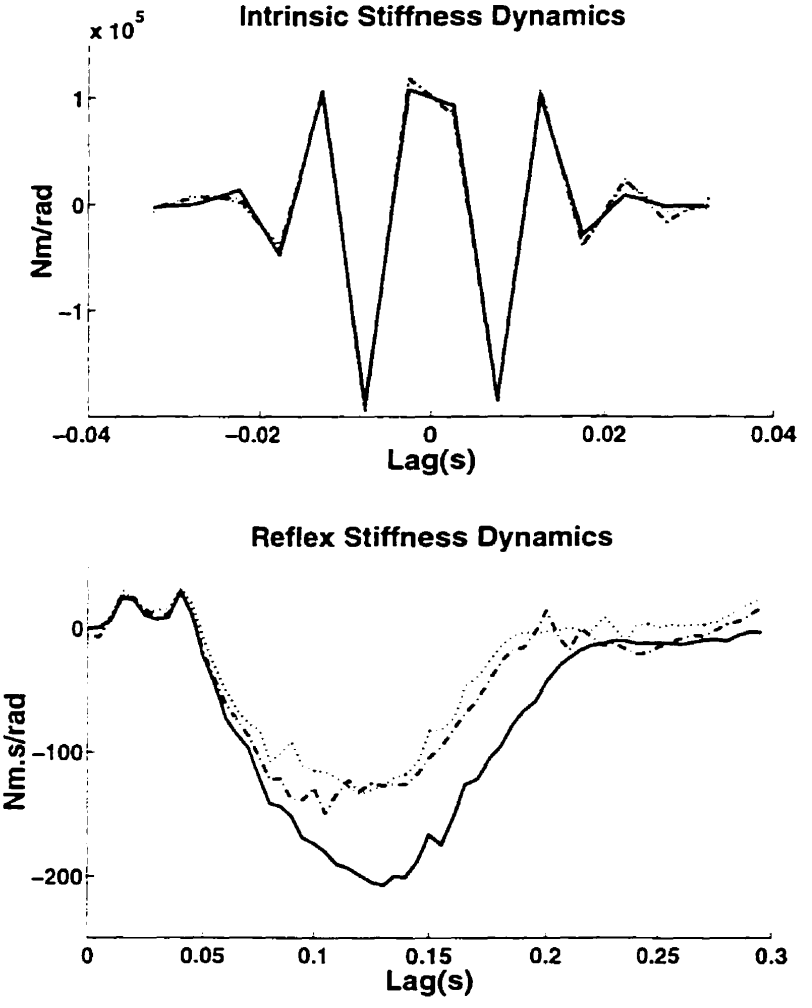

Figure 4.6: Intrinsic Stiffness and Reflex Stiffness IRF's obtained for different input perturbation velocities (*dotted line : RMS vel = 0.32 rad/s; dashdot line : RMS vel = 0.30 rad/s; solid line : RMS vel 0.23 rad/s*). Subject - TR

The IRF's estimated for the reflex stiffness dynamics were observed to depend on the root mean square (r.m.s.) velocity of the applied displacement. As shown in Fig. 4.6, increasing the average velocity of the input perturbation from 0.23 rad/s to 0.32 rad/s decreased the magnitude of the reflex stiffness IRF. In contrast, the intrinsic stiffness

IRF seemed to be independent of the displacement velocity.

The magnitude of the reflex stiffness IRF is a measure of the static gain of the reflex loop. As shown in Fig. 4.7, increasing the r.m.s. velocity of the perturbation from 0.25 rad/s to 0.50 rad/s decreases the static gain by 50 %.

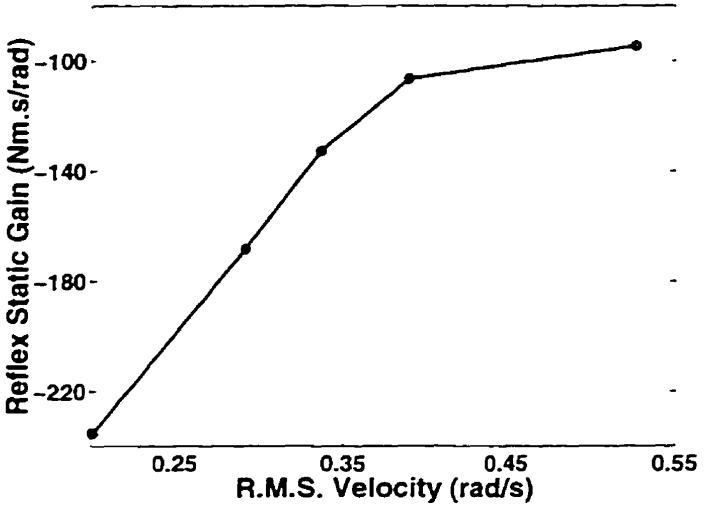

Figure 4.7: Effect of movement on the magnitude of the identified reflex stiffness IRF magnitude. The data was acquired at voluntary contraction levels between -5.1 and -5.9 Nm. Subject - AK

A passively imposed movement seems to decrease the gain of the reflexes, while having no effect on the passive mechanics.

Consequently, the relative importance of intrinsic and reflex components are altered by the average velocity of the input signal. As demonstrated in Fig. 4.8, the reflex contribution decreased progressively as displacement velocity increased. At low velocity, the reflex mechanism contributed approximately 25 % of the output torque variance; as the velocity reached 0.5 rad/s, the contribution fell to less than 5 %. The intrinsic mechanisms displayed a complementary behaviour: the % VAF by the intrinsic pathway increased with velocity and maintained the % VAF by the total model at a constant level. These results have been presented elsewhere [66].

The velocity-dependent behaviour of the reflex mechanisms imply that stochastically perturbing the ankle joint reduces the gain (and relative importance) of the stretch reflex. It is possible that the system identification techniques alter the dynamics of the system under study. The effects could be due to either system identification

estimation problems, or to reflex attenuation. The latter explanation seemed to be more probable: previous research has shown that the stretch reflex response decreases in the presence of an ongoing perturbation [90].

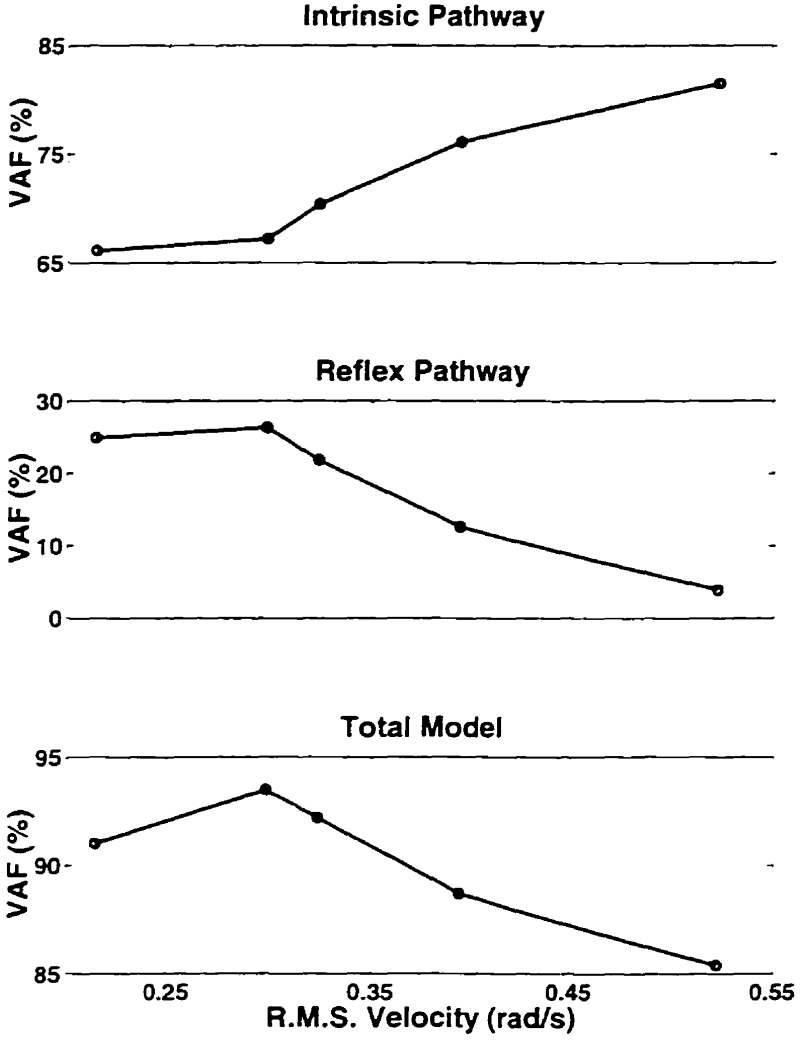

Figure 4.8: % of output torque variance accounted for by the intrinsic pathway, the reflex pathway and the whole parallel-cascade model plotted as a function of the r.m.s velocity of the superimposed perturbation. The data was acquired at voluntary contraction levels between -9.1 and -9.7 Nm. Subject - TR

In order to comprehensively investigate the effect of stochastically vibrating the ankle, experiments utilising transient stimuli were used. The hypothesis that reflexes were progressively attenuated as the displacement velocity increased was studied explicitly.

4.4 Reflex Attenuation

Reflexes were evoked by stretching the TS muscle, as shown in Figure 4.1.

Fig. 4.9 illustrates the effect of superimposing a stochastic (FGWN) signal with a peak-to-peak amplitude of 0.013 rad and a bandwidth flat to 30 hz onto a series of reflex-evoking pulse displacements (with amplitudes of about 0.025 rad). As expected, the reflex torque and EMG response decreased.

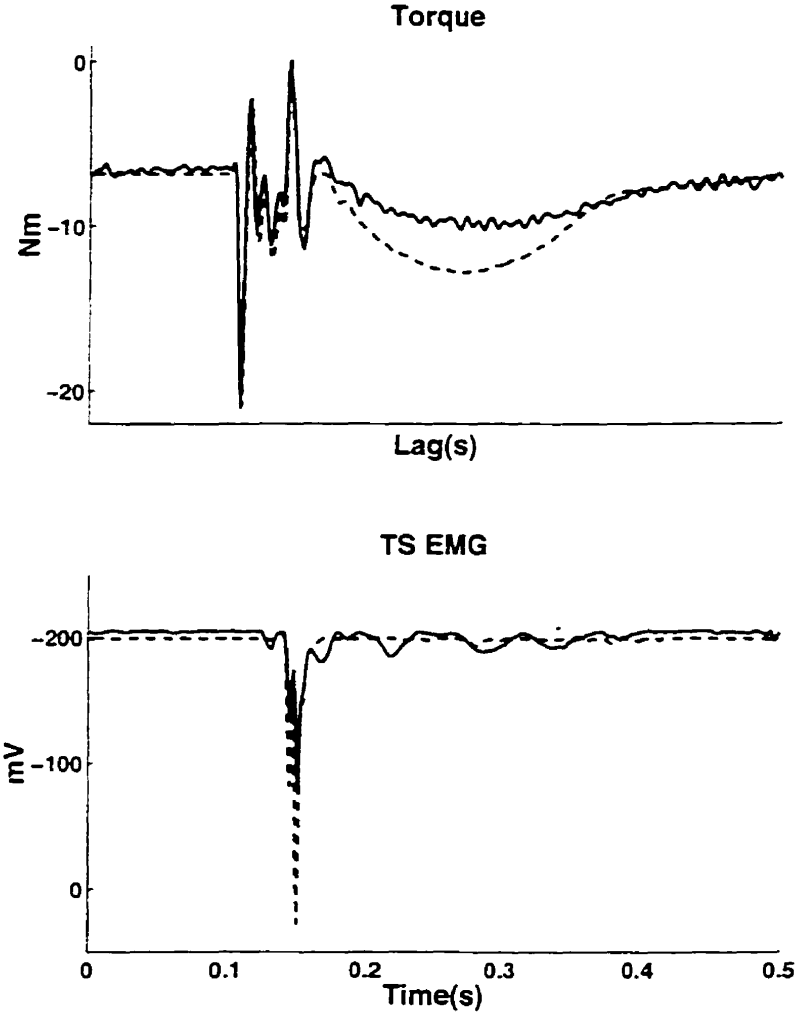

Figure 4.9: Effect of an imposed perturbation on the reflex torque and EMG response evoked by a series of dorsiflexing pulse displacements. The plot shows the ensemble-averaged data record. The dashed lines represent the responses obtained after the superposition of the imposed movement. Subject - RH

The presence of a passively applied movement attenuated the TS stretch reflex in a graded fashion. As demonstrated in Fig. 4.10, the torque generated by reflex mech-

anisms decreased as the average velocity of the superimposed movement increased. In the figure, the response to a dorsiflexing pulse displacement of 0.035 rad decreased from 8 Nm to 2 Nm in the presence of an ongoing PRBS sequence with a peak-to-peak amplitude of 0.011rad and a switching interval of 20ms (approximately equal to a zero-crossing rate of 25/s). The data, presented previously [80], corroborates the findings of Stein and Kearney [90].

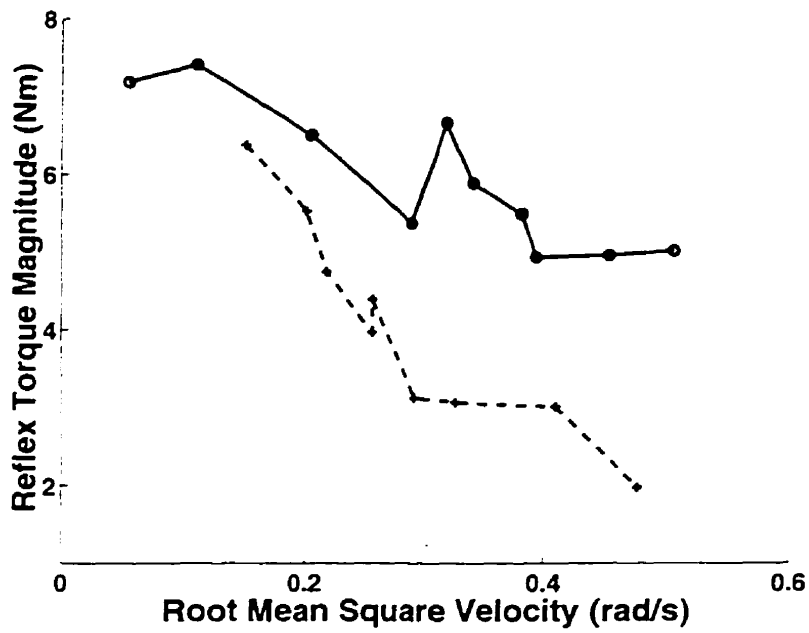

Figure 4.10: Attenuation of TS stretch reflex torque as a function of RMS velocity of the imposed perturbation (passive movement). The solid line represents a FGWN signal while the dashed line represents a PRBS input. Subject - BH

Of additional interest is the observation that a PRBS signal attenuates the reflex to a greater extent than a superimposed FGWN signal. For a given average velocity, the two signals have a different degree of reflex attenuation.

Since the level of attenuation seemed to depend on the *type* of signal, the following question was raised :

Which properties of the input perturbation are responsible for the velocity - mediated effects ?

Multiple Regression Analysis

In addition to the r.m.s. velocity and the unknown properties of the imposed movement, the reflex response has been shown to depend on the mean joint position, displacement pulse velocity and the level of voluntary contraction. In order to separate and quantify the relative importance of these factors, stepwise regression techniques were used.

The regression models generated to explain the reflex response data were intended to be tools used to guide experimental design. The conclusions of the tests for statistical significance are therefore not presented here. Empirical data generated by experiments are of greater significance; these results are presented below.

4.5 Perturbation Parameters

Since stochastic signals are described by their amplitude distributions and frequency spectra, the reflex attenuation experiments were repeated using signals with varying peak-to-peak amplitudes and zero-crossing rates.

The zero-crossing rate and the r.m.s. velocity appeared to be the statistically significant variables capable of modelling the reflex torque and EMG responses. Closer examination revealed that these two variables exhibited a high degree of collinearity. The r.m.s. velocity of a signal is a function of the zero-crossing rate and the peak-to-peak amplitude.

Consequently, experiments were redesigned such that the average perturbation velocity could be manipulated independently of the zero-crossing rate; signals possessing similar zero-crossing rates could have different average velocities.

4.5.1 Effect of ZC rate - Spectral Content

The results of the experiment described above are shown in Figure 4.11. For a given r.m.s. velocity, reflex attenuation is independent of the zero-crossing rate.

Since the zero-crossing rate reflects the spectral content of a signal, it is reasonable

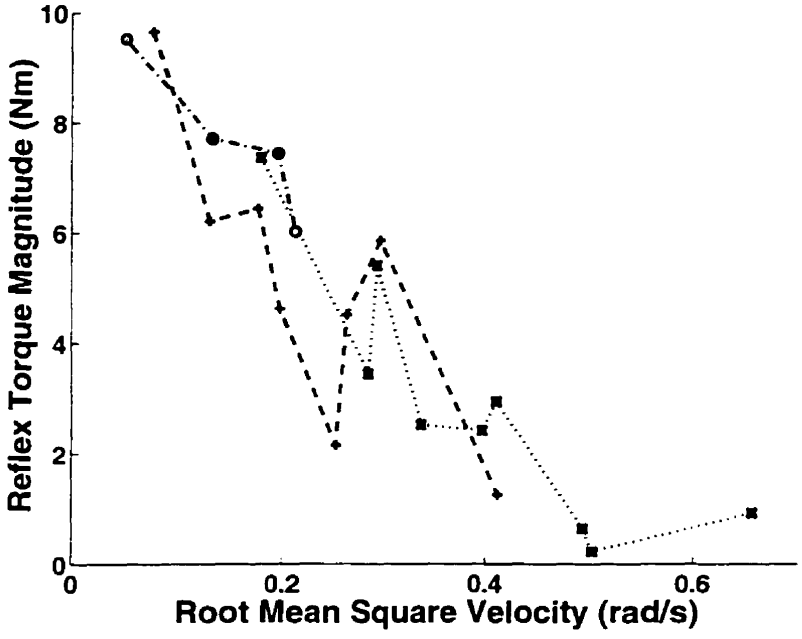

Figure 4.11: Effect of spectral content on the stretch reflex response to a dorsiflexing pulse displacement (*Dashed line : zero-crossing (zc) rate = 5; Dashdot line : zc rate = 13; Dotted line : zc rate = 26*). Subject - BH

to conclude that the frequency content of an applied movement is not explicitly responsible for the attenuation of the TS stretch reflex response. One must remember, however, that the r.m.s. velocity, instrumental in reflex attenuation, is influenced by the zero-crossing rate of the signal.

4.5.2 Effect of Amplitude Distribution

Multiple regression analyses of experiments designed to eliminate the collinear effects of the zero-crossing rate pointed towards the peak signal velocity and the r.m.s signal velocity as being the factors responsible for reflex attenuation.

In order to prevent covariation of peak velocity (dependent on peak-to-peak amplitude) and r.m.s velocity (dependent on peak-to-peak amplitude and zero-crossing rate), two new signals were created. The quaternary sequence(PRQS) and triangular sequence(PRTS) allow for the independent manipulation of peak velocity and r.m.s velocity.

Fig. 4.12 shows the effect of superimposing PRQS inputs onto a series of reflex-

evoking pulse displacements. The analysis was constrained to trials performed at a voluntary contraction level between -6 Nm and -7.5 Nm using displacement pulse velocities between 1.88 and 2.03 rad/s.

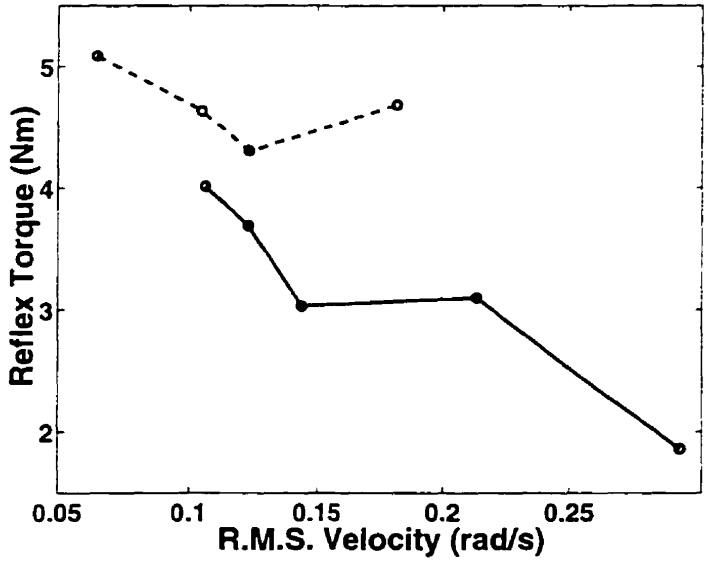

Figure 4.12: Effect of peak velocity on the stretch reflex response to a dorsiflexing pulse displacement (*Dashed line : peak velocity = 0.89 rad/s; Solid line : peak velocity = 1.27 rad/s*). Quaternary sequences (PRQS) were used as the passively applied movement. Subject - TK

Fig. 4.13 demonstrates the effect of applying PRTS movements to the ankle joint. Again the analysis was constrained; the trials were performed at a voluntary contraction level between -6.9 Nm and -8.2 Nm using displacement pulse velocities between 2.2 and 2.4 rad/s.

The r.m.s. velocity-mediated attenuation of the reflex response is apparent in both cases. This confirms previous conclusions reached using the Gaussian and binary sequence inputs. Passively applying a perturbation reduces the reflex response at the ankle joint.

From the graphs, the peak velocity seems to have an attenuating effect; for a given signal r.m.s velocity, the magnitude of the reflex torque response is smaller for a larger input peak velocity. Recall from Fig. 4.10 that the PRBS input exerted a greater degree of attenuation than the FGWN input; the PRBS signal has a larger peak velocity than the FGWN signal.

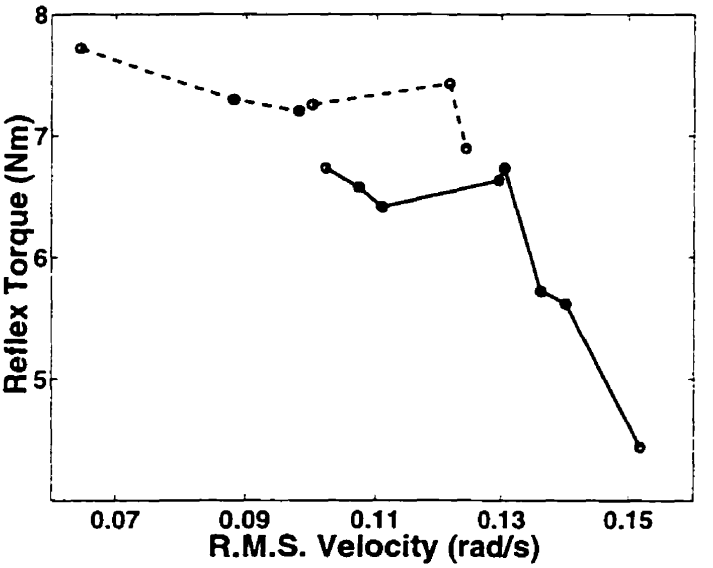

Figure 4.13: Effect of peak velocity on the stretch reflex response to a dorsiflexing pulse displacement (*Dashed line : peak velocity = 1.26 rad/s; Solid line : peak velocity = 1.47 rad/s*). Triangular sequences (PRTS) were used as the passively applied movement. Subject - TK

However, the difference between the dashed curves (lower peak velocity) and the solid curves (higher peak velocity) is not large in either Fig. 4.12 or Fig. 4.13. Hence, one cannot confidently conclude that peak velocity is one of the kinematic parameters responsible for reflex attenuation.

The experiments do show that the TS stretch reflex response decreases during passive movement of the ankle joint. The static gain of the reflex loop seems to be a function of the r.m.s velocity as well as some other, as yet unknown, features of the applied motion. The kinematic parameters affecting this mediation appear to be those describing the amplitude distribution rather than the frequency content of the perturbation.

Chapter 5

Discussion and Conclusions

We shall not cease from exploration
And the end of all our exploring
Will be to arrive where we started
And know the place for the first time.

- T.S. Eliot [34].

The objective of the preceding work was to ascertain the effects of passive motion on the stretch reflex dynamics at the human ankle joint. The modulation of the identified reflex dynamics and the attenuation of the reflex response to a brief stretch were demonstrated. An attempt was made to identify which kinematic parameters of the applied movement were responsible for diminishing the TS stretch reflex.

5.1 Summary of Results

The TS stretch reflex can generate torques of significant (up to 30 % of the MVC) magnitudes. Reflex mechanics are thus functionally important. An ongoing movement alters the magnitude of the impulse response function describing the reflex dynamics: the static gain decreases as the average velocity (expressed as a root mean square value) of the motion increases. The velocity-mediated modulation is due, in part, to the attenuation of the reflex response. The intrinsic dynamics do not appear

to change with the average velocity of an applied perturbation.

The ankle joint's reflex response to a brief dorsiflexing pulse displacement is diminished, in a graded fashion. The kinematic parameters responsible for the attenuation appears to be related to the amplitude distribution characteristics of the ongoing movement. The spectral content has no explicit effect on reflex diminishment.

The r.m.s. velocity is the most obvious parameter - reflex attenuation is proportional to the average velocity. However, it is not the sole signal property of importance. Although the significance of the signal's peak velocity may be inferred, there is a lack of conclusive evidence to support the hypothesis.

5.2 Original Contributions

A portion of this study deals with the analysis of data gathered from a series of system identification experiments performed with the PRBS signal. The analysis demonstrated the velocity-mediated modulation of the static gain of the stretch reflex dynamics. The second part of this work builds upon the results of Stein and Kearney[90]. The velocity-dependent attenuation of the stretch reflex response was shown in the presence of stochastic perturbations that differed from the FGWN signal used by Stein and Kearney. Although the r.m.s. velocity of the imposed movement was a significant determinant of the level of reflex attenuation, this study revealed that it was not the only factor involved. The study also showed that the movement parameters responsible for the observed effects appeared to be related to amplitude distribution characteristics rather than the spectral content.

5.3 Related Behaviour

5.3.1 H-Reflex Attenuation during Cyclical Movement

The attenuation of the reflex response to brief stretches of the TS in the presence of an ongoing passively-applied stochastic perturbation has been shown by Stein and Kearney (1995). The authors inferred that the inhibition was proportional to the

average velocity of the applied perturbation [90].

The velocity-mediated reflex gain noted here and in previous research [66, 90] seems to be consistent with the observation that H-reflex gain is lower during voluntary cyclical movements such as locomotion[20] running[88] and cycling[12]. The gain was noted to decrease as the speed of the motion increased: H-reflexes were lowest in running and highest while standing.

Attenuation of the H-reflex was also noted when the leg was *passively* rotated in a motion akin to cycling. The inhibition occurred in both the ipsilateral (same side) limb[73] and in the contralateral limb[25]. The decrease in reflex activity was found to be directly proportional to the speed of passive rotation.

5.3.2 Tonic Vibration Reflex

High-frequency vibration has been shown to decrease H-reflex and stretch reflex activity in a graded fashion. Furthermore, researchers have employed tendon vibration to decrease the effectiveness of the reflex response at the human ankle[5]. Increasing the amplitude and frequency of the vibration increases reflex attenuation[2]. However, there have been reports of H-reflex activity increasing with increased vibration frequency[28]. Despite the confusion, the TVR and the behaviour presented in this study are probably related. The present study, however, establishes that reflex modulation can occur over a wide range of perturbation frequencies; the effects were noted even when the bandwidth was limited to 5Hz. The preservation of the afferent volley evoked by a tendon tap or H-reflex in the presence of external vibration favors pre-synaptic mechanisms over occlusion as the primary determining mechanism [84].

5.3.3 Inhibition after Stretch

Decreased reflex activity has been noted after a muscle stretch. Aldridge and Stein (1992) noted that the response to two stretches or H-reflex stimuli, in a decerebrate cat, differs from what could be expected on the basis of a single stretch [4]. For intervals shorter than 100ms, the EMG produced by the second stretch was attenu-

ated. For a series of stretches at random intervals, the average reflex response was attenuated in proportion with the stretch rate. Afterhyperpolarization and synaptic mechanisms were cited as possible reasons.

Studies by Berardelli et al[10] and Kirsch et al[68], in humans, have yielded similar observations. Kirsch et al deduced that pre-synaptic inhibition was the mechanism responsible for the modulation. Stein and Kearney noted that the response to a dorsiflexing stretch was attenuated if preceded by a plantarflexing stretch [90]: the attenuation diminished as the time between the stretches was increased.

5.4 Physiological Explanations

Intrinsic dynamics are determined by the behaviour of the passive joint structures combined with the contractile and activation mechanisms. On the other hand, comprehension of the reflex dynamics involves taking the additional mechanics of proprioceptor function and the characteristics of nerve and synaptic transmission into account.

The presence of reflex modulation with small amplitude perturbations and the covariation of reflex EMG and torque during the pulse experiments suggest that the mechanisms responsible are neural rather than mechanical [90]. The velocity-mediated inhibition of reflexes during passively applied movement is to be expected: the spindles are known to be highly sensitive to velocity[72].

With the exception of the studies by Stein and Kearney and by Kearney et al, research on the effect of passively applied movement on the reflexes evoked by muscle stretch has been scant. The numerous H-reflex studies during cyclical movement have yielded similar results and seem to be the most relevant experiments for discussing the present findings. Although the H-reflex differs from the stretch reflex[19], studies using the former are widespread due to experimental convenience. Akazawa et al found that the H-reflex and stretch reflex were modulated similarly during locomotion in decerebrate cats[3]. It would therefore be useful to review movement H-reflex studies and the reasons used to explain them.

5.4.1 Afterhyperpolarization and Occlusion

Afterhyperpolarization has been used to explain the effect of previous stretches on the stretch reflex response in cats [4]. The preceding movement could successfully recruit a significant fraction of the motorneuron(MN) pool and place the motorneurons in a refractory state. When studied intracellularly, the depression in MN discharge was estimated to be of similar magnitude as that due to the maximum autogenic recurrent (postsynaptic) inhibition if the stimulation spikes were placed less than 25ms apart [45].

In humans, however, the relative refractory period is 4-5ms and the highest discharge rate of soleus motor units is an impulse every 60-100ms; only a small fraction of motor units will be refractory at a given time[20]. Kirsch et al discounted the possiblity even after a large stretch and reflexive burst [68]. Hence, it is doubtful that the small amplitude perturbations used in the present study could put the MN pool into a refractory state.

Occlusion of the spindle afferent nerves (the "busy-line" phenomenon), due to the presence of a constant discharge volley provoked by the ongoing movement, could explain the present behaviour. Once again, it is unlikely that the weak stochastic perturbations could attenuate the stretch reflex response using this mechanism [84, 90].

5.4.2 Postsynaptic Inhibition

The variation of the H-reflex magnitude with the soleus EMG level during walking suggested that post-synaptic effects might alter and attenuate reflex behaviour [20]. Later studies involving walking and running [88] observed that the motorneuron pool excitability (quantified by EMG) was not the only factor affecting H-reflex modulation. Capaday and Stein (1989) demonstrated that post-synaptic mechanisms could not regulate the magnitude of the H-reflex independently of the motorneuron recruitment level in cats [21]. Yang et al(1993) reiterated that soleus H-reflex modulation was not a reflection of the background excitability of the motorneuron pool. By

exclusion, the above-mentioned researchers settled on pre-synaptic inhibition as the causative mechanism.

5.4.3 Presynaptic Inhibition

Pre-synaptic inhibition was the favoured explanation for H-reflex modulation during the passive cycling studies by McIlroy et al(1992) and Collins and colleagues(1993) [25, 73]. It has also been used to explain reflex attenuation after a stretch [68] and during high-frequency tendon vibration. In a converse study, Capaday (1995) demonstrated that administering baclofen, a specific $GABA_B$ receptor agonist that increased pre-synaptic inhibitory effects, decreased the response to a soleus muscle stretch for a given background force in pre-mammilary cats, without affecting the intrinsic muscle properties [22].

Descending Control vs. Peripheral Control

Pre-synaptic inhibition can be exerted from a variety of sources. A study by Brooke et al (1995) attempted to find the source of the assumed pre-synaptic inhibitory effects. H-reflex gain was found to be attenuated at a latency of 50ms after passive pedalling began: the time is insufficient for supraspinal effects to be realized [13]. The immediate onset of reflex depression following an imposed stretch was similarly attributed (by Kirsch et al. 1993) to inhibition arising in peripheral sources [68]. Brooke et al(1995) also showed that the reflex modulation was present in people with clinically complete spinal cord lesions.

Unequivocally determining the source of possible pre-synaptic mechanisms is not currently feasible and is certainly beyond the scope of the present study.

5.4.4 Spindle Afferent Response

H-reflex studies are relatively independent of peripheral effects such as fusimotor drive: synaptic mechanisms are thus favoured as the important modulators. Primary spindle afferent response is known to be velocity-sensitive and to have a high-pass

dynamic response. The afferents are also known to be more sensitive to smaller perturbations [72].

The sensitivity of primary spindle afferents can be modulated by γ motorneuron activity. Fusimotor modulation was found to be important in high decerebrate cats walking on a treadmill [89]. Another study by Akazawa et al(1982) stated that the cyclic variation in reflex magnitude during midbrain stimulated locomotion in cats could not be accounted for by fusimotor activity and offered pre-synaptic inhibition as the responsible mechanism.

5.4.5 Closing Statements

Given the predisposition of researchers towards attributing H-reflex modulation and attenuation during cyclical movements to pre-synaptic inhibition, it is an attractive explanation for the present findings. Furthermore, the experiments were all performed at a constant level of voluntary activation: the reflex modulation was present without modulation in the background EMG level. The spindle afferent activity cannot be excluded as a possible contributor to velocity-mediated reflex attenuation.

5.5 Related Phenomena

5.5.1 Second-Order Models

Second-order systems have successfully been used to model the overall joint dynamics even though they do not account for the reflex dynamics or delay [62]. As demonstrated above the overall dynamics are a combination of the both intrinsic and reflex effects.

On examining the protocols used in these identification experiments [58, 46, 70, 97, 98, 96], one notices that the signals had peak-to-peak amplitudes between 0.05 rad and 0.09 rad and had bandwidths that were flat to 25 Hz and contained significant power to 50Hz. Although signal velocities were not reported, they can be inferred from the amplitude and spectral data provided. During the attenuation trials de-

scribed in Chapters 3 and 4, an FGWN perturbation have a peak-to-peak amplitude of 0.01 rad and a bandwidth of 50HZ was found to attenuate the reflex response by 35%. Consequently, it can be assumed that the perturbations used in these earlier experiments attenuated the reflex mechanics and decreased the significance of the reflex pathway due to high velocities imposed onto the system.

5.5.2 Previous Parallel-Cascade Model

The current parallel-cascade model is based on a previous attempt by Perreault et al [81] to separate the intrinsic and reflex components of ankle joint dynamics. The FGWN inputs used by Perreault had peak-to-peak amplitudes of 0.065 rad and a bandwidth flat to 20Hz with a 40dB/decade rolloff. The high average velocity of the signal probably attenuated the reflex dynamics resulting in the low VAF in some subjects and the apparent absence of reflex mechanisms in others.

5.5.3 Effect of Input Amplitude on Reflex Stiffness Identification

In a previous study investigating the dynamic relation between half-wave rectified ankle velocity and TS EMG, Kearney and Hunter (1983) demonstrated that the reflex gain decreased systematically with increased peak-to-peak amplitude of the input position perturbation[59]. Considering that an increasing peak-to-peak amplitude translates into a higher average signal velocity, these results are consistent with the findings of the present study.

5.5.4 Effect of Input Amplitude on Overall Stiffness Identification

The dependence of the overall joint stiffness on the peak-to-peak amplitude of the perturbing input has been stated in numerous studies. Kearney and Hunter (1982) demonstrated the decrease in the viscous and elastic parameters (and in the reso-

nant frequency) when input signal peak-to-peak amplitudes were increased. Brown et al(1982) found that large amplitude sinusoidal movements did not generated correspondingly large reflex responses in the human thumb. Similar findings were reported by Cooker et al(1980) and Evans et al(1983) in the human jaw[26] and ankle joint[36]. Both Joyce et al(1974) and Bennet and colleagues(1992) have reported a decrease in the resonant frequency[52] and a drop in the elastic stiffness[9] at the elbow joint with increased displacement amplitude.

It is possible that the reflex contribution to the overall stiffness was attenuated to a greater degree as the displacement amplitude increased. The parallel-cascade model used in this study demonstrated how reflex activity can augment the overall joint stiffness. Increasing the displacement amplitude increases the average displacement velocity and consequently decreases the reflex gain.

5.5.5 Effect of Stochastic Perturbations on Reflex Evocation

Kirsch et al(1993) explicitly assessed the effect of stochastic perturbations on stretch reflex properties at the human ankle. The reflex EMG generated by an imposed ramp stretch was compared to the response when a superimposed perturbation was added[68]. The reflex response was observed to not be significantly affected by the addition of the perturbation.

Kirsch et al used a ramp displacement of 0.13 rad (with a peak velocity of 6 rad/s) while the subject was exerting a voluntary contraction equal to 15% of the MVC. In the present study, the peak velocity of the reflex-evoking displacement was generally in the range of 2–3 rad/s. It is probable that the ramp displacement in the Kirsch study was supramaximal and caused the saturation of the reflex activation dynamics; superimposing a stochastic perturbation with a displacement amplitude of 0.036 rad may have not been sufficiently attenuating to reduce the reflex response below its saturation level.

5.6 Possible Implications – Reflex Function and Modulation

The deceptively simple monosynaptic stretch reflex has proven to be context-sensitive and highly modulated during a task. The reflex modulation is of great functional importance. Yang et al inferred that the stretch reflex could potentially generate between 30% and 60% of the soleus EMG generated during the walking cycle. The H-reflex gain was found to vary systematically with the phases of leg movement during pedalling, running and walking. The reflexes were most pronounced during the power-producing phase in locomotion and cycling, when they can substantially contribute to force generation. They are strongly depressed during the swing phase in locomotion; their presence would be a hindrance to movement.

Given the previous findings, it is not surprising that reflexes might be attenuated under vibratory conditions or during movement. An active stretch reflex that responds to every movement would be an impediment to functioning in a environment replete with passively applied motions.

5.7 Experimental Considerations

Analyzing biological systems by empirical means often requires the tedious repetition of experimental trials to ascertain the best possible protocol. In this section, I have outlined the reasoning behind the methods used in this project.

The subjects were asked not to resist the pulse displacements in order to avoid evoking long-latency reflexes.

A 3 second interval was used between successive pulses to prevent reflex modification; the effects of ongoing perturbations and passively applied stretches have been documented above. Sinkjaer et al noted that the response to the first of a series of stretches was greater than the responses to subsequent stretches [86].

5.7.1 Muscle Fatigue

A constant sub-maximal isometric contraction will become progressively difficult to hold and will be accompanied by an increase in EMG variance [62]. The increase in neural activation required to sustain a constant force is deemed muscle fatigue. Provided that the mean voluntary level of contraction was held constant, ankle dynamic stiffness was shown to be invariant [48]. Nevertheless, the onset of fatigue is detrimental to a volunteer's comfort and his/her desire to participate in a subsequent experiment.

The experiments were designed to inhibit fatigue onset. The subjects were asked to maintain small tonic contractions (5 - 15 % of MVC) during the experimental trials. Target torque matching was discontinued if a subject became too tired. The perturbations superimposed onto the reflex-evoking pulse displacements had small peak-to-peak amplitudes; this limited the required degree of ensemble averaging and consequently reduced the length of an experimental trial. The use of small-amplitude perturbations minimized nonlinear effects. One downfall of the approach was that it limited the range of perturbation velocities that could be investigated. The new boot design permitted easy ingress and egress of the foot into and out of the boot. Frequent breaks could thus be taken during the course of an experiment.

The attenuation trials were randomized so that the possible presence of fatigue would contribute to variability in the data rather that systematic modifications. Pulse displacements of fixed amplitude and applied at constant voluntary torques were used as controls before and after attenuation trials.

The variation in EMG, with fatigue, is greater than the variation in torque (see references cited in [98]). Hence, the velocity-mediated modulation of reflex responses to pulse displacements was demonstrated in terms of the reflex torque rather than the reflex EMG.

5.7.2 Problems with Axis Determination

Although problems with ankle fixation and subject discomfort have been removed, one area of the boot construction protocol requires substantial improvement. Accurately locating the ankle's axis of rotation has proven to be rather difficult. An off-axis estimate results in the infliction of pain onto the subject and necessitates the construction of a new boot.

The current method infers the axis location from anatomical landmarks [51]. As Isman and Inman stated[51], the variation from subject to subject (standard deviations of 4–5 mm) requires individual determination to accurately pinpoint the axis position.

Myre used a 6 degree-of-freedom position sensor coupled with a least-squares estimation procedure to determine the axis of rotation [78]. Although reasonable estimates were obtained, the assumption of rigid-body motion was contravened when relative motion occurred between the sensor attached to the skin and the skeletal structure beneath. Attempts to practically apply the estimation procedure are currently being undertaken.

5.8 Future Work

Factors involved in reflex attenuation

Previous studies have revealed that the magnitude of the short-latency reflex EMG response increases with the acceleration of the reflex-evoking ramp displacement [10], and that the reflex response could be modelled using joint acceleration as one of the inputs [32]. Furthermore, the primary spindle afferents have been shown to be sensitive to acceleration [72].

It is consequently possible that the average or peak acceleration of an applied perturbation may be an additional signal property responsible for reflex attenuation. The present study could not distinguish acceleration effects since the acceleration parameters covaried closely with the corresponding velocity parameters. Future in-

vestigation would require the design of an input signal that possessed independently modifiable acceleration and velocity parameters.

System Identification Techniques

It has been established that perturbing the ankle joint attenuates reflex responses. Hence, system identification techniques, which involve the stochastic vibration of the foot, will alter the system as it is being "identified." System identification does have numerous benefits though; it is a non-invasive method of analyzing the dynamic properties of both intrinsic and reflex mechanisms in the neuromuscular system. The parallel-cascade technique, presented here, separates the intrinsic and reflex contributions by exploiting the delay inherent in all reflex systems. As long as the conduction delay is longer than the IRF describing the intrinsic mechanics, the techniques can be extended to other joints (in principle) [66].

Of necessity is the development of an input perturbation signal rich enough in amplitude and spectral content to adequately excite the system without depressing the stretch reflex response.

The optimal input signal should have a low average velocity; it would resemble the PRBS input (as opposed to the FGWN input). The frequency structure of the signal would be important in that it should be limited to the range of frequencies necessary for the experiment. The stretch reflex contribution is significant over a narrow range of frequencies (5–10 Hz) due to the combination of low-pass muscle activation dynamics[37] and the high-pass spindle dynamic response[72]. An ideal input signal consequently should have a velocity spectrum with power in that frequency range.

Reflexes in Posture

Previous experiments that characterised the dynamic stiffness of the ankle at various operating points must be repeated with an input perturbation that does not inhibit reflex mechanisms.

Reflexes during Locomotion

By superimposing the reflex-evoking pulse displacements onto a simulated walking trajectory, reflex attenuation can be studied at various points in the gait cycle. In addition, superimposing small-amplitude stochastic perturbations onto the simulated walking trajectory would enable the identification of time-varying reflex dynamics during locomotion.

Other Joints

The techniques developed to study the ankle can be extended to other joints in the human body. The knee and elbow joints are currently under investigation in the Neuromuscular Control Lab.

5.9 Closing Remarks

Due to the highly non-linear interaction between the reflex and intrinsic mechanisms which are in turn strongly modulated by voluntary actions, ascertaining the reflex contribution to posture and movement remains an ongoing effort. Additional work is also required to clarify how much of the reflex modulation is due to peripheral feedback and how much is due to CNS mechanisms. Armed with the knowledge gained about reflex attenuation, the current parallel-cascade technique can be improved to study the complex workings of the human neuromuscular system in terms of its joint dynamics.

Appendix A

Stochastic Input Generation

The MATLAB code used to generate the binary sequence, quaternary sequence and triangular sequence inputs is displayed below. The m-file was designed to work with a host of other programs developed to execute the experimental protocol with the aid of graphical user interfaces. *These files are stored in a common directory in the resident workstations of the Neuromuscular Control Lab. The current directory address is : /home/ralph/REKLAB/matlab/exp/ .*

```
function  exp_sequence_setup (mode)
%function  exp_sequence_setup (mode)
%mode = 'binary' : binary (2-level) perturbation
%mode = 'quat'   : quaternary (4-level) perturbation
%mode = 'tri'    : triangular (2-level with sloped sides) perturbation
disp('Define sequence characteristics');
global DISPLAY_FIG
global RANDOM_DA DA_DISPLAY_RATE
global BIN_SEQUENCE_STIM QUAT_SEQUENCE_STIM TRI_SEQUENCE_STIM
global BIN_SEQUENCE_COMMENT QUAT_SEQUENCE_COMMENT TRI_SEQUENCE_COMMENT
global SEQ_INTERVAL SEQ_LEN SEQ_AMP TRI_SEQ_SLOPE
exp_menu('update', 'h_status','Set parameters for sequence perturbation');
rand('seed',sum(100*clock));
% {{{ Get stimulus parameters
```

```
da_incr = 1000/DA_DISPLAY_RATE; nswitch= SEQ_LEN*1000/SEQ_INTERVAL;
disp(['Number of transitions =' int2str(nswitch)]);
stim = rand(nswitch,1);
% }}}
% {{{ Generate binary sequence stimulus
if (strcmp(mode,'binary'))
  stim = (stim>=.5);  stim = (stim*SEQ_AMP*10/range(stim));
  stim = (stim-mean(stim));  np = SEQ_INTERVAL/da_incr; seq_stim =[];
  for i=1:length(stim),
    seq_stim = [seq_stim zeros(1,np)+stim(i)];
  end
  BIN_SEQUENCE_COMMENT=[ 'BinSeq; A='  num2str(SEQ_AMP), ...
    ';L=' num2str(SEQ_LEN) ';R=' int2str(SEQ_INTERVAL)];
% }}}
% {{{ Plot stimulus sequence
  figure (DISPLAY_FIG); subplot(111); plot_d (seq_stim,da_incr/1000,0);
  drawnow; title ('Binary Sequence Stimulus');
% }}}
  exp_menu('update', 'h_status','Binary sequence setup done');
  BIN_SEQUENCE_STIM = seq_stim;
% {{{ Generate quaternary sequence stimulus
elseif (strcmp(mode,'quat'))
  stim1 = (stim>=(3/4));
  stim1 = (stim1*SEQ_AMP*10/range(stim1));
  stim2 = (stim<(3/4)&stim>=(2/4));
  stim2 = (stim2*SEQ_AMP*(10*2/3)/range(stim2));
  stim3 = (stim<(2/4)&stim>=(1/4));
  stim3 = (stim3*SEQ_AMP*(10*1/3)/range(stim3));
  stim = (stim1+stim2+stim3);  stim = (stim-mean(stim));
  np = SEQ_INTERVAL/da_incr; seq_stim =[];
  for i=1:length(stim),
    seq_stim = [seq_stim zeros(1,np)+stim(i)];
```

```
  end
  QUAT_SEQUENCE_COMMENT=[ 'QuatSeq; A='  num2str(SEQ_AMP), ...
    ';L=' num2str(SEQ_LEN) ...
    ';R=' int2str(SEQ_INTERVAL)];
% }}}
% {{{ Plot stimulus sequence
  figure (DISPLAY_FIG); subplot(111); plot_d (seq_stim,da_incr/1000,0);
  drawnow; title ('Quaternary Sequence Stimulus');
% }}}
  exp_menu('update', 'h_status','Quaternary sequence setup done');
  QUAT_SEQUENCE_STIM = seq_stim;
% {{{ Generate TRIANGULAR sequence stimulus
elseif (strcmp(mode,'tri'))
  stim = (stim>=.5);
  stim = (stim*SEQ_AMP*10/range(stim)); stim = (stim-mean(stim));
  np = SEQ_INTERVAL/da_incr; slope = TRI_SEQ_SLOPE;
  seq_stim = []; seq_stim = [seq_stim zeros(1,np)+stim(1)];
  counter = rand(nswitch,1);
  for i=2:length(stim),
      if (stim(i) > stim(i-1))
if (counter(i) >= .667)
  seq_stim = [seq_stim zeros(1,np)+stim(i)];
elseif (counter(i) < .667)
  seq_stim = [seq_stim  stim(i-1):(range(stim)/slope):stim(i)...
          zeros(1,(np-slope-1))+stim(i)];
        end
      elseif (stim(i) < stim(i-1))
if (counter(i) >= .667)
  seq_stim = [seq_stim zeros(1,np)+stim(i)];
elseif (counter(i) < .667)
          seq_stim = [seq_stim  stim(i-1):-(range(stim)/slope):stim(i)...
           zeros(1,(np-slope-1))+stim(i)];
```

```
        end
      elseif (stim(i) == stim(i-1))
seq_stim = [seq_stim zeros(1,np)+stim(i)];
      end
  end
  TRI_SEQUENCE_COMMENT=[ 'TriSeq; A='  num2str(SEQ_AMP), ...
    ';L=' num2str(SEQ_LEN) ...
    ';R=' int2str(SEQ_INTERVAL) ...
    ';S=' num2str(TRI_SEQ_SLOPE)];
% }}}
% {{{ Plot stimulus sequence
  figure (DISPLAY_FIG); subplot(111); plot_d (seq_stim,da_incr/1000,0);
  drawnow; title ('Triangular Sequence Stimulus');
% }}}
  exp_menu('update', 'h_status','Triangular sequence setup done');
  TRI_SEQUENCE_STIM = seq_stim;
end
% {{{ Emacs local variables
%$$$ Local variables:
%$$$ folded-file: t
%$$$ end;
%$$$
% }}}
```

Appendix B

Multiple Linear Regression

B.1 Background

The voluntary level of contraction in addition to the various kinematic parameters of the superimposed stochastic perturbations and the reflex-evoking pulse displacement were all considered to be potentially important factors contributing to the magnitude of the reflex response. Due to the servo-controller, the joint position was always maintained at a fixed level and could thus be ignored as a contributor.

Regression enables the prediction of a model that expresses a dependent variable in terms of independent variables. Specifically, multiple regression explains how much of the variation in the dependent variable can be attributed to changes in the independent variable. Statistical hypothesis testing could then be used to ascertain the significance of the independent variables.

Detailed information on the terms and concepts outlined below can be obtained from any statistics text [75].

B.1.1 Independent and Dependent Variables

The dependent variables used in this study were the maximum reflex torque generated and the corresponding value of reflex EMG.

The independent variables included the voluntary level of contraction, the peak

amplitude, velocity and acceleration of the reflex-evoking pulse as well as the the peak-to-peak amplitude and zero-crossing rate of the superimposed perturbation. The mean absolute, root mean square and peak velocities and accelerations of the imposed passive movement were also included.

B.1.2 Model

A probabilistic model, consisting of a deterministic portion and a random error was used for the regression analysis :

$$Y = XB + E \tag{B.1}$$

Y and E represent the dependent variable and the random error respectively. X is a row matrix containing 1 and the 3 independent variables X_1, X_2, and X_3. B is a column matrix constituted of the unknown parameters, B_0, B_1, B_2 and B_3. A least squares estimation procedure is used to ascertain B :

$$\hat{B} = (X'X)^{-1}X'Y \tag{B.2}$$

A number of important assumptions were essential for the development of the model. The mean and variance of the probability distribution of the error, E are 0 and a constant respectively. E was also assumed to have a normal probability distribution. The errors associated with any two different observations were regarded as being independent.

B.1.3 Model Testing

Stepwise regression techniques were used to screen out the unimportant "independent" variables. The afore-mentioned assumptions were validated using *residual analysis.*

The *adjusted multiple coefficient of determination*, R_{A2}, defined as the percentage

of the sample variation attributable to or explained by the independent variables, was used to quantify the model's adequacy. R_{A2} takes the sample size and number of B parameters into consideration.

The importance of the independent variables were judged by using statistical tests at a 95% confidence level. The overall model adequacy was examined by checking the hypothesis that one of the B parameters were equal to 0 (F-test). 2-sided T-tests were used to dispell the hypothesis that each B parameter had a value of 0. A non-zero value of B_i indicates that the coefficients are significant contributors to the model.

B.1.4 Limitations

Multiple linear regression implicitly assumes that the independent variables are independent. In order to avoid the spurious results associated with *multicollinearity*, linear correlation tests were used to examine the level of correlation between independent variables. The *Pearson product moment coefficient of correlation*, r, was used as a measure of the strength of the linear relationship between two variables.

In conclusion, one should note that statistical models and tests are tools used to guide the direction of future research. Statistical significance does not establish a cause-and-effect relationship.

B.2 M-files

B.2.1 Multiple Regression with 3 independent variables

```
function[J]=ferret(names, string)
%function[J]=ferret(names, string)
%Determines a vector identifying the location of specific data from
%the tables generated by the table_read command
J=[];
for i=1:length(names)
  if findstr(names(i,:),string)
    j=1;
```

```
    else
    j=0;
  end
  J=[J j];
end

function[OUT]=SS(X,Y)
%function[OUT]=SS(X,Y)
%SS(X,Y)=Summation(i = 1 --> N)[[Xi-mean(X)][Yi-mean(Y)]]
%Xi and Yi are the ith elements of vectors X and Y respectively
%X and Y must have the same length (N)
OUT=0;
OUT=sum(X.*Y)-[(sum(X)*sum(Y))/length(X)];

function[T_stat5,X1,X2,X3,Y,B,VAR,R_sq]=...
mult_reg3(f,c,ind_var1,ind_var2,ind_var3,dep_var,optA,optB)
%function[T_stat5,X1,X2,X3,Y,B,VAR,R_sq]=...
mult_reg3(f,c,ind_var1,ind_var2,ind_var3,dep_var,optA,optB)
%performs multiple linear regression with 3 independent variables
%works with data tables generated by the pulse_batch command
%     T_stat5=test statistic
%     X1=independent variable data set 1
%     X2=independent variable data set 2
%     X3=independent variable data set 3
%     Y=dependent variable data set
%     B=parameters that fit the following model
%          Y=XB+e; e = vector of random error; B = [Bo;B1;B2;B3];
%          E{Y}=expected value of Y = Bo + B1*X1 + B2*X2 + B3*X3
%     VAR=variance of the random error, e
%     R_sq=multiple coefficient of determination
%     f=filelb file from which the table is obtained
%     c=case number
```

```
%     ind_var=independent variable name
%     dep_var=dependent variable name
%     optA and optB allow for changes to the module
%     their default values are 1 (if no values are entered)
%optA=1 : the whole module will be used
%optA=2 : part of the module is used (calc of T_stat(n) for stepreg.m)
%optB=1 : zero elements are removed from X and Y vectors
%optB=2 : zero elements are NOT removed from X and Y vectors
%f,ind_var,dep_var are strings and
%should be entered using single quotes
%the assumptions associated with statistical regression analysis are
%applicable here (see lin_reg.m)
if (nargin<8)
  optB=1;
  end
if (nargin<7)
  optA=1;
  end
[table,names,comment]=table_read(f,c);
[s]=ferret(names,ind_var1);[t]=ferret(names,ind_var2);
[u]=ferret(names,ind_var3);[v]=ferret(names,dep_var);
X1=table(:,s);X2=table(:,t);X3=table(:,u);Y=table(:,v);
% if the linear regression is being performed on variables related to
% the stochastic perturbation, the entries corresponding to the
% perturbation parameters should not be taken into account
% (they will have values of 0)
if (optB==1)
ind_s1=findstr(ind_var1,'pert_');
if (ind_s1==1)
  s1=find(X1);
  X1=X1(s1); X2=X2(s1); X3=X3(s1); Y=Y(s1);
  end
```

```
ind_s2=findstr(ind_var2,'pert_');
if (ind_s2==1)
  s2=find(X2);
  X1=X1(s2); X2=X2(s2); X3=X3(s2); Y=Y(s2);
  end
ind_s3=findstr(ind_var3,'pert_');
if (ind_s3==1)
  s3=find(X3);
  X1=X1(s3); X2=X2(s3); X3=X3(s3); Y=Y(s3);
  end
dep_s=findstr(dep_var,'pert_');
if (dep_s==1)
  s4=find(Y);
  Y=Y(s4); X1=X1(s4); X2=X2(s4); X3=X3(s4);
  end
end
n=length(Y);  X=[ones(n,1)  X1  X2  X3];
% deterministic model parameters are fit by using a minimum
% least-squares solution
cov=inv(X'*X); proto_B=cov*X'; B=proto_B*Y;
%to find the random error variance associated with the fitted model
%SSE=sum of squared deviations from the fitted model
SSE=(Y'*Y)-(B'*X'*Y);  VAR=SSE/(n-4);
%to compute the multiple coefficient of determination,R_sq
R_sq=1-(SSE/SS(Y,Y));
%to compute the adjusted multiple coefficient of determination,
%R_sq_adj, whcich takes the number of variables into account
R_sq_adj=1-(((n-1)/(n-4))*(1-R_sq));
%to test the overall adequacy of the model, the analysis of variance
%F test is used to examine the null hypothesis : B1=B2=B3=0
%a 2-sided t-test is used to evaluate the individual parameter coeff.
%by examining  the null hypotheses : B1=0,B2=0,B3=0
```

```
%if T_stat,(F_stat) is larger than T_alpha(F_alpha),
%the null hypothesis is rejected with 95 % confidence
F_stat=(R_sq/3)/((1-R_sq)/(n-4));
B1=B(2); B2=B(3); B3=B(4);
SB1=sqrt(VAR)*sqrt(cov(2,2)); SB2=sqrt(VAR)*sqrt(cov(3,3));
SB3=sqrt(VAR)*sqrt(cov(4,4));
T_stat3=B1/SB1; T_stat4=B2/SB2; T_stat5=B3/SB3;
if (optA==1)
F_alpha=input(['Enter the F value for numerator d.o.f.= 3,...
 denominator d.o.f.= ' num2str(n-4) ' and alpha=0.05 : '])
if (F_stat > F_alpha)
  disp('B1,B2 and(or) B3 are(is) NOT EQUAL to 0')
  else
    disp('B1,B2 and(or) B3 are(is) EQUAL to 0')
  end
T_alpha=input(['Enter the T value for ' num2str(n-4) ' d.o.f. and ...
alpha=0.025 : '])
if (abs(T_stat3) > T_alpha)
  disp('B1 is not equal to 0')
  else
    disp('B1 is equal to 0')
  end
if (abs(T_stat4) > T_alpha)
  disp('B2 is not equal to 0')
  else
    disp('B2 is equal to 0')
  end
if (abs(T_stat5) > T_alpha)
  disp('B3 is not equal to 0')
  else
    disp('B3 is equal to 0')
  end
```

```
disp(['The confidence interval for B1 = ...
' num2str(B1-(T_alpha*SB1)) ' to ' num2str(B1+(T_alpha*SB1))])
disp(['The confidence interval for B2 = ...
' num2str(B2-(T_alpha*SB2)) ' to ' num2str(B2+(T_alpha*SB2))])
disp(['The confidence interval for B3 = ...
' num2str(B3-(T_alpha*SB3)) ' to ' num2str(B3+(T_alpha*SB3))])
disp(['R_sq = ' num2str(R_sq)])
disp(['R_sq_adj= ' num2str(R_sq_adj)])
% a RESIDUAL ANALYSIS can be used to detect :
% 1 - model misspecification
% 2 - unequal variances
% 3 - nonnormality of the random error
% 4 - outliers and influential observations
% 5 - time correlated errors (NOTE : necessary for TIME SERIES data)
%  5 is not a concern
%  1 and 2 can be detected visually by plotting the residuals
%  against the independent variables
%  3 is investigated using a histogram of the residuals
%  Outliers are residual points larger than 3*s ; their influence
%  should be determined before eliminating it
Y_est=X*B; Res=Y-Y_est; s=sqrt(VAR);
s_plot1=ones(n,1).*3*s; s_plot2=-1.*s_plot1;
Y_plot=[min(Y_est):(range(Y_est)/(n-1)):max(Y_est)]';
figure(1)
plot(Y_est,Y,'o',Y_plot,Y_plot)
xlabel(['estimated ' num2str(dep_var)])
ylabel(['observed ' num2str(dep_var)])
title([num2str(comment) ' : R squared = ' num2str(R_sq)])
subplot(311)
plot(X1,Y,'+',X1,Y_est,'o')
xlabel([num2str(ind_var1)]); ylabel([num2str(dep_var)])
subplot(312)
```

```
plot(X2,Y,'*',X2,Y_est,'o')
xlabel([num2str(ind_var2)]); ylabel([num2str(dep_var)])
subplot(313)
plot(X3,Y,'*',X3,Y_est,'o')
xlabel([num2str(ind_var3)]); ylabel([num2str(dep_var)])
figure(2)
subplot(411)
plot(X1,Res,'+')
xlabel([num2str(ind_var1)]); ylabel([num2str(dep_var) ' residual'])
subplot(412)
plot(X2,Res,'*')
xlabel([num2str(ind_var2)]); ylabel([num2str(dep_var) ' residual'])
subplot(413)
plot(X3,Res,'*')
xlabel([num2str(ind_var3)]); ylabel([num2str(dep_var) ' residual'])
subplot(427)
[M,H]=hist(Res);
bar(H,M./sum(M))
xlabel([num2str(dep_var) ' residual']); ylabel('percentage')
subplot(428)
plot(Y_est,Res,'x',Y_plot,s_plot1,':',Y_plot,s_plot2,':')
xlabel(['estimated ' num2str(dep_var)])
ylabel([num2str(dep_var) ' residual'])
figure(3)
plot(Y_est,Y,'o',Y_plot,Y_plot)
xlabel(['estimated ' num2str(dep_var)])
ylabel(['observed ' num2str(dep_var)])
title([num2str(comment) ' : R squared = ' num2str(R_sq)])
end
```

B.2.2 Test for Correlation - Linear Regression

```
function[T_stat1,X,Y,B,r,r_sq]=...
lin_reg(f,c,ind_var,dep_var,optA,optB,optC,ind_var2)
%function[T_stat1,X,Y,B,VAR,r,r_sq]=...
lin_reg(f,c,ind_var,dep_var,optA,optB,optC,ind_var2)
%performs linear regression
%works with data tables generated by the pulse_batch command
%     T_stat1=test statistic
%     X=independent variable data set
%     Y=dependent variable data set
%     B=parameters that fit the following linear model
%          Y=XB+e; e = vector of random error
%                  B = [Bo;B1]; Bo=intercept, B1=slope
%                  E{Y} = expected value of Y = Bo + B1*X
%     r=Pearson product moment coefficient of correlation
%     r_sq=Coefficient of determination
%     f=filelb file from which the table is obtained
%     c=case number
%     ind_var=independent variable name
%     dep_var=dependent variable name
%     optA,optB,optC allow for changes
%     their default values are 1 (if no values are entered)
%  optA=1 : the whole module will be used
%  optA=2 : part of the module is used (calc of T_stat1 for stepreg.m)
%  optB=1 : X = X
%  optB=2 : X = X.^2 : E[Y] = Bo + B1*X.^2
%  optB=3 : X = X1*X2 : E[Y] = Bo + B1*X1*X2
%  optC=1 : zero elements are removed from X and Y vectors
%  optC=2 : zero elements are NOT removed from X and Y vectors
%  ind_var2=second independent variable (used when optB=3)
%f,ind_var,dep_var,dep_var2 are strings and should be entered using...
%single quotes
 %ASSUMPTIONS involved in a statistical regression analysis
```

```
%  1 - mean of the prob dist of e is 0
%  2 - variance of the prob dist of e is constant for all values of X
%  3 - prob dist of e is normal
%  4 - errors associated with 2 different observations are independent
if (nargin < 5)
  optA = 1;
  end
if (nargin < 6)
  optB = 1;
  end
if (nargin < 7)
  optC = 1;
  end
if (nargin < 8)
  ind_var2 = ' ';
  end
[table,names,comment]=table_read(f,c);
[u]=ferret(names,ind_var);
[v]=ferret(names,dep_var);
[w]=ferret(names,ind_var2);
if (optB==1)
  X=[table(:,u)];
elseif (optB==2)
  X=[table(:,u).*table(:,u)];
elseif (optB==3)
  X=[table(:,u).*table(:,w)];
end
Y=table(:,v);
% if the linear regression is being performed on variables related to
% the stochastic perturbation, the entries corresponding to the
% pertbn parameters should not be taken into account
% (they will have values of 0)
```

```
if (optC==1);
ind_s=findstr(ind_var,'pert_');
if (ind_s==1)
  s1=find(X);  X=X(s1);  Y=Y(s1);
  end
dep_s=findstr(dep_var,'pert_');
if (dep_s==1)
  s2=find(Y);  Y=Y(s2);  X=X(s2);
  end
end
n=length(X); X_calc=[ones(n,1) X];
% deterministic model parameters are fit by using a minimum
%least-squares solution
p_inv=inv(X_calc'*X_calc); proto_B=p_inv*X_calc'; B=proto_B*Y;
%SSE=sum of squares of deviations of the y values about their
%predicted values; the least squares line has a smaller SSE than
%any other straight line model
%VAR=unbiased estimator of the variance of the random error,e
%SDV=estimated standard deviation of e
%most of the observed y values are expected to lie within 2s of their
%respective predicted values
B0=B(1); B1=B(2);
SSE=SS(Y,Y)-(B1*SS(X,Y)); VAR=SSE/(n-2); SDV=sqrt(VAR);
%to test the model utility
%a 2-sided t-test is used to examine the null hypothesis : B1=0
%if the test-statistic, T_stat, is larger than T_alpha,
%the null hypothesis is rejected with 95 % confidence
SB1=SDV/sqrt(SS(X,X)); T_stat1=B1/SB1;
if(optA==1)
T_alpha=input(['Enter the T value for ...
' num2str(n-2) ' d.o.f. and alpha=0.025 : '])
disp(['T_stat = ' num2str(T_stat1)])
```

```
if abs(T_stat1) > T_alpha
  disp('B1 is not equal to 0')
  else
    disp('B1 is equal to 0')
  end
  disp(['The confidence interval for B1 = ...
' num2str(B1-(T_alpha*SB1)) ' to ' num2str(B1+(T_alpha*SB1))])
%to compute the product moment coefficient of correlation,r
%r gives a measure of the strength of the linear relation
%between X and Y;
%warning - a high correlation does not imply causality
%one can test the null hypothesis, r=0 using T_stat2
%disproving the null hypothesis yields the same information
%as disproving : B1=0
r=SS(X,Y)/sqrt(SS(X,X)*SS(Y,Y));
T_stat2=(r*sqrt(n-2))/sqrt(1-r^2);
if abs(T_stat2) > T_alpha
  disp('r is not equal to 0')
  else
    disp('r is equal to 0')
  end
%to compute the coefficient of determination,r_sq
%r_sq represents the proportion of the sum of squares of deviations
%of the y values from their predicted values that can be attributed
%to a linear relation between Y and X
r_sq=1-(SSE/SS(Y,Y));
%to plot the data, the fitted line and the 2*SDV interval
X_plot=[min(X):(range(X)/(n-1)):max(X)]';
X_est=[ones(n,1) X_plot];
Y_est=X_est*B;
plot(X,Y,'o',X_plot,Y_est,'-',X_plot,Y_est+(2*SDV),':',...
X_plot,Y_est-(2*SDV),':')
```

```
if (optB==1)
  xlabel([num2str(ind_var)])
elseif (optB==2)
  xlabel([num2str(ind_var) ' * ' num2str(ind_var)])
elseif (optB==3)
  xlabel([num2str(ind_var) ' * ' num2str(ind_var2)])
  end
ylabel(num2str(dep_var))
title(['r = ' num2str(r) ';  r_sq = ' num2str(r_sq) ';...
  slope = ' num2str(B1) ';  intercept = ' num2str(B0)])
end
```

B.2.3 Stepwise Regression

```
function step_reg(f,c,dep_var,option,ind_var1,ind_var2,ind_var3)
%function step_reg(f,c,dep_var,option,ind_var1,ind_var2,ind_var3)
%Stepwise regression is used as a screening procedure to determine
%which independent variables are important
%  f=filelb file from which the table is obtained
%  c=case number
%  dep_var=dependent variable
%  option=1 : one variable models;option=2 : two variable models
%  option=3 : three variable models; option=4 : four variable models
%  ind_var1 = independent variable 1(used when option=2)
%  ind_var2 = independent variable 2(used when option=3)
%  ind_var3 = independent variable 3(used when option=4)
%  f,ind_var,dep_var are strings and should be entered using
%  single quotes
if (nargin < 5)
  ind_var1 = ' ';
  end
if (nargin < 6)
```

```
  ind_var2 = ' ';
  end
if (nargin < 7)
  ind_var3 = ' ';
  end
[table,names,comment]=table_read(f,c);
if (option==1)
%All possible one-variable models of the form
%   E[y] = B0 + B1*X
%are fit to the data
disp ('models of the form E[y] = B0 + B1*X')
for (i=2:22)
  [T_stat1]=lin_reg(f,c,names(i,:),dep_var,2,1,2);
  disp([names(i,:) ': ' num2str(T_stat1)]);
end
disp ('models of the form E[y] = B0 + B1*X.^2')
for (i=2:22)
   [T_stat1]=lin_reg(f,c,names(i,:),dep_var,2,2,2);
   disp([names(i,:) ': ' num2str(T_stat1)]);
end
elseif(option==2)
%All possible two-variable models of the form
%    E[y]=B0 + B1*X1 + B2*X2
%are fit to the data
disp (['models of the form E[y] = B0 + B1*' num2str(ind_var1) ' +...
B2*X2'])
for (i=2:22)
  [T_stat4]=mult_reg2(f,c,ind_var1,names(i,:),dep_var,2,2);
  disp([names(i,:) ': ' num2str(T_stat4)]);
end
elseif(option==3)
%All possible three-variable models of the form
```

```
%    E[y]=B0 + B1*X + B2*X2 + B3*X3
%are fit to the data
disp (['models of the form E[y] = B0 + B1* ' num2str(ind_var1) ' + ...
B2* ' num2str(ind_var2) ' + B3*X3'])
for (i=2:22)
  [T_stat5]=mult_reg3(f,c,ind_var1,ind_var2,names(i,:),dep_var,2,2);
  disp([names(i,:) ': ' num2str(T_stat5)]);
  end
elseif(option==4)
%All possible three-variable models of the form
%    E[y]=B0 + B1*X + B2*X2 + B3*X3 + B4*X4
%are fit to the data
disp (['models of the form E[y] = B0 + B1* ' num2str(ind_var1) ' + ...
B2* ' num2str(ind_var2) ' + B3* ' num2str(ind_var3) ' + B4*X4'])
for (i=2:22)
   [T_stat6]=mult_reg4(f,c,ind_var1,ind_var2,ind_var3,...
   names(i,:),dep_var,2,2);
   disp([names(i,:) ': ' num2str(T_stat6)]);
 end
end
```

Appendix C

Axis Location

Locating the ankle (or talocrural) joint is an essential step in constructing the "boot." The following figures (obtained from [51]) were used as references.

Fig. C.1 illustrates the position of the axis joint on the medial side of the foot with respect to the tibial malleolus. Fig. C.2 demonstrates the axis location with respect to the fibular malleolus on the lateral side of the foot. The figures also show the distribution of values quantifying the axis location.

Note that the values represent averaged data from a study of 46 cadaver legs and at best represent an estimate of the actual axis location in a given individual.

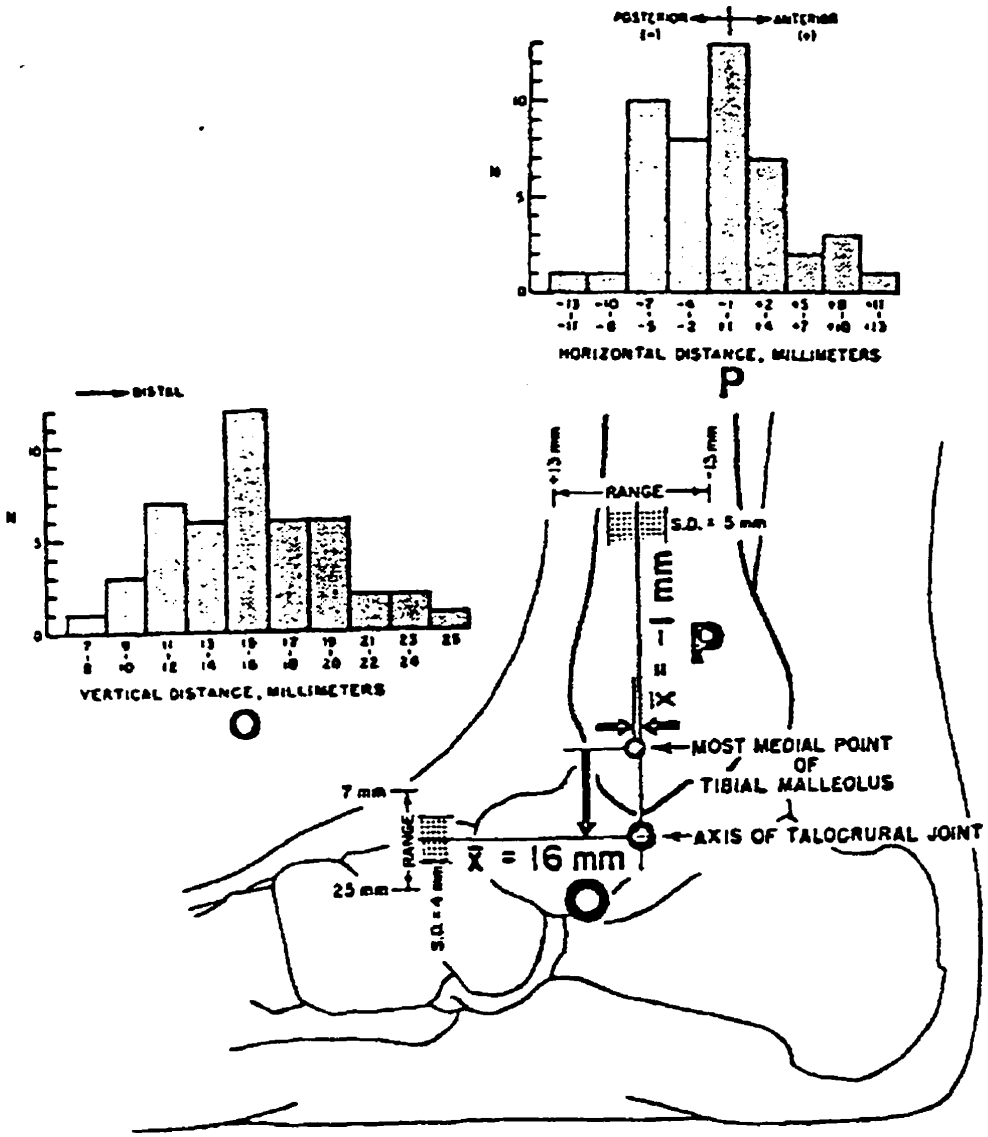

Figure C.1: Position of the axis joint with respect to the most medial point of the tibial malleolus.

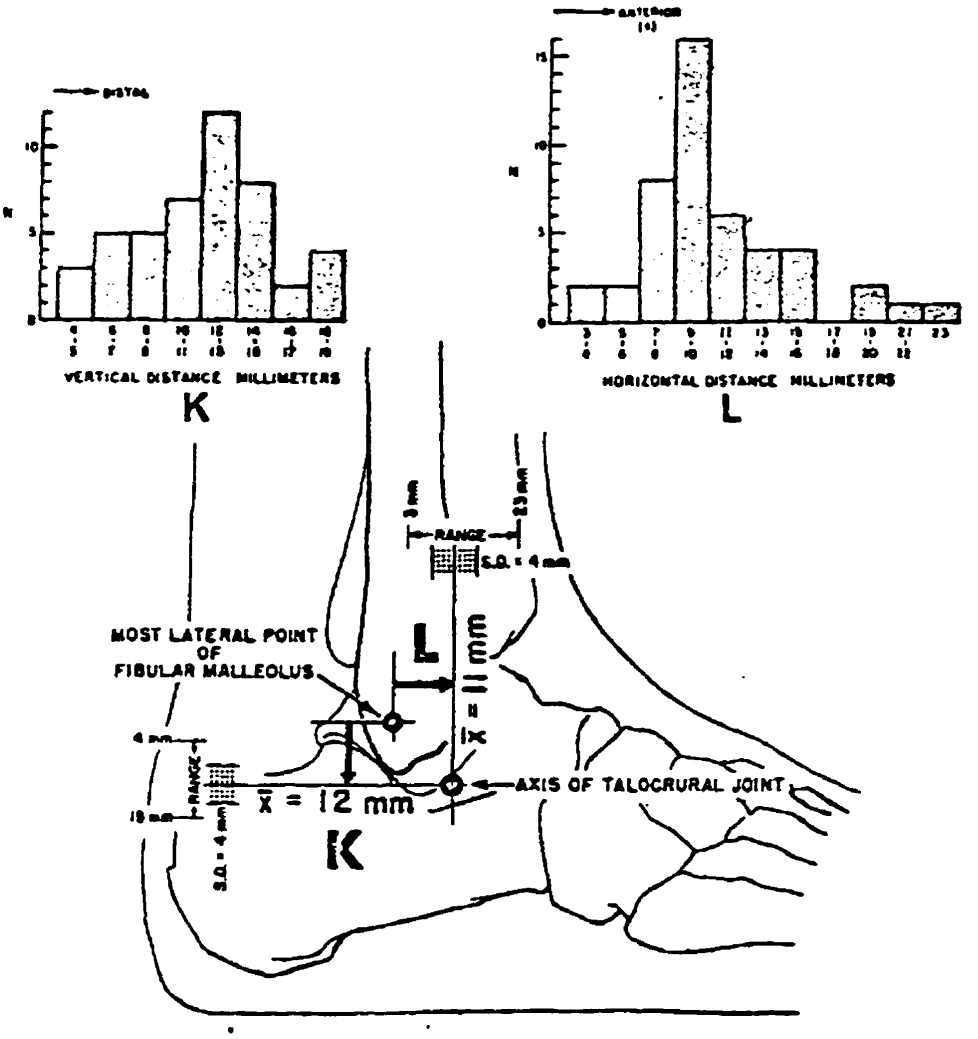

Figure C.2: Position of the axis joint with respect to the most lateral point of the fibular malleolus

Bibliography

[1] G.C. Agarwal, B.M. Berman, P. Löhnberg, and L. Stark. Studies in postural control systems part II - tendon jerk input. *IEEE Transactions on Systems Science and Cybernetics*. SSC-6(2):122-126, 1970.

[2] G.C. Agarwal and G.L. Gottlieb. Effect of vibration on the ankle stretch reflex in man. *Electroencephalography and Clinical Neurophysiology*. 49:81-92, 1980.

[3] K. Akazawa, J.W. Aldridge, J.D. Steeves, and R.B. Stein. Modulation of stretch reflexes during locomotion in the mesencephalic cat. *Journal of Physiology*. 329:553-567, 1982.

[4] J.W. Aldridge and R.B. Stein. Nonlinear properties of stretch reflex studied in the decerebrate cat. *Journal of Neurophysiology*. 47(2):179-192, 1982.

[5] J.H.J. Allum, K.H. Mauritz, and H. Vögele. The mechanical effectiveness of short latency reflexes in human triceps surae muscles revealed by ischaemia and vibration. *Experimental Brain Research*. 48:153-156, 1982.

[6] J.H.J. Allum, K.H. Mauritz, and H. Vögele. Stiffness regulation provided by short-latency reflexes in human triceps surae muscles. *Brain Research*. 234:159-164, 1982.

[7] E.K. Antonsson and R.W. Mann. The frequency content of gait. *Journal of Biomechanics*. 18(1):39-47, 1985.

[8] J.V. Basmajian and C.J. DeLuca. *Muscles Alive : Their Functions Revealed by Electromyography*. Williams and Wilkins Company, 5th edition, 1985.

[9] D.J. Bennet. J.M. Hollerbach. Y. Xu. and I.W. Hunter. Time-varying stiffness of human elbow joint during cyclical voluntary movement. *Experimental Brain Research.* 88:433–442. 1992.

[10] A. Berardelli. M. Hallett. C. Kaufman. E. Fine. W. Berenberg. and S.R. Simon. Stretch reflexes of triceps surae in normal man. *Journal of Neurology. Neurosurgery and Psychiatry.* 45:513–525. 1982.

[11] E. Bizzi. P. Dev. P. Morasso. and A. Polit. Effect of load disturbances during centrally initiated movements. *Journal of Neurophysiology.* 41(3):542–556. 1978.

[12] J.D. Brooke. W.E. McIlroy. and D.F. Collins. Movement features and h-reflex modulation - I. pedalling versus matched controls. *Brain Research.* 582:78–84. 1992.

[13] J.D. Brooke. W.E. McIlroy. D.F. Collins. and J.E. Misiaszek. Mechanisms within the human spinal cord suppress fast reflexes to control the movmement of the legs. *Brain Research.* 679:255–260. 1985.

[14] V.B. Brooks. *Neural Basis of Motor Control.* Oxford University Press. 1986.

[15] M.C. Brown. A. Crowe. and P.B.C. Matthews. Observations on the fusimotor fibres of the tibialis posterior muscle of the cat. *Journal of Physiology.* 177:140–159. 1965.

[16] M.C. Brown. I. Engberg. and P.B.C. Matthews. Fusimotor simulation and the dynamic sensitivity of the secondary ending of the muscle spindle. *Journal of Physiology.* 189:545–550. 1967.

[17] M.C. Brown. I. Engberg. and P.B.C. Matthews. The relative sensitivity to vibration of muscle receptors of the cat. *Journal of Physiology.* 192:773–800. 1967.

[18] T.I.H. Brown. P.M.H. Rack. and H.F. Ross. A range of different stretch reflex responses in the human thumb. *Journal of Physiology.* 332:101–112. 1982.

[19] D. Burke. Critical exmaination of the case for or against fusimotor involvement in disorders of muscle tone. In J.E. Desmedt. editor. *Advances in Neurology - Motor control mechanisms in health and disease.* volume 39. pages 133–150. Raven Press. 1983.

[20] C. Capaday and R.B. Stein. Amplitude modulation of the soleus h-reflex in the human during walking and standing. *The Journal of Neuroscience*, 6(5):1308–1313, 1986.

[21] C. Capaday and R.B. Stein. The effects of postsynaptic inhibition on the monosynaptic reflex of the cat at different levels of motoneuron pool activity. *Experimental Brain Research*, 77:577–584, 1989.

[22] Capaday95. The effects of baclofen on the stretch reflex parameters of the cat. *Experimental Brain Research*, 104:287–296, 1995.

[23] R.R. Carter, P.E. Crago, and M.W. Keith. Stiffness regulation by reflex action in the normal human hand. *Journal of Neurophysiology*, 64(1):105–118, 1990.

[24] C.W.Y. Chan and R.E. Kearney. Is the functional stretch response servo-controlled or preprogrammed ? *Electroencephalography and Clinical Neurophysiology*, 53:310–324, 1982.

[25] D.F. Collins, W.E. McIlroy, and J.D. Brooke. Contralateral inhibition of soleus h-reflexes with different velocities of passive movement of the opposite leg. *Brain Research*, 603:96–101, 1993.

[26] H.S. Cooker, C.R. Larson, and E.S. Luschei. Evidence that the human jaw stretch reflex increases the resistance of the mandible to small displacements. *Journal of Physiology*, 308:61–78, 1980.

[27] C. Darwin. *The Origin of the Species and The Descent of Man*. Modern Library, 1859.

[28] J.E. Desmedt and E. Godaux. Mechanism of the vibration paradox : Excitatory and inhibitory effects of tendon vibration on single soleus muscle motor units in man. *Journal of Physiology*, 285:197–207, 1978.

[29] F. Doemges and P.M.H. Rack. Changes in the stretch reflex of the human first dorsal interosseus muscle during different tasks. *Journal of Physiology*, 447:563–573, 1992.

[30] F. Doemges and P.M.H. Rack. Task-dependent changes in the response of the human wrist joint to mechanical disturbance. *Journal of Physiology*, 447:575–585, 1992.

[31] J.R. Dufresne, J.F. Soechting, and C.A. Terzuolo. Electromyographic response to pseudo-random torque disturbances of human forearm position. *Neuroscience*, 3:1213–1226, 1978.

[32] J.R. Dufresne, J.F. Soechting, and C.A. Terzuolo. Reflex motor output to torque pulses in man : identification of short– and long–latency loops with individual feedback parameters. *Neuroscience*, 4:1493–1500, 1979.

[33] J.A. Duha and R.E. Kearney. A client-server system for real-time control. Technical report, Neuromuscular Control Laboratory - McGill University, 1994.

[34] T.S. Eliot. *Little Gidding in Four Quartets*. Faber and Faber, 1944.

[35] *Proceedings of the IEEE EMBS*, volume 17, 1995.

[36] S.J. Evans, C.M.and Fellows, H.F. Ross, and D.K.W Walters. Response of the normal human ankle joint to imposed sinusoidal movements. *Journal of Physiology*, 344:483–502, 1983.

[37] W.F. Genadry, R.E. Kearney, and I.W. Hunter. Dynamic relationship between emg and torque at the human ankle : Variation with contraction level and modulation. *Medical & Biological Engineering & Computing*, 26:489–496, September 1988.

[38] G.L. Gottlieb and G.C. Agarwal. Modulation of postural reflexes by voluntary movement - I. modulation of the active limb. *Journal of Neurology, Neurosurgery and Psychiatry*, 36:529–539, 1973.

[39] G.L. Gottlieb and G.C. Agarwal. Response to sudden torques about ankle in man : myotatic reflex. *Journal of Neurophysiology*, 42:91-106, 1979.

[40] G.L. Gottlieb and G.C. Agarwal. Response to sudden torques about ankle in man - III suppression of stretch-evoked responses during phasic contraction. *Journal of Neurophyiology*, 44(233–246), 1980.

[41] K.-E. Hagbarth and G. Eklund. Tonic vibration reflexes (TVR) in spasticity. *Brain Research*, 2:201–203, 1966.

[42] J.A. Hoffer and S. Andreassen. Regulation of soleus muscle stiffness in pre-mammilary cats – intrinsic and reflex components. *Journal of Neurophysiology*, 45(2):267–285, 1981.

[43] J.C. Houk. Regulation of stiffness by skeletomotor reflexes. *Ann. Rev. Physiol.*, 41:99–114, 1979.

[44] H. Hultborn, S. Lindström, and H. Wigström. On the function of recurrent inhibition in the spinal cord. *Experimental Brain Research*, 37:399–403, 1979.

[45] H. Hultborn, E. Pierrot-Deseilligny, and H. Wigström. Recurrent inhibition and afterhyperpolarization followin neuronal discharge in the cat. *Journal of Physiology*, 297:253–266, 1979.

[46] I.W. Hunter and R.E. Kearney. Dynamics of human ankle stiffness : variation with mean ankle torque. *Journal of Biomechanics*, 15(10):747–752, 1982.

[47] I.W. Hunter and R.E. Kearney. Generation of random sequences with jointly specified probability density and autocorrelation functions. *Biological Cybernetics*, 47:141–146, 1983.

[48] I.W. Hunter and R.E. Kearney. Invariance of ankle dynamic stiffness during fatiguing muscle contractions. *Journal of Biomechanics*, 16(12):985–991, 1983.

[49] I.W. Hunter and R.E. Kearney. Two-sided linear filter identification. *Medical & Biological Engineering & Computing*, 21:203–209, 1983.

[50] V.T. Inman. *The Joints of the Ankle*. Williams and Wilkins, 1976.

[51] R.E Isman and Inman V.T. Anthropometric studies of the human foot and ankle. *Bulletin of Prosthetics Research*, Spring 1969.

[52] G.C. Joyce, P.M.H. Rack, and H.F. Ross. The forces generated at the human elbow joint in response to imposed sinusoidal movements of the forearm. *Journal of Physiology*, 240:351–374, 1974.

[53] R.E. Kearney. *Experimental and simulation studies of ankle reflexes in man.* PhD thesis, McGill University, Department of Mechanical Engineering and Biomedical Engineering Unit, 1976.

[54] R.E. Kearney. Simulation of the human neuromuscular response to ankle rotation with a segmental reflex model. *Comput. Biol. Med.*, 8:229–341, 1978.

[55] R.E. Kearney. Peripheral neuromuscular control. *Selected Topics in Biomedical Engineering - Class Notes - McGill Univ. Course 399-501A*, 1992.

[56] R.E. Kearney. Electromyography. *Biomedical Instrumentation and Measurement Techniques - Class Notes - McGill Univ. Course 399-503B*, 1993.

[57] R.E. Kearney and C.W.Y. Chan. Contrasts between the reflex responses of tibialis anterior and triceps surae to sudden ankle rotation in normal human subjects. *Electroencephalography and Clinical Neurophysiology*, 54:301–310, 1982.

[58] R.E. Kearney and I.W. Hunter. Dynamics of human ankle stiffness : variation with displacement amplitude. *Journal of Biomechanics*, 15(10):753–756, 1982.

[59] R.E. Kearney and I.W. Hunter. System identification of human triceps surae stretch reflex dynamics. *Experimental Brain Research*, 51:117–127, 1983.

[60] R.E. Kearney and I.W. Hunter. System identification of human stretch reflex dynamics : Tibialis anterior. *Experimental Brain Research*, 56:40–49, 1984.

[61] R.E. Kearney and I.W. Hunter. Nonlinear identification of stretch reflex dynamics. *Annals of Biomedical Engineering*, 16:79–94, 1988.

[62] R.E. Kearney and I.W. Hunter. System identification of human joint dynamics. *Critical Reviews in Biomedical Engineering*, 18(1):55–87, 1990.

[63] R.E. Kearney, I.W. Hunter, Weiss P.L., and Spring K. Tilt-table/ankle-actuator system for the study of vestibulospinal reflexes. *Medical & Biological Engineering & Computing*, 21:301–305, May 1983.

[64] R.E. Kearney, R.B. Stein, and L. Parameswaran. Differential identification of passive and reflex mechanisms in human ankle stiffness dynamics. In *Proceedings of the IEEE Engineering in Medicine and Biology Society*, volume 16, 1994.

[65] R.E. Kearney, R.B. Stein, and L. Parameswaran. Identification of passive and reflex contributions to human ankle joint mechanics. In *Proceedings of the Canadian Medical and Biological Engineering Society*, volume 18, 1994.

[66] R.E. Kearney, R.B. Stein, and L. Parameswaran. Identification of intrinsic and reflex contributions to human ankle stiffness dynamics. Submitted to IEEE Transactions on Biomedical Engineering, 1995.

[67] R.E. Kearney, P.L. Weiss, and R. Morier. System identification of human ankle dynamics : intersubject variability and intrasubject reliability. *Clinical Biomechanics*, 5:205–217, 1990.

[68] R.F. Kirsch and R.E. Kearney. Identification of time-varying dynamics of the human triceps surae stretch reflex – II rapid imposed movement. *Experimental Brain Research*, 97:128–138, 1993.

[69] R.F. Kirsch, R.E. Kearney, and J.B. MacNeil. Identification of time-varying dynamics of the human triceps surae stretch reflex – I rapid isometric contraction. *Experimental Brain Research*, 97:115–127, 1993.

[70] J.B. MacNeil, R.E. Kearney, and I.W. Hunter. Identification of time-varying biological systems from ensemble data. *IEEE Transactions on Biomedical Engineering*, 39(12):1213–1225, 1992.

[71] P.Z. Marmarelis and P.Z. Marmarelis. *Analysis of Physiological Systems : The White-Noise Approach*. Plenum Press, 1978.

[72] P.B.C. Matthews. *Mammalian Muscle Receptors and Their Central Actions*. Edward Arnold, 1972.

[73] W.E. McIlroy, D.F. Collins, and J.D. Brooke. Movement features and h-reflex modulation – II. passive rotation, movement velocity and single leg movement. *Brain Research*, 582:85–93, 1992.

[74] T.A. McMahon. *Muscles, Reflexes, and Locomotion*. Princeton University Press, 1984.

[75] W. Mendenhall and T. Sincich. *Statistics for Engineering and the Sciences*. Dellen Publishing Comp., 3rd edition, 1992.

[76] M. Mirbagheri, R.E. Kearney, and H. Barbeau. Modulation of intrinsic and reflex contributions to dynamic ankle stiffness with the level of voluntary contraction. In EMBS17 [35].

[77] R.L. Morier, P.L. Weiss, and R.E. Kearney. Low inertia, rigid limb fixation using glass fibre casting bandage. *Medical & Biological Engineering & Computing*, 28:96–99, January 1990.

[78] R. Myre. A method for estimating the instantaneous axis of rigid body motion. Master's thesis, McGill University, Departments of Electrical Engineering and Biomedical Engineering, 1992.

[79] T.R. Nichols and J.C. Houk. Improvement in linearity and regulation of stiffness that results from actions of stretch reflex. *Journal of Neurophysiology*, 29:119–142, 1976.

[80] L. Parameswaran and R.E. Kearney. The effects of passive joint movement on stretch reflex gain at the human ankle. In EMBS17 [35].

[81] E.J. Perreault. System identification of the reflex contribution to human ankle dynamics. Master's thesis, McGill University, Departments of Electrical Engineering and Biomedical Engineering, 1991.

[82] E.J. Perreault, Hunter I.W., and R.E. Kearney. Quantitative analysis of four EMG amplifiers. *Journal of Biomedical Engineering*, 15, September 1993.

[83] E.J. Perreault and R.E. Kearney. A method for the evaluation of reflex contribution to ankle dynamics. In *Proceedings of the IEEE Engineering in Medicine and Biology Society*, volume 13, 1991.

[84] J.C. Rothwell. *Control of Human Voluntary Movement.* Aspen, 1987.

[85] T. Sinkjaer and I. Magnussen. Passive, intrinsic and reflex-mediated stiffness in the ankle extensors of hemiparetic patients. *Brain*, 117:355–363, 1994.

[86] T. Sinkjaer, E. Toft, S. Andreassen, and B.C. Hornemann. Muscle stiffness in human ankle dorsiflexors : intrinsic and reflex components. *Journal of Neurophysiology*, 60(3):1110–1121, 1988.

[87] B. Smith. The human machine. *Mechanical Engineering*, page 4, August 1993. Letters to Editor.

[88] R.B. Stein and C. Capaday. The modulation of human reflexes during functional motor tasks. *Trends in Neuroscience*, 11(7):328–332, 1988.

[89] R.B. Stein, S.J. Deserres, and R.E. Kearney. Modulation of stretch reflexes during behaviour. In W.R. Ferrel and U. Proske, editors, *Neural Control of Movement*, pages 151–158. Plenum Press, 1995.

[90] R.B. Stein and R.E. Kearney. Nonlinear behaviour of muscle reflexes at the human ankle joint. *Journal of Neurophysiology*, 73(1):65–72, 1995.

[91] M. Steszyn. Experimental apparatus for the investigation of human knee dynamics. Master's thesis, McGill University, Department of Biomedical Engineering, 1995.

[92] J.P. Trainor. Identification of the time-varying human joint dynamics during an electrically-stimulated twitch. Master's thesis, McGill University, Departments of Mechanical Engineering and Biomedical Engineering, 1994.

[93] R.L. Valmassy. *Clinical Biomechanics of the Lower Extremities*. Mosby, 1996.

[94] A.J. Vander, J.H. Sherman, and D.S. Luciano. *Human Physiology : The Mechanisms of Body Function*. McGraw-Hill, 5th edition, 1990.

[95] P.L. Weiss. *Position Dependence of Ankle Joint Dynamics*. PhD thesis, McGill University, Department of Physiology and Biomedical Engineering Unit, 1985.

[96] P.L. Weiss, I.W. Hunter, and R.E. Kearney. Human ankle joint stiffness over the full range of muscle activation levels. *Journal of Biomechanics*, 21(7):539–544, 1988.

[97] P.L. Weiss, R.E. Kearney, and I.W. Hunter. Position dependence of ankle joint dynamics - I passive mechanics. *Journal of Biomechanics*, 19(9):727–735, 1986.

[98] P.L. Weiss, R.E. Kearney, and I.W. Hunter. Position dependence of ankle joint dynamics - II active mechanics. *Journal of Biomechanics*, 19(9):737–751, 1986.

[99] P.L. Weiss, R.E. Kearney, and I.W. Hunter. Position dependence of stretch reflex dynamics at the human ankle. *Experimental Brain Research*, 63:49–59, 1986.

[100] D.T. Westwick. *Methods for the Identification of Multiple-Input Nonlinear Systems.* PhD thesis. McGill University. Departments of Electrical Engineering and Biomedical Engineering, 1995.

[101] J.F. Yang, R.B. Stein, and K.B. James. Contribution of peripheral afferents to the activation of the soleus muscle during walking in humans. *Experimental Brain Research*, 87:679–687, 1991.

[102] B.Y. Yunan. The design and construction of a high performance electro-hydrauli actuating system used to identify the human ankle joint mechanics. Master's thesis. McGill University. Department of Mechanical Engineering and Biomedical Engineering Unit, 1989.

IMAGE EVALUATION
TEST TARGET (QA-3)

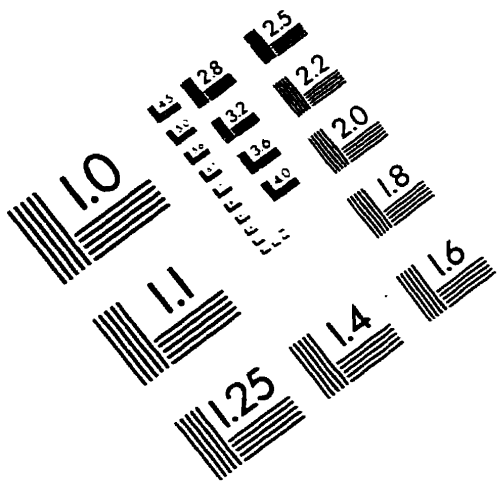

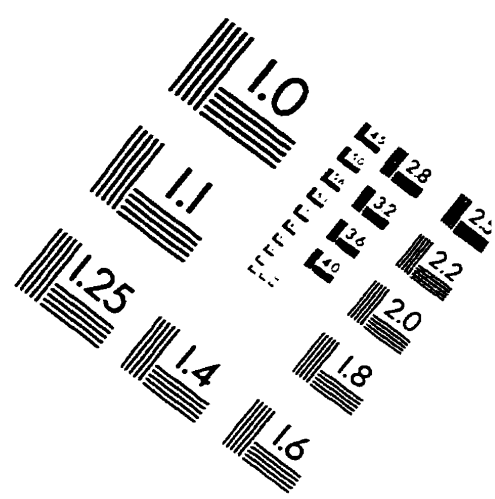

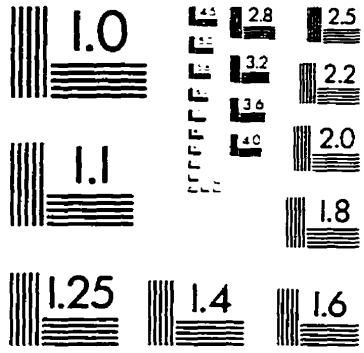

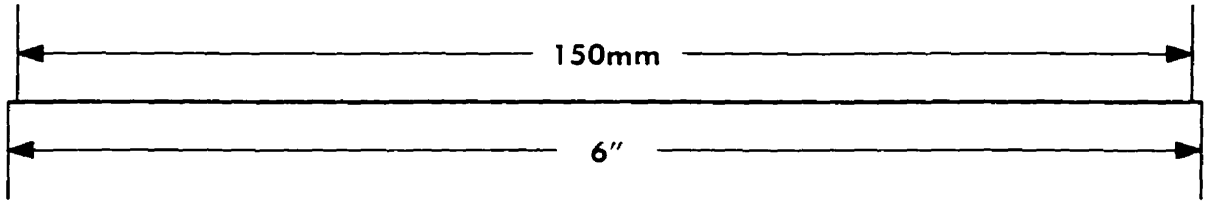

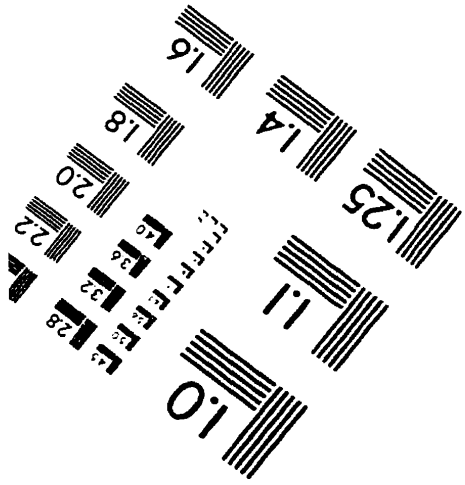

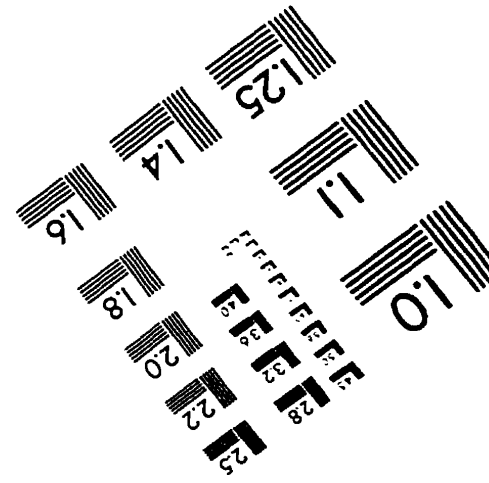

APPLIED IMAGE, Inc
1653 East Main Street
Rochester, NY 14609 USA
Phone: 716/482-0300
Fax: 716/288-5989